Charles University

Faculty of Science

Department of Plant Experimental Biology

Study programme: Biology

Branch of study: Experimental Plant Biology

A role of *Arabidopsis* Phosducin-like2 (AtPhLP2) in regulation of plant growth and development

Role phosdicin-like2 (AtPhLP2)
při regulaci růstu a vývoje u *Arabidopsis*

Diploma thesis

Bc. Veronika Poláková

Supervisor: Mgr. Denisa Oulehlová, PhD.

Consultant: Mgr. Matyáš Fendrych, PhD.

Prague, 2024

Prohlašuji, že předkládanou diplomovou práci jsem vypracovala samostatně pod vedením Mgr. Denisy Oulehlové, PhD. Předkládaný text je výsledkem mé vlastní práce, použité informační zdroje jsou vždy řádně citovány. Tato práce ani žádná její část nebyla předložena k získání jiného nebo stejného akademického titulu.

I hereby confirm that my diploma thesis was prepared independently under the guidance of Mgr. Denisa Oulehlová, PhD. This study represents my own work and results, otherwise the source is always properly cited. This work or a substantial part has not been submitted to obtain another or the same academic degree.

Prague, August 1st 2024 Veronika Poláková

Acknowledgements

First of all, I would like to thank my supervisor, Denisa Oulehlová, and my consultant, Matyáš Fendrych, for their patience, experienced guidance, worthwhile advice and indispensable support throughout the process of my research and writing this thesis. I am grateful for the time and effort they dedicated to help me overcome obstacles and challenging tasks.

I would also like to extend my gratitude to all lab members for their support and for creating a great balance of a professional and friendly environment in the lab. The inspiring atmosphere they fostered was a great opportunity to work in.

I am also deeply thankful to my family and friends for their significant support and encouragement. Their companionship has been invaluable through all my studies.

Abstract

Recently, we identified Phosducin-like2 (AtPhLP2) in *Arabidopsis* as a possible regulator of growth and development that could be involved in the non-transcriptional auxin response in roots. Based on preliminary data, this protein could also be crucial for other developmental processes, as the progeny of knock-out mutants is not viable.

The aim of this thesis is to elucidate the function of AtPhLP2 in *Arabidopsis thaliana* root development by analyzing the expression of PhLP2 and characterizing the *phlp2* knock-down line. I prepared transgenic *Arabidopsis thaliana* lines to monitor the activity of the putative PhLP2 promoter. The promoter was active in the aboveground parts of the plant as well as in the vascular bundles of the root and in the root meristem. The localization of the protein was consistent with promoter activity, and strong expression was additionally observed in germinating pollen. At the cellular level, the signal was visible in the nucleus and cytoplasm. To estimate a possible link to auxin signaling and other processes in which PhLP2 might be involved, I characterized the phenotype of *phlp2* knock-down lines available in the laboratory and quantified the general growth characteristics and responses of these seedlings to gravistimulation or IAA treatment. I show that the PhLP2 knock-down line exhibited severe root waving, a short meristem and minimal number of lateral root primordia, yet there was no insensitivity to IAA observed and the rapid auxin response was not impaired. The distinct phenotypic expression of the knock-down mutant cannot be explained by disruption of auxin signaling, and further research is needed to unravel the function of PhLP2 in *Arabidopsis thaliana* development.

Keywords: phosducin-like 2, rapid auxin response, phosphorylation, root development

Abstrakt

Nedávno jsme u huseníčku identifikovali Phosducin-like2 (AtPhLP2) jako možného regulátora růstu a vývoje, který by se mohl účastnit netranskripční auxinové odpovědi v kořenech. Na základě předběžných údajů by tento protein mohl být klíčový i pro další vývojové procesy, protože potomstvo knock-out mutantů není životaschopné.

Cílem této diplomové práce je objasnit funkci AtPhLP2 ve vývoji kořene *Arabidopsis thaliana* pomocí analýzy exprese PhLP2 a charakteristiky knock-down linie. Připravila jsem transgenní linie *Arabidopsis thaliana* pro sledování aktivity předpokládaného promotoru PhLP2. Promotor se ukázal jako aktivní v nadzemních částech rostliny a také v cévních svazcích kořene a v kořenovém meristému. Lokalizace proteinu odpovídala aktivitě promotoru, silná exprese byla navíc pozorována u klíčícího pylu. Na buněčné úrovni byl signál viditelný v jádře i cytoplazmě. Pro odhadnutí možného spojení s auxinovou signalizací a dalších procesů, kterých by se PhLP2 mohl účastnit, jsem charakterizovala fenotyp knock-down linií dostupných v laboratoři a kvantifikovala jsem obecné růstové charakteristiky a reakce těchto semenáčků na gravistimulaci nebo ošetření IAA. Uvádíme, že PhLP2 knock-down linie vykazovala silné zvlnění kořene, krátký meristém a minimum primordií laterálních kořenů, avšak nebyla zjištěna necitlivost na IAA a rychlá auxinová odpověď nebyla porušena. Výrazný fenotypový projev knock-down mutanta nelze vysvětlit narušením auxinové signalizace a k odhalení funkce PhLP2 ve vývoji *Arabidopsis thaliana* je nutný další výzkum.

Klíčová slova: phosducin-like 2, rychlá auxinová odpověď, fosforylace, vývoj kořene

Contents

Abbreviations

ABCB	ATP-binding cassette B
ALF4	ABERRANT LATERAL ROOT FORMATION 4
ABP1	AUXIN BINDING PROTEIN 1
AHA1	H+-ATPase
ARF	AUXIN RESPONSE FACTOR
ARP2/3	ACTIN RELATED PROTEIN 2/3
ATP	adenosin triphosphate
Aux/IAA	Auxin/Indole-3-Acetic Acid
AUX/LAX	Auxin1/Like-AUX1
AXR	AUXIN RESISTANCE
BRL2	BRI1-Like 2
CCT	CHAPERONIN CONTAINING TAILLESS COMPLEX POLYPEPTIDE
CKA2	CASEIN KINASE II: ALPHA CHAIN 2
Col-0	Columbia-0 background (NASC ID N70000)
COP13	CONSTITUTIVE PHOTOMORPHOGENIC 13
DZ	differentiation zone
ELK4	ERECTA-LIKE4
EZ	elongation zone
GB	Golden Braid
GRK2	G-PROTEIN COUPLED RECEPTOR KINASE 2
GOS12	GOLGI SNARE 12
IAA	indole-3-acetic acid
JAZ3	JASMONATE-ZIM-DOMAIN PROTEIN 3

LB	Luria-Bertani
LR	lateral root
LRP	lateral root primordia
MS	Murashige-Skoog
MZ	meristematic zone
NLS	nuclear localization signal
PDCL2	PHOSDUCIN-LIKE 2 (human)
PEO-IAA	α-(2-oxo-2-phenylethyl)-1H-indole-3-acetic acid
PhLP2	PHODUCIN-LIKE 2
PI	propidium iodide
PID	PINOID
PIN	PIN-formed
PLT	PLETHORA
PM	plasma membrane
QC	quiescent center
RAPTOR1	TOR REGULATORY PROTEIN
RGS1	REGULATOR OF G-PROTEIN SIGNALING 1
RHIP1	RGS1-HXK1 INTERACTING PROTEIN 1
RISC	RNA-INDUCED SPLICING COMPLEX
RNAi	RNA interference
ROP	RHO OF PLANTS
SCF	SKP1 CULLIN-F-BOX (COMPLEX)
SCL15	SCARECROW-LIKE 15
SCL30	SC35-LIKE SPLICING FACTOR 30
SNT	Simple Neurite Tracer
SNX1	SORTING NEXIN 1

SYP51	SYNTAXIN OF PLANTS 51
SYP53	SYNTAXIN OF PLANTS 53
TIR1/AFB	TRANSPORT INHIBITOR RESPONSE 1/ AUXIN SIGNALLING F-BOX (receptor)
TMK1	TRANSMEMRANE KINASE 1
TOR	TARGET OF RAPAMYCIN
TRiC	TAILLESS COMPLEX POLYPEPTIDE 1 RING COMPLEX
VAP27-1	VESICLE ASSOCIATED PROTEIN 27-1
VGI	vertical growth index
VH1	VASCULAR HIGHWAY 1
WAV2	WAVED GROWTH 2
WINK8	WITH NO LYSINE KINASE 8
WRM	WORM ARM MOTIF 1
WT	wild type
Y2H	yeast two hybrid
ZHD2	ZINC-FINGER HOMEODOMAIN PROTEIN 2

Introduction

Auxin is a phytohormone that regulates plant growth and development via well studied transcriptional pathway. However, there are auxin-dependent processes happening so rapidly that there is not enough time for transcription to occur. Non-transcriptional pathway of auxin signaling is known as a rapid auxin response. In a model plant *Arabidopsis thaliana*, some of the crucial components of the rapid auxin response pathway were recently identified (Dubey et al., 2021; Prigge et al., 2020; Serre et al., 2021), yet other players remain unknown. To identify novel regulators of this process, we took advantage of existing datasets and picked candidate genes. Based on swift auxin-promoted phosphorylation changes, Phosducin-like Protein 2 (PhLP2; At5g14240) was identified as a potential player in the rapid auxin response.

Surprisingly, it was not possible to obtain knock-out mutants from public databases and CRISPR-Cas9 mutants generated in our laboratory were not viable. Knock-down mutants with lower expression of *PhLP2* can be propagated, yet they exhibit strongly afflicted phenotype, which indicates the essential role of this protein in *Arabidopsis thaliana* development. In this thesis, I would like to describe the relation of PhLP2 to rapid auxin response and other developmental processes based on its expression and the phenotype of the knock-down line.

Aims and hypotheses

Established hypotheses:

PhLP2 is dephosphorylated immediately after IAA application

PhLP2 knock-out mutants are not viable

Phenotype of PhLP2 knock-down mutant is strongly affected

Aim of the thesis is to elucidate following questions:

Where in the plant is PhLP2 expressed?

Does PhLP2 participate in the rapid auxin response or other auxin-related processes?

What other processes could be PhLP2 involved in?

Is PhLP2 involved in gametophytic or embryonic development?

1. Literature overview

1.1 Plant morphogenesis

Plant development requires proper organ and structure formation, a morphogenesis. It is a complex process consisting of many overlapping steps leading to the plant structure initiation, growth and maintenance through ontogenesis. It determines organ shape and function with respect to external conditions (Huang et al., 2018).

Despite a huge diversity of plant structures and their biological functions, the process of morphogenesis begins at a cellular level and depends on the meristem activity and cell differentiation. In other words, cells gain their function and at the same time, they form tissues. (Barlow, 1989; Huang et al., 2018).

Growth depends on the cell division, cell expansion or, at most times, the combination of both. So to shape the organ, it is crucial to coordinate meristematic activity and subsequent differentiation of newly formed cells, which is regulated by many factors. One of them is the phytohormone auxin (Hilty et al., 2021; Marconi and Wabnik, 2021).

1.2 Auxin and its transport

Plant morphogenetics is in many aspects regulated by the phytohormone auxin. Its significant role in different processes was predicted by Charles Darwin and his son Francis in the 1880s. Later, the first characterized (and as was found out, also the most abundant) representative was the indole-3-acetic acid (IAA). It is a small molecule derived from tryptophan (Leyser, 2010; Zhao, 2012).

The majority of auxin is synthesized in the apical meristem from where it is distributed to other tissues. Auxin transport is mediated via specific facilitators, whose distribution at the cell membrane moreover enables polarity of the transport. AUXIN1/LIKE-AUX (*AUX/LAX*) is a gene family of 4 *Arabidopsis* influx carriers mediating transport of auxin from apoplast to symplast working as $2H^+$ symporters. When entering a slightly alkaline environment of cytoplasm,

auxin dissociates to its deprotonated form IAA^- and thus can not pass through the plasma membrane (PM) back to the apoplast (Péret et al., 2012). On the other hand, transport of auxin from the cytosol to the apoplast is driven by the PIN-formed (PIN) protein family. *Arabidopsis thaliana* possesses 8 PIN proteins and their distribution on the PM determines the direction of the auxin flow. Distribution of auxin transporters on the PM enables polar auxin transport (Friml, 2003; Okada et al., 1991; Ung et al., 2022).

Mutation of either PINs or their positive regulators encoded by PINOIDs (*PID*s) leads to strongly disrupted organ development (Benjamins et al., 2001; Mudgett et al., 2023). Both cases exhibit a typical pin-formed shoot with very little or no flowers (Fig. 1 and 2).

Another transporters participating in auxin fluxes are P-glycoproteins (PGP) belonging to the ATP-BINDING CASSETTE B (ABCB) family, providing both efflux and influx. These carriers are distributed non-polarly on the PM (Ng et al., 2015) and its mutation also causes visible phenotype (Fig. 2). Auxin transport at the cellular level is visualized in Fig. 3.

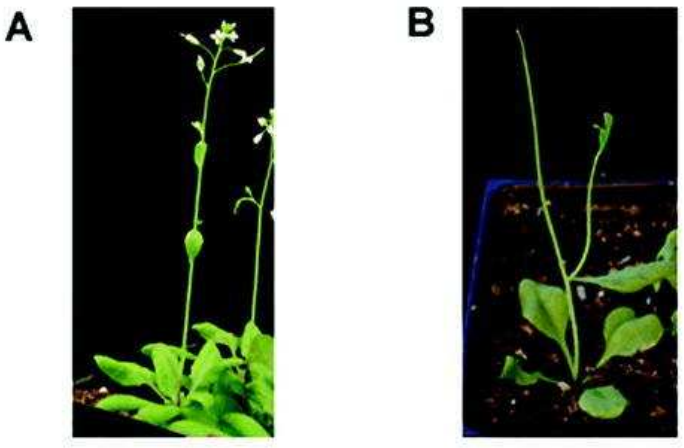

Fig. 1: **A** - Col-0 typical shoot phenotype, **B** - mutation of PID exhibits pin-formed phenotype (Wang et al., 2007, edited)

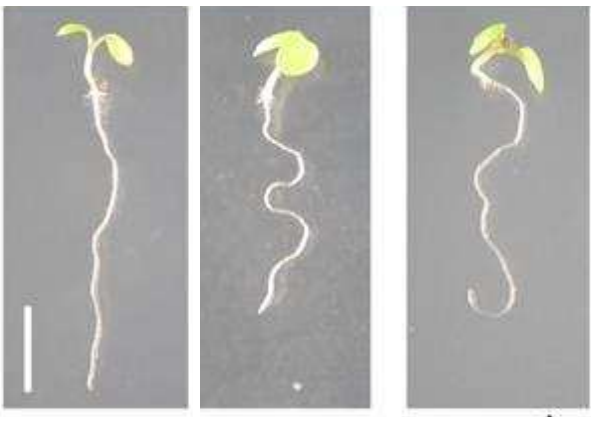

Fig. 2: comparison of Col-0 (left) to *pgp1pgp19* double mutant (center) and *pin2* mutant (right), bar = 1 cm (Blakeslee et al., 2007, edited)

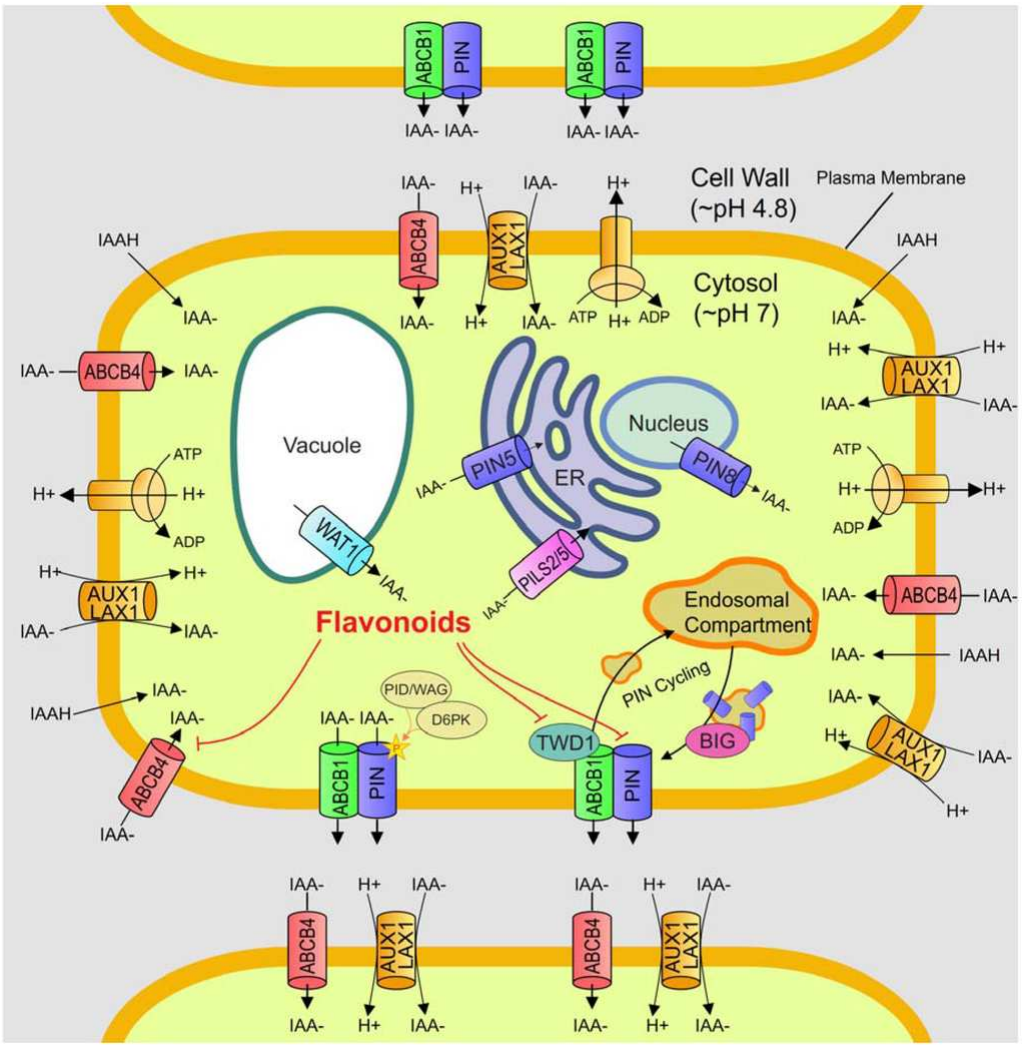

Fig. 3: Scheme of the auxin transport on the cell level (Ng et al., 2015)

1.3 Mechanisms of auxin signaling

Presence of auxin in the cell induces a specific reaction and there are different mechanisms of how it happens. One of them is the effect on expression of specific genes. Auxin transcriptional signaling pathway has been studied for a long time. It was proposed that without auxin presence (or when auxin is present minimally) AUXIN RESPONSE FACTORs (ARF), which activate the expression of auxin-responsive genes, binds with their repressor AUXIN/INDOLE-3-ACETIC ACID (Aux/IAA), therefore transcription of following genes is disabled. When present, auxin mediates interaction between ubiquitin ligase complex (SKP1 CULLIN-F-BOX) $SCF^{TIR1/AFB}$ (TRANSPORT INHIBITOR RESPONSE 1 / AUXIN SIGNALING F-BOX (TIR1/AFB) and Aux/IAA. As a result, the Aux/IAAs get ubiquitinated and degraded by the 26S proteasome. Since ARFs are then not inhibited by Aux/IAAs, they are able to regulate related gene transcription (Gray et al., 2001; Kepinski and Leyser, 2004).

The process of transcription and translation itself, in the case of 400 amino acids long protein, takes at least 2 minutes - with other signaling steps neglected (Milo et al., 2010). However, some auxin-related processes are happening in a shorter time. There is another, non-genomic mechanism of auxin action in the cell known as a rapid auxin response. This pathway goes along with various reactions at the cell level, such as apoplastic alkalinization, Ca^{2+} influx to the cytoplasm and membrane potential changes (Dindas et al., 2018; Monshausen et al., 2011; Serre et al., 2021). These rapid auxin responses require AFB1, which is a cytoplasmic auxin receptor (Dubey et al., 2023). Mechanism of its action is not understood, however, it seems SCF complex-independent (Dubey et al., 2023; Yu et al., 2015).

One of the players that has for long been connected with the non-transcriptional responses to auxin is the AUXIN BINDING PROTEIN 1 (ABP1). TRANSMEMBRANE RECEPTOR-LIKE KINASE 1 (TMK1) was shown to

create a complex with ABP1 on PM which enables auxin sensing and subsequently activation of intracellular GTPases RHO OF PLANTS (ROPs) (Friml et al., 2022; Xu et al., 2014).

TMKs are closely connected to plant morphogenesis via participating in many processes, such as pavement cells development, formation of lateral roots or apical hook growth (Cao et al., 2019; Huang et al., 2019). TMK1 is also related to pH changes in apoplast. Auxin mediated phosphorylation of H^+-ATPase through TMK1 on PM happens in several seconds (Lin et al., 2021).

As an example of rapid auxin response, the root growth inhibition can be mentioned: application of auxin inhibits root growth within tens of seconds, and after its removal, root growth is quickly restored. This rapid reaction does not occur in absence of AFB1. However, rapid auxin response is a quite recent concept and still a lot remains unclear about its molecular mechanism. (Fendrych et al., 2018).

1.4 Auxin in regulation of root growth and development

During ontogenesis, auxin is crucial for the proper root development. Nanomolar concentrations of auxin inhibit cell elongation but promote cell division, and the ability of the cells to either divide or elongate is regulated by auxin gradient. In the root, auxin is transported through the vasculature to the distal part (where auxin concentration reaches the highest values) and subsequently is directed to the lateral cap and epidermis from where it continues in proximal direction. This gradient is formed by specific PIN distribution and is known as the “reverse fountain” model (Blancaflor and Masson, 2003). The quiescent center (QC) is a pool of stem cells where new tissues are derived from and where the auxin maximum can be found. Along the auxin gradient in the proximal direction from QC, cells progress through the following developmental stages: meristematic zone (MZ), elongation zone (EZ) and differentiation zone (DZ) (Fig. 4) (Petricka et al., 2012).

Continuous growth is kept by activity of the root meristem. Concentration of auxin in MZ promotes cell division and the further from the QC, the lower the auxin concentration is (Fig. 5). It was shown that disturbances in auxin transport lead to disorders in the primary root formation (Hadfi et al., 1998; Petricka et al., 2012). PLETHORA (*PLT*) is a family of genes involved in maintenance of the stem cell activity (Aida et al., 2004). Expression of *PLT* is regulated by auxin. Prolonged auxin action triggers expression of *PLT* which maintains the stem cell activity. Multiple mutants in *PLT* genes exhibit short meristem phenotype. Gradient of PLT is affected by PIN-mediated polar transport of auxin (Galinha et al., 2007; Mähönen et al., 2014).

Cells are losing the ability to divide in the EZ. As the border of this zone can not be clearly determined, the area of receding cell division is called a transition zone (TZ) and overlaps with its neighboring zones. Expansion of cells in EZ is caused by intracellular changes, such as vacuole enlargement or cytoskeleton reorganization (Del Bianco and Kepinski, 2011). In the cell, auxin promotes activity of proton pumps transporting H^+ to apoplast. Acidification of apoplasts is closely related to cell growth. Cells are bounded by the cell wall, which is a stiff structure ensuring mechanical support and stability. For the cell growth, cell wall loosening is required without losing its integrity. Loosening of the cell wall components is dependent on decreased pH. The assumption is that decreased pH activates expansins, proteins present in the cell wall initiating its remodeling. Cell turgor creates a pressure on the acidified cell wall, which provides a vector of growth, resulting in cell elongation (Routier-Kierzkowska and Smith, 2013).

Finally, EZ is followed by DZ, where cells gain their final function and morphological attributes (Konstantinova et al., 2021).

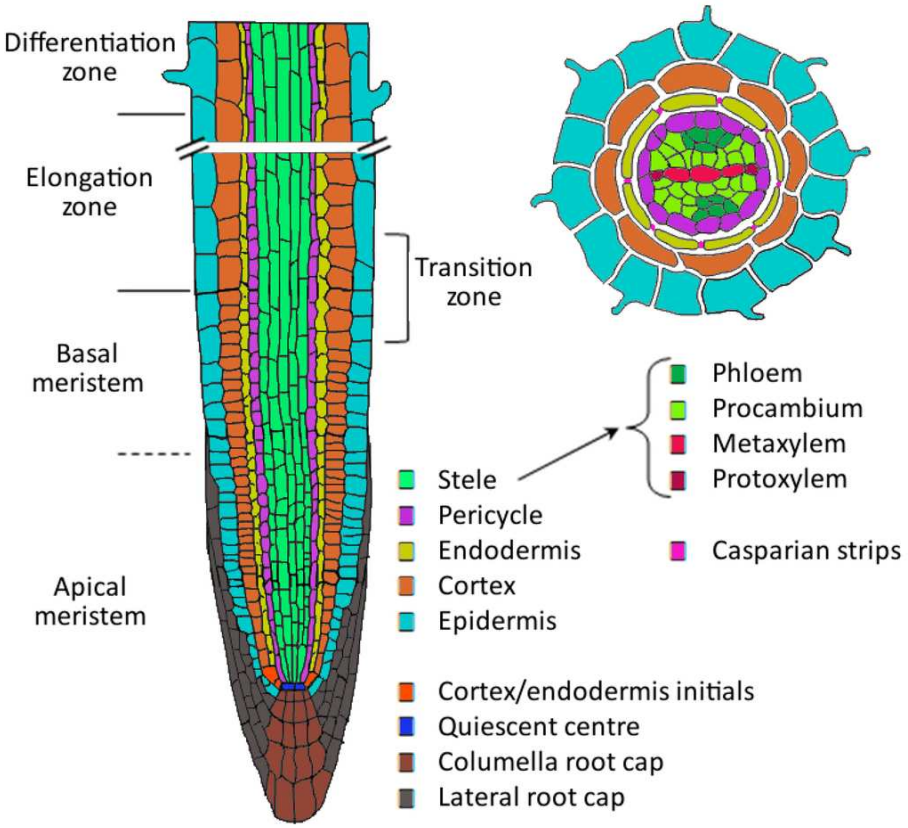

Fig. 4: Scheme of the root zonation (De Smet et al., 2015)

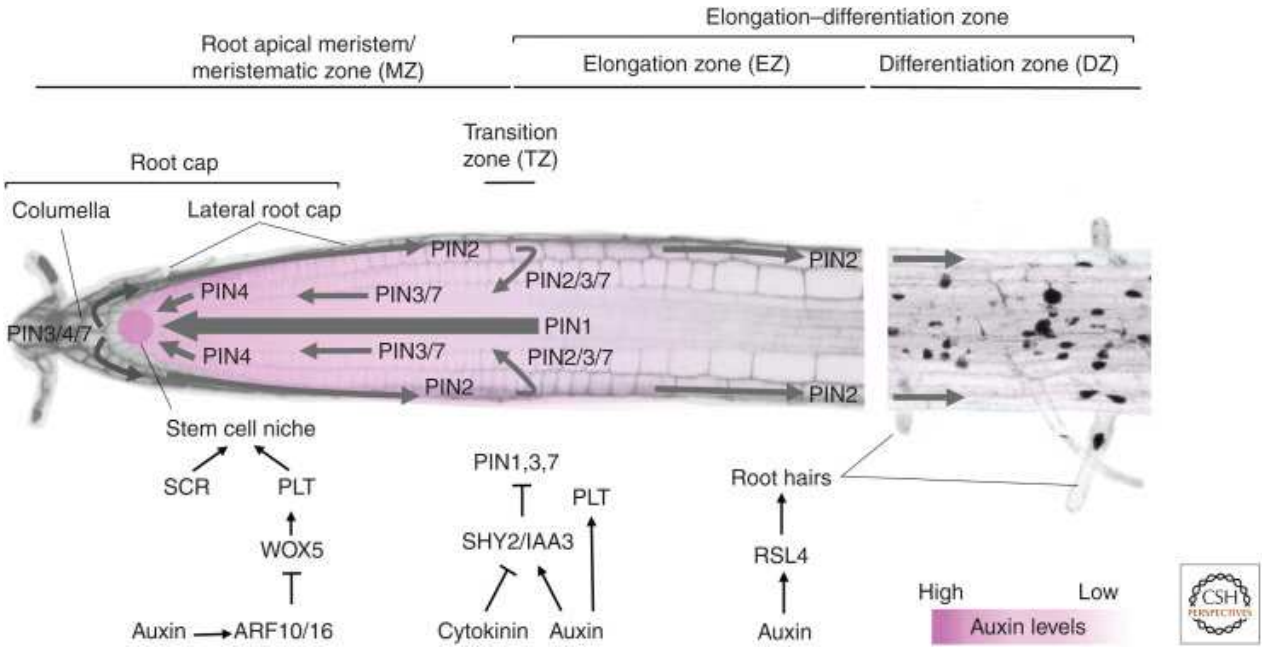

Fig. 5: Auxin levels and its distribution in context of the root development and zonation (Roychoudhry and Kepinski, 2021)

In dicotyledons, primary roots branch through the formation of lateral roots (LR) (Fig. 6). The main function of LRs is to enlarge the volume of the accessible soil. In case of *Arabidopsis thaliana*, these roots are initiated from the cells of the pericycle adjacent to the xylem pole cells. Origin of LR begins with a lateral root primordium (LRP) formation, initiated from a single pericycle foundation cell in the xylem pole (Torres-Martínez et al., 2020, 2019; Von Wangenheim et al., 2016).

The sites, where the primordia are initiated, are determined by an auxin accumulation enhancing cell division. This process begins with a single pericycle founder cell, whose division is triggered by a local auxin maximum. Subsequently, this cell recruits its neighboring pericycle cells for the primordium formation (Vermeer et al., 2014).

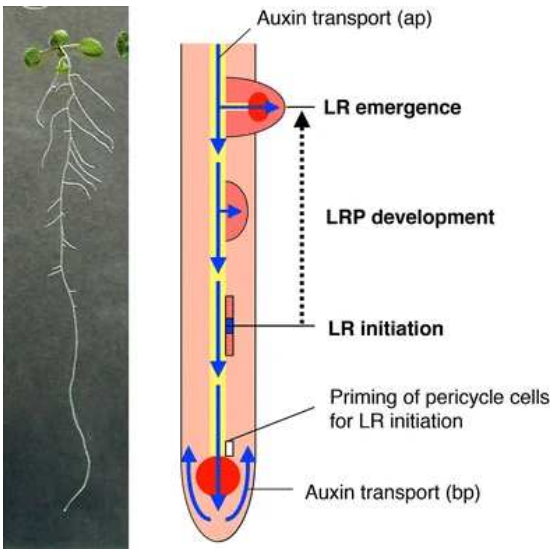

On the other hand, the emergence of LR is dependent on acropetal auxin distribution. Endogenous signals influence localization of PIN proteins, which leads to directional flow of auxin towards the tip of developing primordium, promoting growth of the lateral root (Fig. 7) (Benková et al., 2003; Wu et al., 2007).

Fig. 6: Lateral roots and their initiation in *Arabidopsis thaliana*, (Fukaki and Tasaka, 2009)

There were various mutants in auxin signalization or distribution reported to exhibit lower numbers of LRs in comparison to control. One of the important mechanisms is the endomembrane trafficking system which regulates PIN recycling to PM (Okumura et al., 2013).

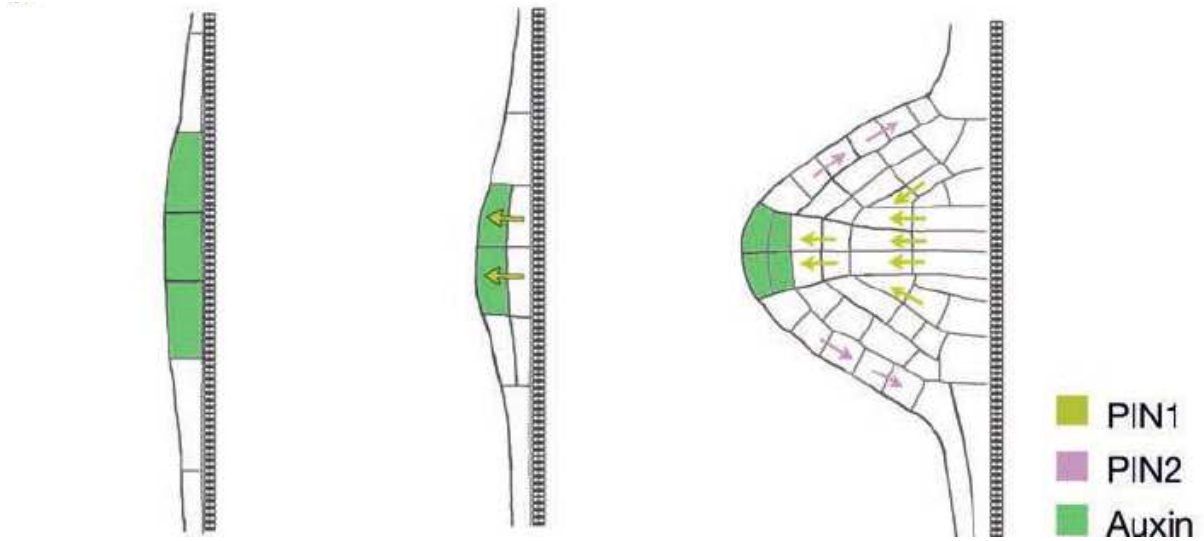

Fig. 7: Scheme of PIN-mediated auxin distribution in the context of LRP development (Tanaka et al., 2006)

1.5 Auxin-related processes

1.5.1 Root waving and skewing

When *Arabidopsis* seedlings are cultivated on the surface of the agar medium, roots exhibit a sinusoid pattern called waving, which occurs due to many different factors. A model potentially explaining this phenomenon describes waving as a result of gravity sensing, mechanosensitive reaction and circumnutation. A root naturally exhibits spiral growth, which enables it to penetrate into the substrate, simultaneously the root tip grows towards gravity vector and gets in touch with the medium, which leads to the thigmotropic response. Combination of all processes mentioned leads to the sinusoid root phenotype on the surface of the medium (Roy and Bassham, 2014). A part of the wave-forming phenotype mechanism is auxin-dependent and disruption in auxin transport leads to visible phenotype in the context of waving. Auxin influx carriers *pgp1pgp19* double mutant (Fig. 2) exhibits a strong phenotype in context of the root waving (Blakeslee et al., 2007), as well as a mutant in WAG1 and WAG2, kinases closely related to PID, PIN-phosphoryltaing kinases: *wag1/wag2* double mutant display strong wavy patterns of the primary root on inclined plates (Fig. 8) (Santner and Watson, 2006).

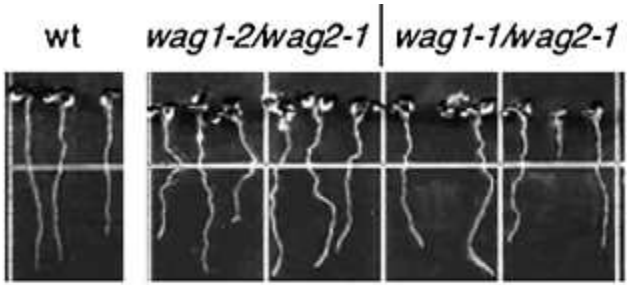

Fig. 8: Phenotype of double *wag* mutants compared to Col-0 (wt). Roots of *wag* mutant seedlings exhibit waved phenotype (plants grown vertical plates, tilted on 100 ° from the 3rd day, depicted by the white line), (Santner and Watson, 2006)

Root of a seedling growing vertically on the medium surface is usually skewed to the left side according to the vertical axes (Fig. 9) (Rutherford and Masson,

1996). One of potential explanations of this phenomena is epidermal cell file rotation, which is supported by observing right-handed growth in case of mutants slanting towards the right. But there are other mechanisms that can take place instead and influence this root deflection. Although skewing is closely related to waving, the origin of both of these processes seems independent (Oliva and Dunand, 2007; Schultz et al., 2017).

Skewing occurs even in microgravity conditions, indicating that it is not dependent on gravitropic response. Skewing is affected by proteins interacting with microtubules and remodeling of microtubules leads to differences in root skewing. Auxin in this process acts on skewing through TARGET OF RAPAMYCIN (TOR) kinase involved in cytoskeleton remodeling (Califar et al., 2020).

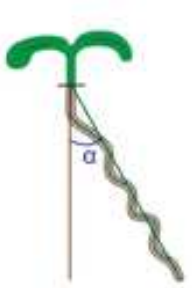

Fig. 9: Scheme of the root skewed according to the vertical axes, (Villaecija-Aguilar et al., 2019)

1.5.2 Gravitropic response

Plants exhibit growth movements called tropisms as a reaction to different stimuli. Gravity represents an environmental factor determining plant growth orientation in space. Unlike other factors, the gravity vector remains stable and plants have their mechanism of perceiving it. Although gravity is perceived in columella cells, the gravitropic movement is happening in the cells of the elongation zone (EZ) (Band et al., 2012; Blancaflor et al., 1998). As was mentioned above, nanomolar concentrations of auxin inhibit cell elongation. Gravitropic stimulation promotes reorientation of the auxin transport to the lower part of the root. As a result, growth of cell files on the bottom side is inhibited, while the growth of upper cell files is not. It leads to the asymmetrical growth of the whole organ (Moritaka Nakamura, 2019). PIN auxin efflux

carriers are important for redirecting the flow of auxin towards the lower part of the root (Fig. 10). Their activity is controlled by phosphorylation mediated by kinases as PID, WAG1 and WAG2 or the family of serine/threonine AGC kinases (Barbosa et al., 2014; Sato et al., 2015; Su et al., 2017).

Several processes were reported to accompany the gravitropic response. As one of the first reactions to the gravitropic stimulus, influx of Ca^{2+} to the cytoplasm of columella cells was described. Interestingly, Ca^{2+} influx after gravitropic stimulation was observed even in the case of starch-less mutants, however, it seems that starch grains are required for optimal reaction (Caspar and Pickard, 1989; Li et al., 2024). Reaction of TZ and EZ to the incoming auxin is also accompanied by Ca^{2+} influx. Complexity of the signal transduction was not fully explained yet (Kulich et al., 2024; Serre et al., 2023; Shih et al., 2015).

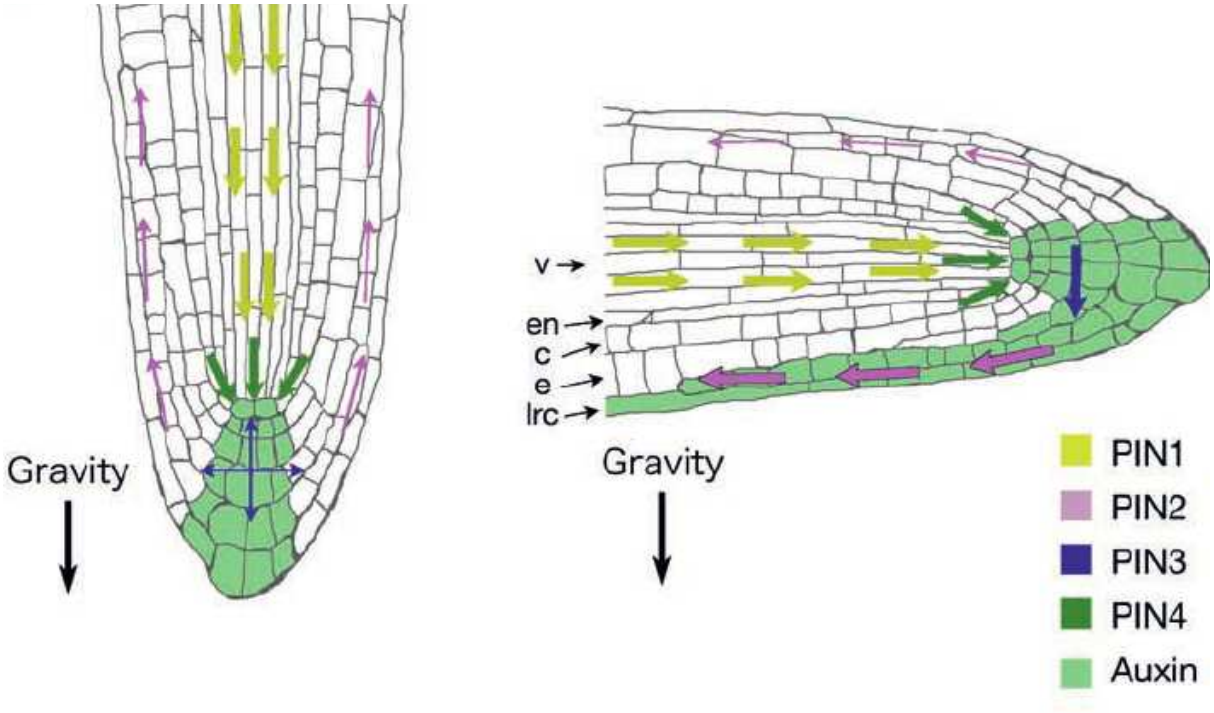

Fig. 10: Distribution of auxin in root tip following gravitropic stimulation, (Tanaka et al., 2006)

In *Arabidopsis*, both canonical and rapid auxin responses are required for bending of the root towards the gravity stimulus and mutation in their participating components exhibits defects in gravitropic response. Rapid response controls mainly the initial steps (its main player *afb1* mutant is defective in the early stages of gravitropic response, yet the bending occurs eventually) (Fig. 11) (Dubey et al., 2023). The TIR1/AFB pathway takes over later on. *AXR3-1* (the dominant mutant in the IAA17 repressor of ARF) interferes with the transcriptional pathway. Upon inducible overexpression, roots become agravitropic despite their rapid response remains unaffected (Fig. 12) (Kubalová et al., 2023).

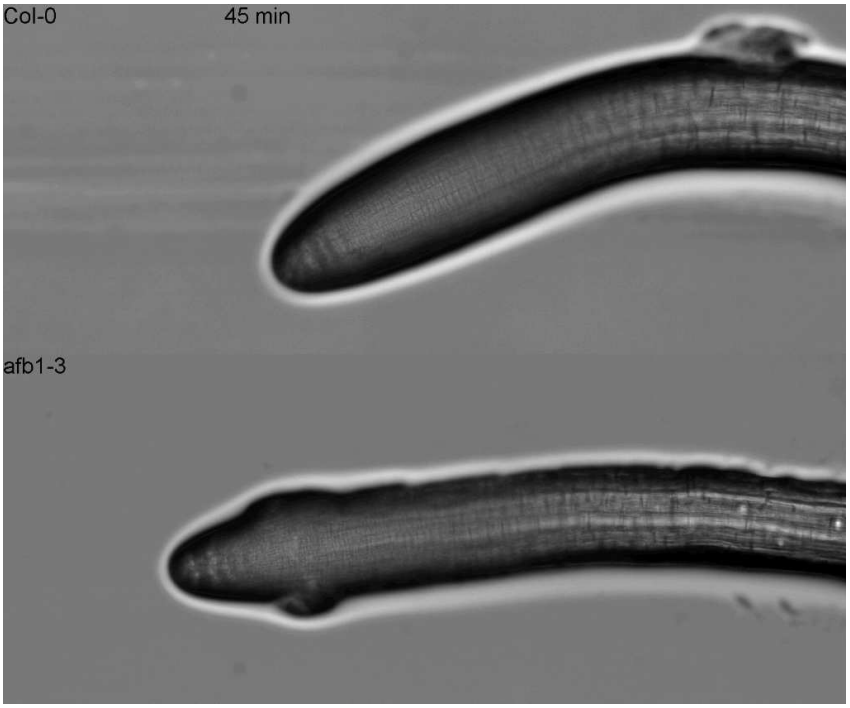

Fig. 11: Comparison of gravitropic bending in 45 minutes after gravistimulation in Col-0 (upper) and *afb1-3* (bottom) (Dubey et al., 2023)

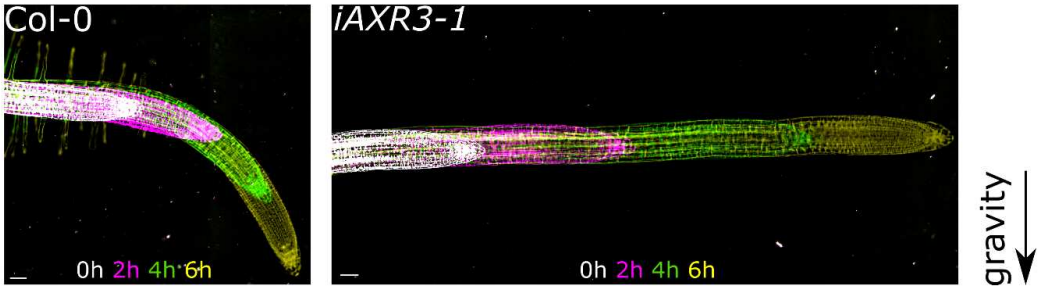

Fig. 12: Comparison of the gravitropic response of Col-0 (left) and *iAXR3-1* (right). (Kubalová et al., 2023)

Importance of the polar auxin transport in the gravitropic response could be illustrated by the phenotypes of its mutant. Gravitropic response in *pgp1pgp19* double mutant remains conserved, while *pin2* mutant is agravitropic (Fig. 2) (Blakeslee et al., 2007).

1.6 Auxin role in protein phosphorylation

Phosphorylation was identified as a mechanism potentially participating in the rapid auxin response. Phosphorylation is an enzymatically mediated modification of protein activity without a need of *de-novo* protein synthesis and is distributed widespread among eukaryotes (Jin and Pawson, 2012). Auxin-dependent phosphorylation was reported for many proteins including SORTING NEXIN 1 (SNX) involved in endomembrane trafficking (Zhang et al., 2013). H^+-ATPase (*AHA1*) is phosphorylated by the TMK1 receptor and controls apoplast acidification (Lin et al., 2021). Finally, it was shown that exogenous application of IAA triggers a substantial and ultra-rapid phosphorylation of many proteins, and this response was present in *Arabidopsis thaliana*, *Marchantia polymorpha* and *Klebsormidium nitens* (Kuhn et al., 2024a). As the TIR1 and AFB1 receptors are not present in algae, there has to be another mechanism steering the phosphorylation response. The PhLP2 protein has been discovered as one of the proteins the phosphorylation of which

reacts to application of auxin and auxin analogs (Han et al., 2021a; Kuhn et al., 2022).

1.7 PhLP2 and phosducin family

Based on revealed phosphorylation changes in a short time after IAA application, previously uncharacterized PhLP2 was selected as a potential candidate participating in rapid auxin response (Han et al., 2021a).

PhLP2 belongs to the phosducin family, which is a group of cytosolic proteins found in all eukaryotes. These proteins contain helical N-terminal domain and thioredoxin C-terminal domain. The helical domain was observed to interact with βγ subunits of the heterotrimeric G-protein complex (described below). The thioredoxin domain contains the Cys-X-X-Cys motif in the active site and possesses a disulfide oxidoreductase activity. The Cysteine residues are important for disulfide bonds disconnection in oxidized substrates. Thioredoxins in plants participate in multiple processes like membrane transport, hormone metabolism, photorespiration or adenosine triphosphate (ATP) synthesis (Collet and Messens, 2010).

Phosducins are evolutionary conserved and branch into three monophyletic groups, phosducin-I, phosducin-II and phosducin-III (Fig. 13). Known mechanisms of phosducin function slightly differ among groups mentioned (Blaauw, 2003).

In general, phosducins are so far better studied in animal systems. In human, phosducin I occurs within various tissues including retina, where it participates in visual sight transduction (Lee et al., 1990; Reig et al., 1990).

In the yeast two hybrid (Y2H), interaction with CYTOSOLIC CHAPERONIN COMPLEX (CCT) (also known as T-complex protein ring complex; TRiC) was reported for PhLP1 and this protein was shown to participate in a proper cytoskeleton components folding (Castellano and Sablowski, 2008).

Human phosducin-like 2 (PDCL2) is expressed in both male and female reproductive tissues and also was identified as related to CCT (Li et al., 2022). So far, there is very little known about phosducins in plants. *Arabidopsis thaliana* encodes two functionally redundant proteins from the group III; PhLP3a and PhLP3b (Castellano and Sablowski, 2008; De Mendoza et al., 2014). It was shown that these proteins are necessary for proper microtubule folding and their double knock-down mutant exhibits defects in various microtubule-dependent processes, such as mitotic spindle formation or cell wall structure. PhLP3 knock-down mutant in *Caenorhabditis elegans* exhibited a slower growth and even embryonic lethality due to defects in microtubule organization (Castellano and Sablowski, 2008). PhLP2 (Fig. 17) was recently identified as the third known protein from phosducin family present in *Arabidopsis thaliana*, moreover, it is the sole representative from the second clade (Blaauw, 2003; Roosjen et al., 2022). According to the G-protein signaling interactome in *Arabidopsis thaliana*, the second group of phosducins might be involved in the heterotrimeric G-protein signaling in context of proper subunit folding (Humrich et al., 2005; Lukov et al., 2005).

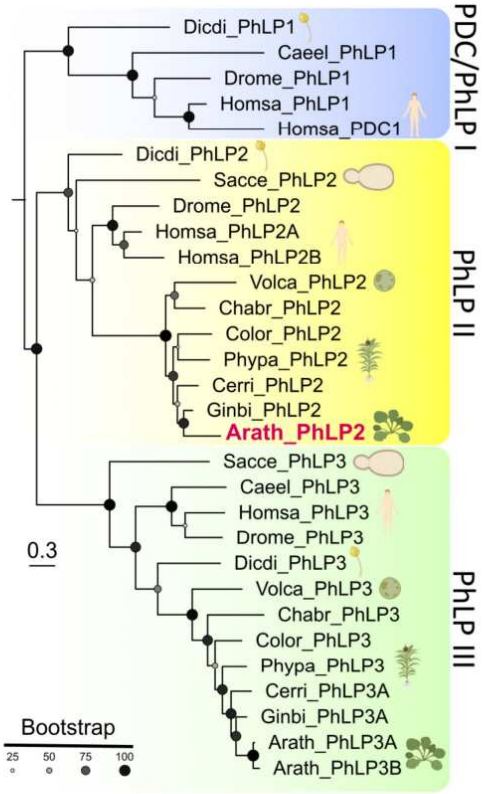

Fig. 13: Phylogenetic tree of phosducin family divided into three monophyletic clades, created by David Ušák

1.8 Heterotrimeric G-protein signalization

Signaling mediated by G-proteins is one of the most common mechanisms of signal transduction among eukaryotes and mediates communication between intercellular and extracellular environments. The G-protein complex itself consists of three subunits, which are able to associate and dissociate: α-subunit containing domain with a GTPase activity and a dimer of β and γ subunits, which binds to the α-subunit in its inactive state to form the heterotrimeric complex. The signaling activity is regulated by a coupled transmembrane receptor (Fig. 14). There are differences between signaling in plant and animal cells, but some processes are similar. The transmembrane receptor is activated by a ligand from outside of the cell, and the subsequent conformational changes lead to activation of G-proteins via exchange of guanine di/triphosphate (GDP to GTP) in α-subunit, which then dissociates from the complex and releases the β/γ dimer. Both α and β/γ subunits are able to transduce the signal to downstream effectors. Inactivation is mediated by a hydrolysis of GTP associated with the α-subunit and re-association of the complex (De Mendoza et al., 2014).

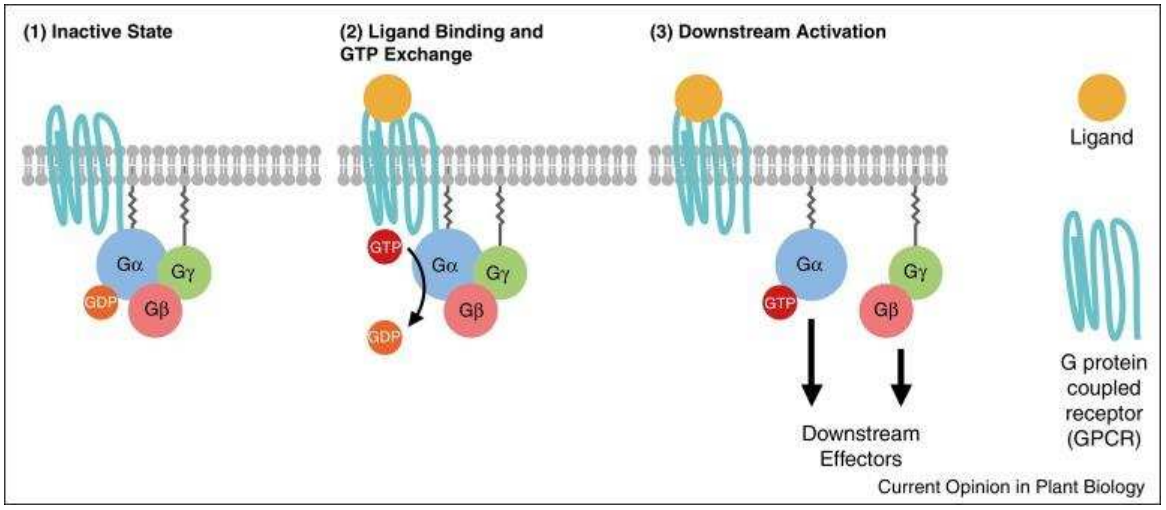

Fig. 14: Heterotrimeric G-protein signaling, animal model (Stateczny et al., 2016)

1.8.1 Plant G-protein signalization

In plants, activation of the α-subunit through GDP → GTP exchange can happen spontaneously without the help of a coupled receptor. In other words, plant α-subunits are capable of self-activation and are constitutively active without additional regulation. REGULATOR OF G-PROTEIN SIGNALING 1 (RGS1) is a known GTPase activating protein in animals acting as a negative regulator of G-protein signaling and its function is also conserved in plants, moreover, this regulator was shown to participate in the sugar signaling. In the presence of glucose (as its signaling molecule), RGS1 is phosphorylated by the receptor like kinase WITH NO LYSINE KINASE 8 (WINK8) and undergoes endocytosis (unlike in animals, plant RGS1 is a transmembrane protein), which leads to the exchange of GDP for GTP on the α-subunit and downstream signaling (Oliveira et al., 2022; Stateczny et al., 2016).

There were reported several phenotype characteristics in connection to G-protein signaling disruption. For example, the G-protein complex affects a sensitivity to auxin towards cell division, including LRP formation. (Ullah et al., 2003).

1.8.2 Phosducin in G-protein signalization

Interactions of the phosducin family with other structures are better studied in animals than in plants. For instance, PhLP1 was in humans identified as a potential co-chaperon for proper Gβ-subunit complex folding via interacting with CCT (Humrich et al., 2005; Lukov et al., 2005; Stirling et al., 2007; S. Wang et al., 2023). This complex consists of various subunits forming a barrel-shaped structure, where unfolded proteins can enter. Each subunit exhibits an ATP-ase activity, thus initiates conformation changes in target protein, which is subsequently released and able to interact with its binding partners. CCT is predicted to mediate folding up to 10 % of cytosolic proteins,

including the Gβ. Participation of PhLP1 in Gβ folding was proven *in vivo* in mice - deletion of PhLP1 in photoreceptor cones, rods and striatal neurons lead to decreased levels of Gβγ and $G\beta_5$-RGS complexes and defects in G-protein signaling (S. Wang et al., 2023). Nevertheless, some phosducins regulate stability and activity of G-protein subunits directly, such as MAU-8, a PhLP from *C. elegans*, which binds Gβ through its C-terminus. This interaction is modulated by de/phosphorylation of the PhLP (Lacoste et al., 2006).

Interestingly, *Arabidopsis* PhLP2 was shown to interact with RGS1 and some of its interactors in a Y2H. (Klopffleisch et al., 2011).

Based on information gained, PhLP2 function in *Arabidopsis* could be related to multiple processes including protein folding, heterotrimeric G-protein signaling or processes related to auxin.

2. Methods

2.1 Medium and treatments used

½ Murashige Skoog medium (½ MS) - salt mixture (Duchefa) -2.15 g/l, MES (MES.H2O) - 0.5 g/l, pH 5,8 adjusted with KOH; 1% sucrose, 1% agar (Duchefa plant agar)

Arabidopsis pollen germination medium - 0,01 % H_3BO_3, 5mM $CaCl_2$, 1mM $MgSO_4$, 5nM KCl, pH 7,5 adjusted with KOH; 10 % sucrose, 1,5 % (low melting point) agarose (Sigma-Aldrich)

IAA treatment medium - IAA (Sigma-Aldrich) in stock solution (10µM concentration in 96% EtOH). From the stock, 35 µl (for 10nM concentration) or 175 µl (for 50nM concentration) was diluted in 35 ml ½ MS medium

Floral dip medium - 100 g sucrose, 500 µl silwet, fill up with dH_2O to 1000 ml

½ MS glufosinate ammonium, phosphinothricin (BASTA) - 15 µg/ml of BASTA in ½ MS medium (described above) (Cayman chemical)

LB (Luria-Bertani) medium - 4 g peptone, 4 g yeast extract, 4 g NaCl, 6,4 g KOBE agar /Roth/, 400 ml distilled water

SOC medium - 20 g peptone, 5 g yeast extract, 0,58 g NaCl, 0,19 g KCl, 10 ml 1M MgCl2, 10 ml MgSO4, water to total volume of 1 l, pH= 6-7 (adjusted with NaOH) + 10 ml 20% (w/v) glucose solution

YEB medium - 5 g beef extract, 1 g yeast extract, 5 g peptone, 5 g sucrose, 300 mg $MgSO_4$, fill up to 1000 ml with dH_2O, 20 g agar, pH = 7,2

Electrophoresis gel - 1% agarose (peqGOLD, Universal agarose, VWR), 0,5x TAE buffer, 1.5% GelRed (GelRedTM Nucleic Acid Gel Stains, Biotium)

2.2 Plant material

The following *Arabidopsis thaliana* transgenic lines were used (Table 1), all were in the Columbia-0 background (*NASC ID N70000*).

Line	Note
35S::RNAi *PhLP2*	Created by Denisa Oulehlová, David Ušák
pPhLP2::PhLP2-NLS-mCherry	Created by Veronika Poláková
pPhLP2::PhLP2-mScarlet	Created by Denisa Oulehlová, David Ušák
pPhLP2::PhLP2-mEGFP	Created by Denisa Oulehlová, David Ušák

Table 1: Transgenic lines used for following experiments

2.2.1 Growth conditions

For *in vitro* experiments, plants were cultivated in the growth room with long day light conditions (16/8 hours) at 22 °C and light intensity approx. 100 µmol m^{-2} sec^{-1}. Seedlings were grown on plates containing ½ MS medium in vertical position (unless otherwise specified). Before transferring plants to the cultivation room, plates were stratified for 1-4 days at 4 °C in constant darkness. Plants cultivated in pots containing Jiffy pellets were placed in the cultivation room with an automatic water irrigation system and the same light conditions as in case of previously described cultivation room.

2.2.2 Sterilization of seeds

Harvested seeds were placed into 2 ml tubes, each line separately. Opened tubes were left in a glass desiccator containing a solution of 50 ml household bleach (Savo) and 1,5 ml 37% HCl. The desiccator was closed and approximately after 90 minutes in conditions of evaporating chlorine gas, tubes were closed, removed and transferred to the laminar flow hood for 30 minutes to get rid of chlorine gas.

2.3 Molecular cloning

To obtain transcriptional fusion of PhLP2, the promoter-containing region was cloned. Cloning was designed using a web tool Goldenbraid (GB) (Sarrion-Perdigones et al., 2013, https://gbcloning.upv.es/). For that procedure, two types of restriction enzymes were used: BsaI and BsmBI. Geneious Prime 2019 2.3 software (https://www.geneious.com/) was used for the *in silico* assembly of the construct. Cloning procedure is depicted in Fig. 16.

The cloning procedure consists of following steps:

1. Creation of a particular GB-part (Fig. 15)
2. Creation of α-plasmid (Alpha) level transcription unit
3. Creation of Ω-plasmid (Omega1) level transcription unit

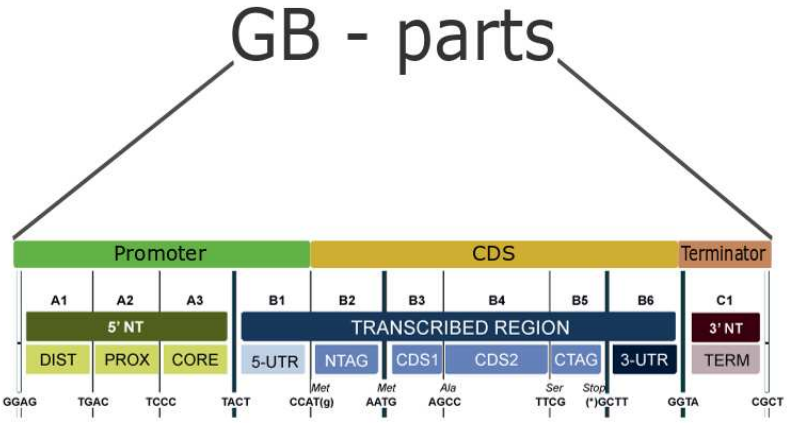

Fig. 15: Scheme of the GB-part composite

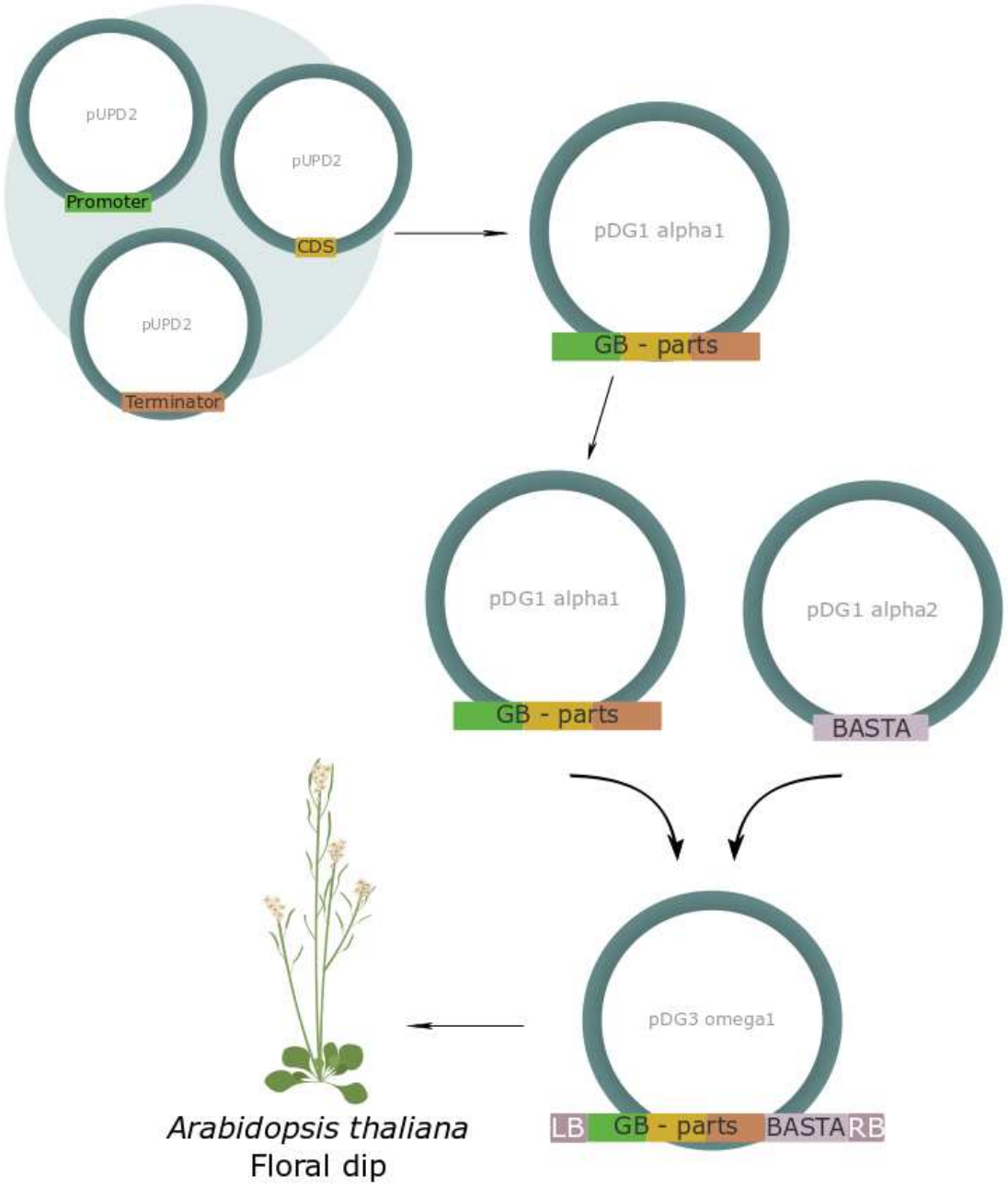

Fig. 16: Scheme of the GB cloning system. The domestication provides the pUPD2 containing a GB-components, which can be subsequently combined into a pDG1alpha1 vector. This vector can be later ligated together with pDG1 alpha2 carrying BASTA resistance into the destination vector (omega1), which is suitable for transformation of *Arabidopsis thaliana.*

2.3.1 Golden Braid components

GB-part	Forward	Reverse
PhLP2 promoter	GCGCCGTCTCGCTCGGGAGCAGCTCCGATCATCTTCGAT	GCGCCGTCTCGCTCAATGGCAAAGTATAACCACCTACGAAG

Table 2: Primers used for PhLP2 promoter, forward and reverse

Position	GB-part	Description	Reference
A1	Promoter	pPhLP2; AT5G14240	Denisa Oulehlová
A2			
B1			
B2	SV40 NLS	Nuclear localization signal	Tomáš Moravec
B3	mCherry	mCherry fluorescent protein sequence	Eva Medvecká
B4			
B5	STOP codon		
B6	Terminator	Ubiquitine terminator-pubq3	Nelson Serre
C1			
Vector backbone	pUPD2	Domestication vector, Chloramphenicol bacterial resistance	Tomáš Moravec

Table 3: GB-individual parts used for cloning of pPhLP2::NLS-mCherry

Position	GB-part	Description	Reference
A1	Promoter	pPhLP2; AT5G14240	Denisa Oulehlová
A2			
B1			
B2	Exon	Exon 1 from AT5G14240	David Ušák
B3			David Ušák
B4	MSPi	Intron	David Ušák
B5	Exon (as)	Antisense orientation according to B3-B4	David Ušák
B6	Terminator	Ubiquitine terminator-pubq3	Nelson Serre
C1			
Vector backbone	pUPD2	Domestication vector, Chloramphenicol bacterial resistance	Tomáš Moravec

Table 4: GB-individual part used for the cloning of pPhLP2::RNAi *PhLP2*

Primers used for the PhLP2 promoter can be found in Table 2. Particular GB parts for pPhLP2::NLS-mCherry (Table 3) and pPhLP2::RNAi *PhLP2* (Table 4) were available in the laboratory collection. Components for PCR reaction are listed in Table 5 and conditions are listed in Table 6. Amplified DNA was checked using TAE electrophoresis and purified using pJET purification kit THERMO SCIENTIFIC GeneJET Plasmid Miniprep Kit.

PCR component	Amount
5x0,5 Q5 buffer	10 µl
dNTP	1 µl
primer forward	0,25 µl
primer reverse	0,25 µl
DNA (20x Scar as a template)	1 µl
G5E	0,5 µl
H_2O	37 µl

Table 5: Components for PCR reaction used for preparation individual GB-part

Step	Temperature (°C)	Duration (s)	Repeats
1. initial denaturation	98	30	1
2. denaturation	98	5	-
3. annealing	60	15	-
4. extension	72	15	go to step 2, 35x
5. final extension	72	300	1

Table 6: The conditions of PCR reactions

2.3.2 Domestication with the pUPD2 vector

In this step, DNA was ligated with the pUPD2 vector containing chloramphenicol (CAM) resistance using components listed in Table 7. The thermal cycler Biometra TOne by Analytik Jena was used for ligation and the procedure was performed under conditions listed in Table 8.

Component	Amount
pUPD2 vector	75 ng
PCR product	40 ng
T4 DNA ligase (3U/µl, NEB)	1 µl
buffer for ligase (10x, NEB)	1 µl
BsmBI (10U/µl, Thermo Fisher)	1 µl
dH_2O	fill up to 10 µl

Table 7: Domestication with pUPD2 vector

Step	Temperature (°C)	Duration (s)	Repeats
1	37	120	25 (alternating 1st and 2nd step)
2	16	300	
3	16	-	

Table 8: The conditions of ligation

2.3.3 Alpha-plasmid level

For creation of α-plasmid level, components listed in Table 9 were used. Procedure followed the steps as are described in Domestication with pUPD2 vector.

Component	Amount
PhLP2 promoter	75 ng
pDGB1 alpha 1	75 ng
NLS; SV40 nuclear localization signal	75 ng
mCherryB3B4-pUPD2	75 ng
STOP codon	75 ng

ubiquitin Terminator-pubq3	75 ng
T4 DNA ligase (NEB)	1 µl
buffer for ligase (NEB)	1 µl
BsaI enzyme (NEB)	1 µl
distilled water	fill to 10 µl

Table 9: Ligation with pDG1 alpha vector

Plasmid was verified using a restriction reaction (components listed in Table 10).

Components were incubated in the tube for 1 hour at 37 °C. Electrophoresis was used for visualization of the fragment length, the result was subsequently compared to the predicted values to verify plasmid accuracy.

Component	**Amount**
DNA	1,5 µl
Restriction enzyme (NEB)	0,1 µl
buffer (10x CutSmart, NEB)	1 µl
dH_2O	filled up to 10 µl

Table 10: Components for the restriction reaction

Then, the sample was also verified using Sanger sequencing (Eurofins Genomics).

A verified plasmid was later transformed into *E.coli* cells using components listed in Table 11. *E.coli* competent cells (TOP10 strain) were melted on ice for 10 minutes. After that, they were carefully mixed with 1 µl of the ligation mixture. The sample was kept on ice for 30 minutes. After that, the heat shock was applied (42 °C for 30 seconds) and the cells were returned to ice for 5 minutes. Room temperature SOC medium was added to the mixture and the

cells were incubated at 37 °C for 45 minutes while shaking (250 rpm). 2% X-β-Gal (5-Bromo-4-chloro-3-indoxyl-beta-D-galactopyranoside; Biosynth) was spreaded on the surface of solid LB medium containing chloramphenicol (c = 50 µl/ml). Bacterial suspension was applied on the prepared stiff medium. Sample was cultivated overnight at 37 °C.

Component	Amount
5 α *E. coli* (NEB)	10 µl
DNA	100 ng
SOC	190 µl
2% X-β-Gal	50 µl

Table 11: Components used for the transformation to *E.coli* competent cells

Transformed colonies were selected according to a blue / white selection. A couple of independent white colonies were inoculated into 3 ml of a liquid LB medium and incubated overnight at 37 °C while shaking (250 rpm).
The next day, DNA was isolated using the THERMO SCIENTIFIC pJET Plasmid Purification Kit containing GeneJet. Procedure was followed according to manufacturer instructions.

2.3.4 Omega-plasmid level

Transformed colonies were selected on Spectinomycin (50 µl/ml) and X-gal containing LB plates and the subsequent verification was performed the same way as in the case of the alpha level-transformation with necessities listed in Table 12 used.

Component	Amount
pDGl alpha 1 transcriptional unit	75 ng
pDG3 omega 1 vector	75 ng
pDG1 alpha 2 vector with BASTA resistance cassette	75 ng
BsmBI enzyme (NEB, 10U/µl)	1 µl
T4 DNA ligase (NEB, 3U/µl)	1 µl
buffer for ligase (10x concentrated, NEB)	1 µl
dH_2O	filled up to 10 µl

Table 12: Components used for the cloning with omega plasmid level

Plasmids were verified using a restriction reaction and sequencing (as described above).

2.3.5 Transformation to *Agrobacterium tumefaciens*

Components used for transformation of *Agrobacterium tumefaciens* are listed and specified in Table 13. Bacterie were thawed on ice and mixed with DNA obtained in the previous step. Sample was transferred to the electroporation cuvette and DNA transformation was performed using electroporation (Eppendorf Eporator 4309) approximately 5 µs at 2 200 V. Then, 200 µl YEB was added to the cuvette for easier removal. Content was transferred to the falcon tube containing the rest of LB medium. Bacteria were cultivated for 2 hours at 28 °C while shaking at 225 rpm. 40 µl of the mixture was spread on the solid LB medium. Plates were cultivated for 2 days at 28 °C.

Component	Amount
DNA Omega-plasmid level	3 µl
YEB medium	800 µl
Agrobacterium tumefaciens (GV 3101)	50 µl
LB containing SPEC, GEN, RIF	200 µl
• Spectinomycin (SPEC)	10 µl/ml
• Gentamicin (GEN)	50 µl/ml
• Rifampicin (RIF)	25 µl/ml

Table 13: Components and their amount used for transformation to *Agrobacterium tumefaciens*

2.3.6 Stable transformation to *Arabidopsis thaliana*

Stable *Arabidopsis thaliana* lines were obtained performing floral dip transformation (Clough and Bent, 1998). Necessities used are stated in Table 14 and procedure was performed via following steps: Colony of *Agrobacterium tumefaciens* carrying desired construct was propagated in a 1 ml liquid LB medium and cultivated at 28 °C while shaking (250 rpm). After 6 hours, 10 ml of LB medium was added and the culture was incubated overnight. Siliques from *Arabidopsis thaliana ecotype Col-0 (NASC ID: N70000)* plants at a flowering stage were removed to reduce the number of seeds not carrying the mutation. Floral dip medium was added to the LB medium containing transformed *Agrobacterium*. Each plant was dipped into the bacterial mixture for approximately 30 seconds. Plants were stored overnight in dark conditions. The next day, plants were transferred to the cultivation room. Seeds were harvested after approximately 3 weeks of cultivation.

Component	Amount
LB medium	11 ml
Transformed *A. tumefaciens* colonies	-
Arabidopsis thaliana Col-0, flowering	3 individuals
Floral dip medium	40 ml

Table 14: Components used for stable transformation to *Arabidopsis thaliana*

2.4 Selection of transgenic plants

T1 seeds of *Arabidopsis thaliana* containing plasmid construct were sterilized the way described above and after that transferred on vertical plates with ½ MS medium containing the BASTA selection. After 7 days, resistant (visibly viable and thriving plants) were selected for further microscopy analysis. Several independent primary transformants with the fluorescent signal were further propagated in Jiffy pellets to obtain T2 generation seeds. This process was repeated to obtain next generations.

2.5 Data acquisition and analysis

2.5.1 Scanning

Images were acquired using a scanner EPSON perfection V37/V370 and EPSON perfection V700 photo. Plates with seedling growing on agar medium were placed vertically to the scanning area with black fabric as a background. Images were taken every 30 minutes during various hours (as specified for each experiment), controlled by an AutoIT script.

2.5.2 Microscopy

For microscopy measurement, vertical stage Zeiss Axio Observer 7 was used, coupled to a Yokogawa CSU-W1-T2 spinning disk confocal unit with 50 µm pinholes and equipped with a VS401 HOM1000 excitation light homogenizer

(Visitron Systems). Different objectives were used - EC Plan-Neofluar 5x/0.16 M27 (FWD=18.5mm), Plan-Apochromat 10x/0.45 M27 (FWD=2.1mm), Plan-Apochromat 20x/0.8 M27 (FWD=0.55mm), LD LCI Plan-Apochromat 40x/1.2 Imm Corr DIC M27 for water or glycerine immersion (CG=0.15-0.19mm) (FWD=0.41mm at CG=0.17mm), 100x/1.46 Oil DIC M27 (FWD=0.10mm), (UV)VIS-IR. Images were acquired using the VisiView software (Visitron Systems). mScarlet and mCherry were excited by the laser 561 nm (emission 582 - 636 nm), mEGFF was excited by the laser 488 nm (excitation 500 - 550 nm). Signal was detected using a PRIME-95B Back-Illuminated sCMOS Camera (1200 x 1200 pixels; Photometrics).

2.6 Experiments setup

IAA-induced root growth inhibition

Seeds of Col-0 and RNAi *PhLP2* were cultivated on plates with ½ MS medium for 5 days in the conditions described above. Plates for treatment were prepared using an IAA treatment medium described above (IAA was no longer than 3 weeks old). Grown seedlings were transferred to three plates: ½ MS with 175 µl EtOH (mock), ½ MS with 10nM IAA and ½ MS with 50nM IAA. Growth of the roots was observed and captured via scanning in 30 min intervals during 12 h using the scanner.

Two images of each treatment were compared: the first one immediately after seedling transfer to the plates, the second one after 11,5 hours. The difference of the length of the roots (from the first image root tip to the second image root tip) describes the increment of the root in a certain time, as specified below.

Gravitropic response - long term

Plates with seedlings cultivated vertically for 5 days inside the agar medium were placed in the scanning area rotated by 90 °. From all images taken with the scanner, a time stack was created, containing 24 images with 30 minute

intervals. Root bending was measured using the ImageJ plugin Manual tracking (mentioned above, following the root tip in every single image of the time series). Data was processed using Excel.

Gravitropic response - short term

5-day old seedlings of Col-0 and RNAi *PhLP2* grown into ½ MS medium were used for this experiment. Plants were transferred from plate to microscopy chamber in the block of the medium and left for one hour in a vertical position to recover before they were rotated and the gravitropic response was followed. Images were captured using microscopic imaging with a 10x objective setup in brightfield in 5 minute intervals.

Phenotype observation on tilted plates

Seedlings were grown on the surface of 1⁄2 MS media in conditions described above. The first 2 days of cultivation plates were placed vertically in the cultivation room to prevent seedlings from growing inside the medium, after that, plates were tilted at 45 °. After 3 days, plates were scanned and immediately transferred back to the cultivation room. After another 4 days, the plates were scanned again. This setup was used for measuring VGI, the number of wave amplitudes and skewing, as specified below.

Root zonation measurement

1mM propidium iodide (PI) in ½ MS medium was spread into the circular Petri dish (35 mm in diameter). 8-day old seedlings were dipped in the dye and incubated in the dark for 10 minutes. After this time, seedlings were transferred to ½ MS agar block and placed in the microscopy chamber. Roots were observed using the vertical spinning disk microscope. This setup was used for root zonation determination and cell counting, as specified below.

Images were captured using microscopic imaging with a 20x objective setup excited by the laser 561 nm.

Lateral roots counting

10-day old seedlings of Col-0 and RNAi *PhLP2* were observed using microscopic imaging with a 20x objective setup in brightfield.

Pollen germination

Arabidopsis pollen germination medium was prepared into a 90 mm diameter Petri dish. Pollen of pPhLP2::PhLP2-GFP plants cultivated in long day (16 / 8 h) conditions in 22 °C was spread on the solid *Arabidopsis* pollen germination medium in the presence of a pistil and stigma to promote germination. The sample was incubated in the dark at root temperature for 2 hours and after that at 28 °C for additional 3,5 hours. Germinated pollen was transferred to the microscopy chamber directly on a piece of solid medium. This method was used for protein expression observation.

2.7. Measurement and calculations

2.7.1 Image analysis

Images obtained from either the scanner or the microscope were processed using software FIJI ImageJ (Schindelin et al., 2012).

Measuring structures in different time points was corrected in the context of shift between time points using ImageJ plugin Registration >> Correct 3D drift (used for correcting drift in time series captured using scanner or microscope; measurement of IAA-induced root growth inhibition and gravitropic response).

2.7.2 Experimental setup

IAA-induced root growth inhibition was measured using Plugins >> Segmentation >> Simple Neurite Tracer (SNT) (Arshadi et al., 2021). Images in the beginning and in the end of observation were overlaid and the difference in root length was measured using SNT.

To calculate root bending angle, measurement of the root tip position through a time-stack containing images in certain time intervals (specified in particular experiments in the chapter Methods, Experimental setup) was performed using ImageJ >> Analyze >> Measure. Coordinates obtained from measurement were processed using Excel for evaluating angle of the tip in every time point relative to initial root base-tip axis.

Vertical growth index (VGI) was calculated as a ratio of base-tip distance to root length measured (Grabov et al., 2005) using ImageJ >> Straight line or ImageJ >> Plugins >> Segmentation >> Simple Neurite Tracer (SNT) (Arshadi et al., 2021).

Amplitude number was counted manually. One amplitude was determined as a root deviating from vertical axes until the direction changes.

Skewing was measured using ImageJ >> Angle tool. Angle was established between root tip, root base and vertical axes.

Meristem length was measured using ImageJ >> Straight line from the tip to the border of the meristematic zone. Meristematic zone was determined as an area between the quiescent center and the last not elongating cell in the cell file.

Cell number was counted manually in one cell file in the area of the meristem (as described above).

Number of lateral roots was established manually.

2.7.3 Statistical analysis

Data processing and statistical analysis were done using Excel, R software (R v4.0.2 and RStudio v1.3.1073) or available online tools (https://www.graphpad.com/quickcalcs/ttest1/?format=C). Plots were created using R software or Google Collab.

3. Results

3.1 Metaanalysis of available data for PhLP2

Currently, there is very little experimental data about phosducins in plants. Therefore, for primary research, I summarized known information and analyzed data obtained from publicly available databases to assume the possible function of PhLP2 based on information acquired.

3.1.1 PhLP2 phosphorylation is regulated by auxin

Based on previous research, the protein phosphorylation was found as a common post-translational modification in protein function, which is energetically more advantageous than *de novo* synthesis (Han et al., 2021a). There were several analyses mentioning phosphorylation changes in PhLP2 related to auxin in a short time, therefore PhLP2 was selected as a potential candidate participating in rapid auxin response. Also, phosphorylation changes were observed in mutants in rapid auxin response-related players: AFB1, TMK1 and ABP1 (Table 15). In Col-0, treatment with an auxin antagonist α-(2-oxo-2-phenylethyl)-1H-indole-3-acetic acid (PEO-IAA) led to high phosphorylation of PhLP2. AFB1 is the main player in rapid auxin response and simultaneously inhibits the canonical pathway (Dubey et al., 2023). TMK1 mediates phosphorylation of H^+-ATPase and apoplast acidification. In the case of *afb1-3* and *tmk1-1* mutants, there was an increased phosphorylation of PhLP2 compared to Col-0 and also in the case of *abp1-TD1* mutant after 2 minute IAA treatment compared to *abp1-TD1* untreated. On the contrary, dephosphorylation of PhLP2 was reported in *abp1-TD1* untreated in comparison to Col-0 untreated (Kuhn et al., 2024a). Residue Ser255 in PhLP2 was shown as a phosphorylation changing site in all cases mentioned (Table 15).

Phosphorylation of PhLP2 in:	LOG2	x-LOG10 (FDR)	Position of phosphorylation	Reference
Col-0 treated with IAA compared to **Col-0 untreated**	2.969	2.048	255	(Han et al., 2021a)
Col-0 PEO compared to **Col-0 untreated**	3.501	3.458	255	(Han et al., 2021b)
afb1-3 compared to **Col-0**	0.283	1.610	255	(Kuhn et al., 2024a)
tmk1 compared to **Col-0**	0.781	2.319	255	(Kuhn et al., 2024a)
abp1-TD1 compared to **Col-0**	-0.55	1.415	255	(Kuhn et al., 2024a)
abp1-TD1 **treated with IAA after 2 minutes** compared to ***abp1-TD1 untreated***	0.917	1.774	255	(Kuhn et al., 2024a)

Table 15: Rate of phosphorylation of PhLP2 in different mutant backgrounds and conditions. Phosphorylation in green, dephosphorylation in red

3.1.2 Characterization of PhLP2 protein

I summarized available information and characteristics of the protein. Protein structure can be highly precisely predicted using AlphaFold (https://alphafold.ebi.ac.uk/), which is an AI system combinating bioinformatics and physical approach (Jumper et al., 2021). Based on the amino acid sequence, it is possible to obtain prediction of the 3D structure. The tool was used for estimation of evolutionary conserved domains, which could hint the protein function and figure out structural aspects of the interaction map.

PhLP2 was identified as a thioredoxin-domain containing protein, indicating disulfide oxidoreductase activity (Collet and Messens, 2010). Length of the protein is 256 amino acids and consists of 4 independent domains (AlphaFold,

https://alphafold.ebi.ac.uk/). The domains are estimated with different reliability. Domains 2 - 4 are predicted with higher confidence indicating more evolutionary conserved sequences in comparison to domain 1. De/phosphorylation was reported for Ser255 located in the C-terminal domain as a penultimate amino acid of the protein (Roosjen et al., 2022). Domain 3 (a core domain) contains the conserved thioredoxin active site Cys135 (Collet and Messens, 2010). Protein structure is depicted in Fig. 17.

In the context of subcellular localization, the highest confidence score of gene product was measured in the nucleus, cytoplasm and mitochondria (Hooper et al., 2017).

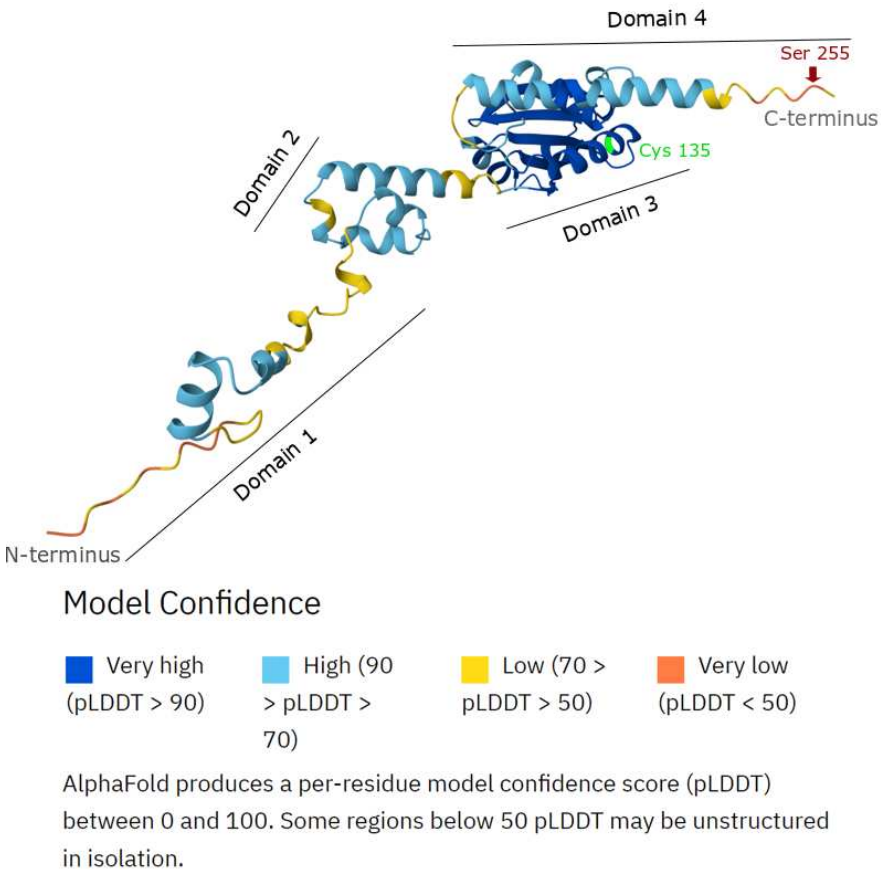

Fig. 17: Prediction of PhLP2 structure visualized using the AlphaFold (https://alphafold.ebi.ac.uk/) with phosphorylation site Ser255 and thioredoxin active site Cys135 labeled and complemented by the model of confidence

3.1.3 Expression of PhLP2 within *Arabidopsis thaliana*

I analyzed the PhLP2 expression data using publicly available databases. It was shown that PhLP2 is expressed in most tissues and developmental stages of the *Arabidopsis thaliana* plant. However, there are several interesting differences in the expression levels (https://bar.utoronto.ca/eplant/). The highest expression was observed in roots and mature pollen. In mature flowers, higher rate of expression was reported for stamen filaments and petals than opened anthers or carpel. *PhLP2* is also expressed in young and mature leaves and petioles (Fig. 18) (Klepikova et al., 2016). In the context of the root, the transcript is rather reported in the xylem pole of vasculature and endodermis; the highest rates were observed in meristematic and transition zones in comparison to elongation zone (Fig. 19) (Schmid et al., 2005) Expression occurs in all developmental stages, although the rate may differ through ontogenesis. PhLP2 expression in siliques was the highest in 3 days post anthesis and later in development, PhLP2 transcript level is gradually decreasing (Mizzotti et al., 2018). In seeds, the level of PhLP2 mRNA increases in time. The highest level of mRNA was measured in 24 hours after desiccated seeds-stratification in 4 °C in dark, while in 24 hours mRNA level slightly decreased. After transferring seeds to constant light, the expression changes exhibited a similar pattern (Narsai et al., 2011). In embryo, the lowest rate of mRNA was reported for the early stage, while the highest rate occurred in the early heart stage. Later on in development, the levels slightly decreased (Hofmann et al., 2019).

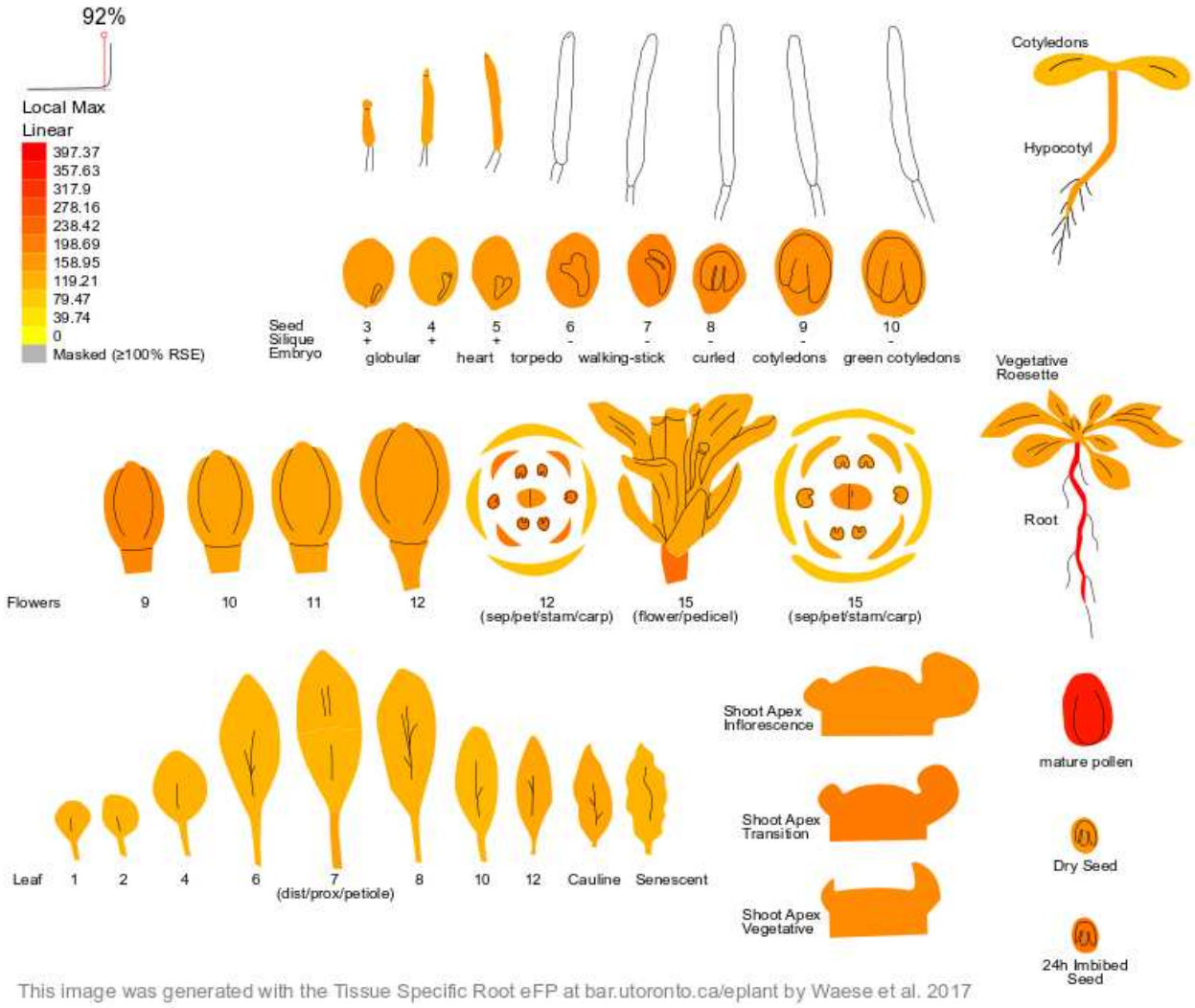

Fig. 18: Transcript levels of PhLP2 in different tissues, (https://bar.utoronto.ca/eplant/), the scale represents absolute values.

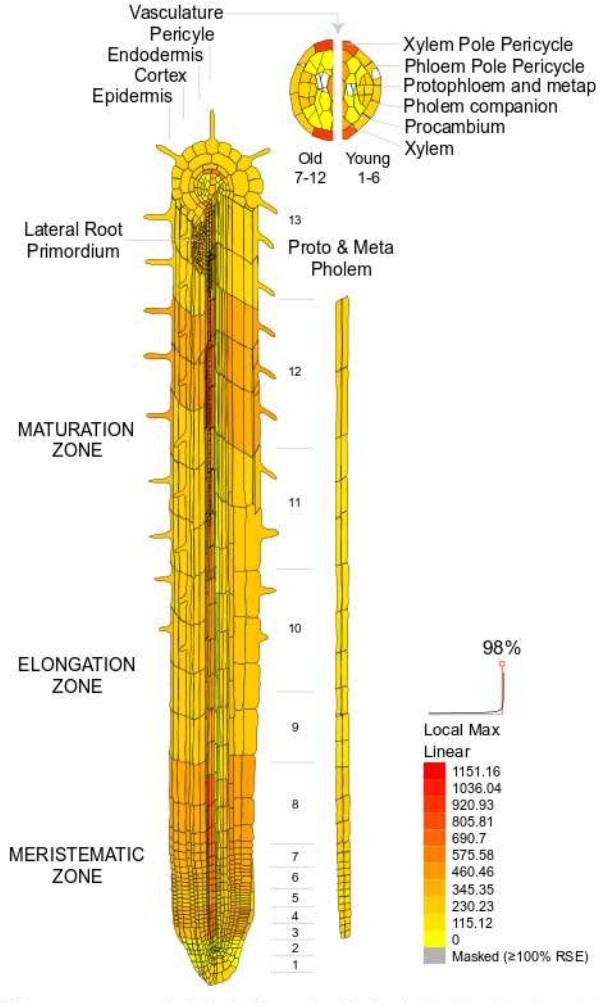

Fig. 19: PhLP2 mRNA levels in the root (https://bar.utoronto.ca/eplant/), the scale represents absolute values.

Regarding condition-dependent changes of *PhLP2* expression, there was significant upregulation in seedlings grown in constant darkness. Similarly, in seedlings grown in short-day conditions (8/16 h), higher levels of the transcript were detected at night (Fig. 20) (Todd P. Michael et al., 2008).

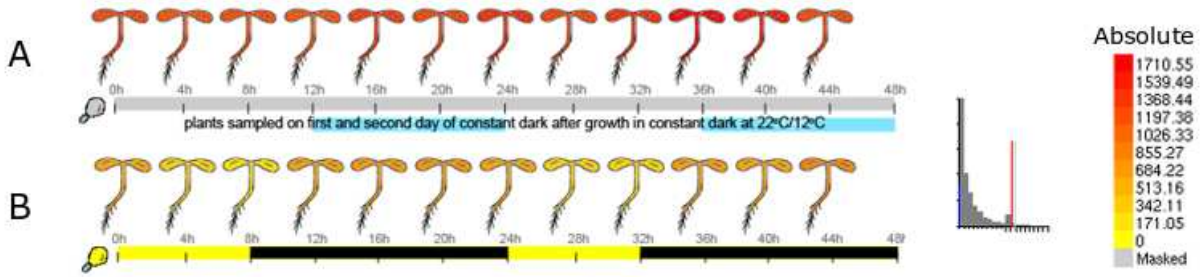

Fig. 20: *PhLP2* mRNA levels in **A** - 8-day old Col-0 seedlings in constant darkness, **B** - 7-day old seedlings of Ler in short-day condition (8/16 h). Both were grown on 3% sucrose agar in 22 °C in different conditions.

3.1.4 Genes co-expressed with PhLP2

When genes exhibit similar expression patterns across various developmental and environmental contexts, they can be considered to potentially participate in the same cellular process; the set of genes co-expressed with *PhLP2* can thus provide hints at its cellular and molecular function. I therefore analyzed the coexpression network of *PhLP2* using the ATTED II online tool (https://atted.jp/) (Obayashi et al., 2022). Overview of the gene co-expression can be found in Table 16.

Gene	Function	Other ID	Co-expression rate
SNX1	SORTING NEXIN 1	AT5G06140	8.2
GOS12	GOLGI SNARE 12	AT2G45200	7.5
CKA2	CASEIN KINASE II: ALPHA CHAIN 2	AT3G50000	7.4
VAP27-1	VESICLE ASSOCIATED PROTEIN 27-1	AT3G60600	7.3
SYP51	SYNTAXIN OF PLANTS 51	AT1G16240	6.6
SCL30	SC35-LIKE SPLICING FACTOR 30	AT3G55460	6.5
AT2G29020	RAB5-INTERACTING FAMILY PROTEIN	AT2G29020	6
WAV2	ALPHA/BETA-HYDROLASES SUPERFAMILY PROTEIN	AT5G20520	6

Table 16: Overview of genes co-expressed with *PhLP2*, Co-expression rate = relative value, the higher value, the higher rate of co-expression, data obtained from ATTED-II database (https://atted.jp/).

The strongest co-expression coefficient was reported for *SNX1*, which is a protein that regulates endomembrane trafficking and as such is also involved in auxin distribution. There are also other co-expressed genes involved in endomembrane trafficking, including GOLGI SNAP RECEPTOR COMPLEX MEMBER 1-2 (*GOS12*), VESICLE ASSOCIATED PROTEIN 27-1 (*VAP27-1*), SYNTAXIN OF PLANTS 51 (*SYP51*) or Rab5-interacting family protein. Co-expression-rate related to *PhLP2* was also reported for ALPHA CHAIN 2 OF CASEIN KINASE II (*CKA2*), which is related to light stimuli and circadian rhythms (Marquès‐Bueno et al., 2011), or an alpha/beta HYDROLASES SUPERFAMILY PROTEIN WAVY GROWTH 2 (*WAV2*) participating in root growth regulation.

In general, there are various highly co-expressed genes involved in membrane trafficking and protein sorting.

3.1.5 Protein-protein interactions of PhLP2

Another approach helping to estimate possible functions of PhLP2 is the overview of its interacting partners. Publicly available databases provide PhLP2 related information based mainly on three publications: Y2H screening by (Klopffleisch et al., 2011), TOR mass spec by (Van Leene et al., 2019) and VH1/BRL2 interactome by (Ceserani et al., 2009). Information traceable using databases and supplementary information can provide further prompter about PhLP2 function. Protein-protein interactions with PhLP2 are visualized in Fig. 21 and 22.

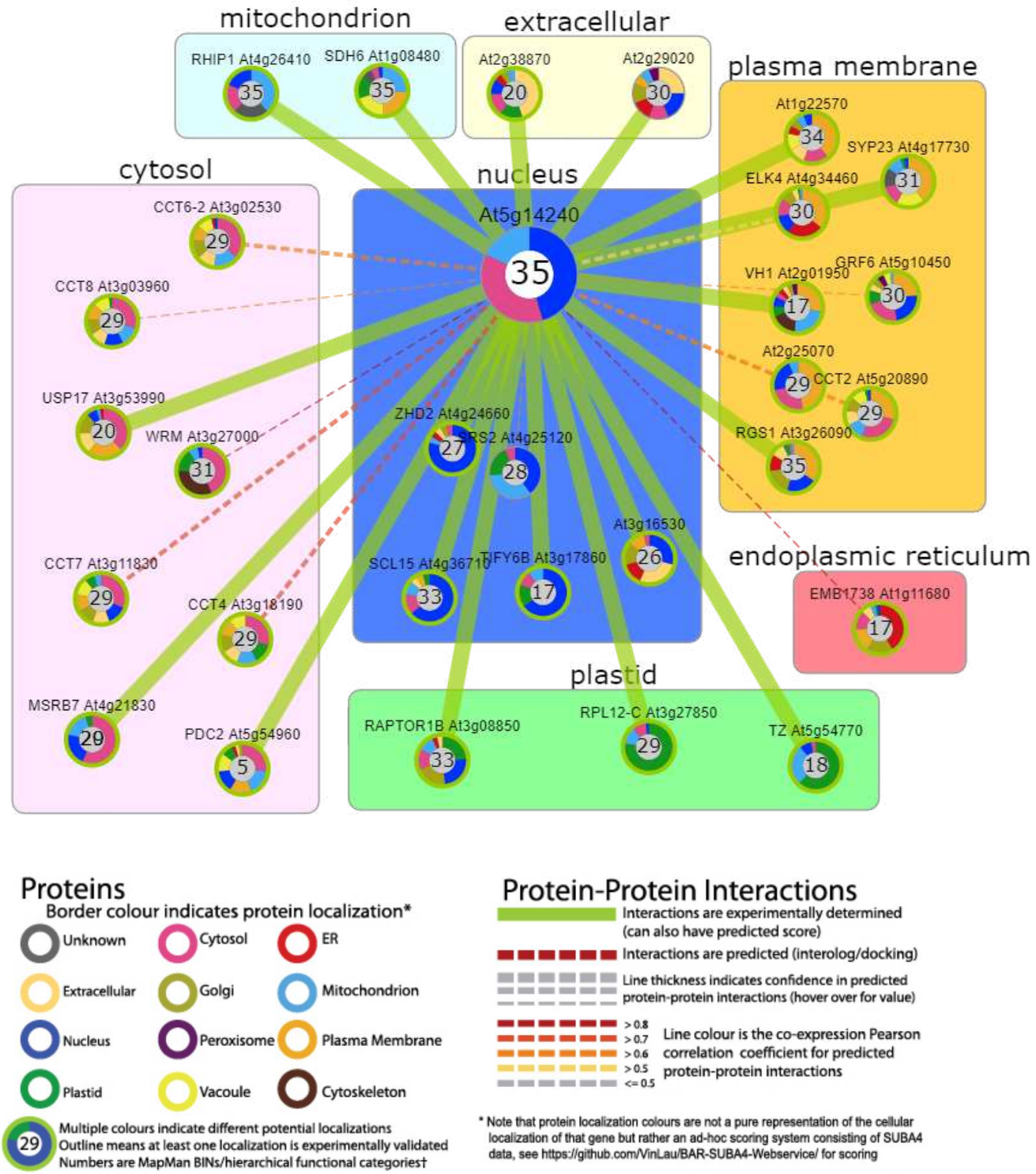

Fig. 21: A map of protein-protein interactions with PhLP2 (AT5G14240, center) obtained from Arabidopsis Interactions Viewer 2.0 (https://bar.utoronto.ca/interactions2/#%7B%7D), edited

Based on the Y2H interaction screen, PhLP2 interacts with RGS1 (Klopffleisch et al., 2011), which is a heterotrimeric G-protein regulator. This is consistent with the stated phosducin engagement in animal heterotrimeric G-protein signaling (Chen and Jones, 2004; Stateczny et al., 2016) and RGS1-related sugar-binding legume lectin family protein, RGS1-HXK1 INTERACTING PROTEIN 1 (RHIP1) (Huang et al., 2015).

For PhLP2, there was also predicted interaction with ERECTA-LIKE 4 (ELK4), which encodes the beta subunit of heterotrimeric G-protein (Lease et al., 2001a).

Several interactors of PhLP are involved in phytohormone regulation: JASMONATE-ZIM-DOMAIN PROTEIN 3 (JAZ3). Among proteins related to auxin, there is MAJOR FACILITATOR SUPERFAMILY involved in auxin transport (Remy et al., 2013), further ZINC-FINGER HOMEODOMAIN PROTEIN 2 (ZHD2) or SCARECROW-LIKE 15 (SCL15).

Leucine rich repeat kinase VASCULAR HIGHWAY 1 (VH1) related to meristem development (Al-Harrasi et al., 2020; Clay and Nelson, 2002), beside others, was also identified as PhLP2 interactor in Y2H (Klopffleisch et al., 2011).

Affinity capture MS proved RAPTOR1, the main interacting partner of the TOR, as an interacting partner (Salem et al., 2018; Van Leene et al., 2019).

Several other interactors are related to vesicle trafficking: such as SNARE-protein SYNTAXIN OF PLANTS (SYP23) or Rab5-interacting family protein (Ibrahim et al., 2020; Klopffleisch et al., 2011).

Additionally, there were also predicted interactions with various proteins (Geisler-Lee et al., 2007). Several of them belong to the CCT group, which are chaperonins essential for proper actin and tubulin molecules assembly (Brackley and Grantham, 2009; Grantham, 2020), expressed by stem cells (Llamas et al., 2021). Another possibly interacting partner is WRM actin related protein 2, which participates in ACTIN RELATED PROTEIN 2/3 (ARP2/3) complex

(Mathur et al., 2003). Orthology-based interactor prediction indicate possible interaction with CYTOCHROME P450 51G1 (CYP51G1) (Geisler-Lee et al., 2007), which is a protein that belongs to the group of cytochromes required for proper plasmatic membrane development and integrity (Geisler-Lee et al., 2007; Kim et al., 2005).

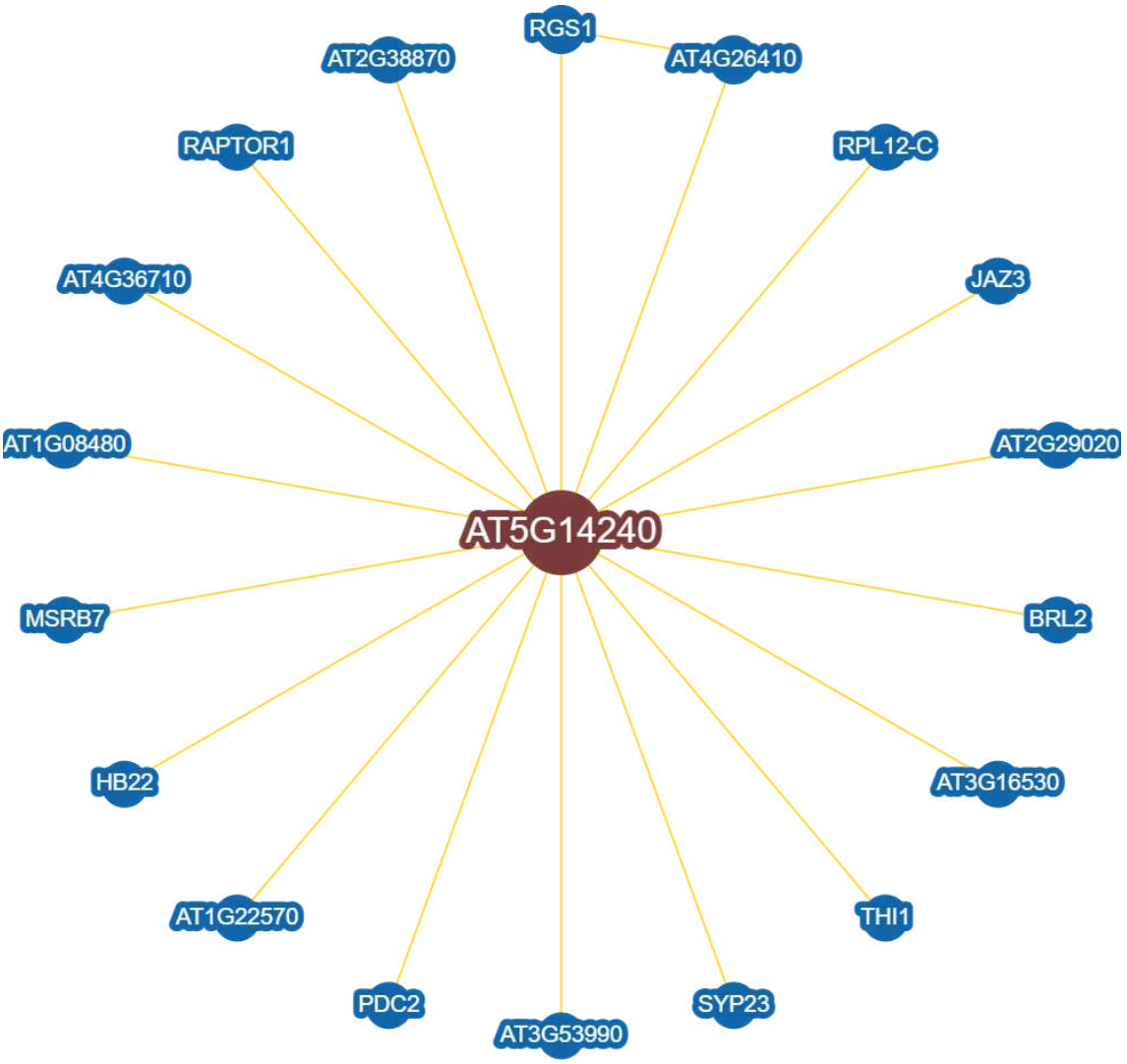

Fig. 22: A map of physical protein-protein interactions with PhLP2 (AT5G14240, center), obtained from BioGRID (https://thebiogrid.org/)

Additional information can be obtained from different database. Serine/threonine-protein kinase BRI1-LIKE 2 (BRL2) was identified as another interactor based on a reconstituted complex - the interaction was detected

between purified proteins *in vitro* (Ceserani et al., 2009).

3.2 Pattern of PhLP2 expression and localization

3.2.1 Observation of promoter activity

Since currently there is very little known about the function of PhLP2, an overview of the tissues in which the promoter is active can provide important insights into the gene function. For this purpose, I prepared a line with a pPhLP2-driven expression of NLS-mCherry, which was used for observation of the promoter activity in different tissues. Native promoter was estimated as a 400 bp long sequence between START codon and a coding sequence of the neighboring gene CONSTITUTIVE PHOTOMORPHOGENIC 13 (*COP13*).

According to my observation, the promoter was active in both young and mature leaves and in trichomes (Fig. 23). In the flower, the promoter was active in petals and style replum. Less intense signal was observed in the stem tissue, fertilized seeds or pollen grains (Fig. 25, 26). In the root, I observed the promoter activity in the root meristem, vasculature and maturation zone in the epidermis and trichoblasts in particular. Signal was also visible outside of the nucleus indicating cleaved particular components. Fluorescent protein detached from NLS could occur in the cytoplasm (Fig. 24).

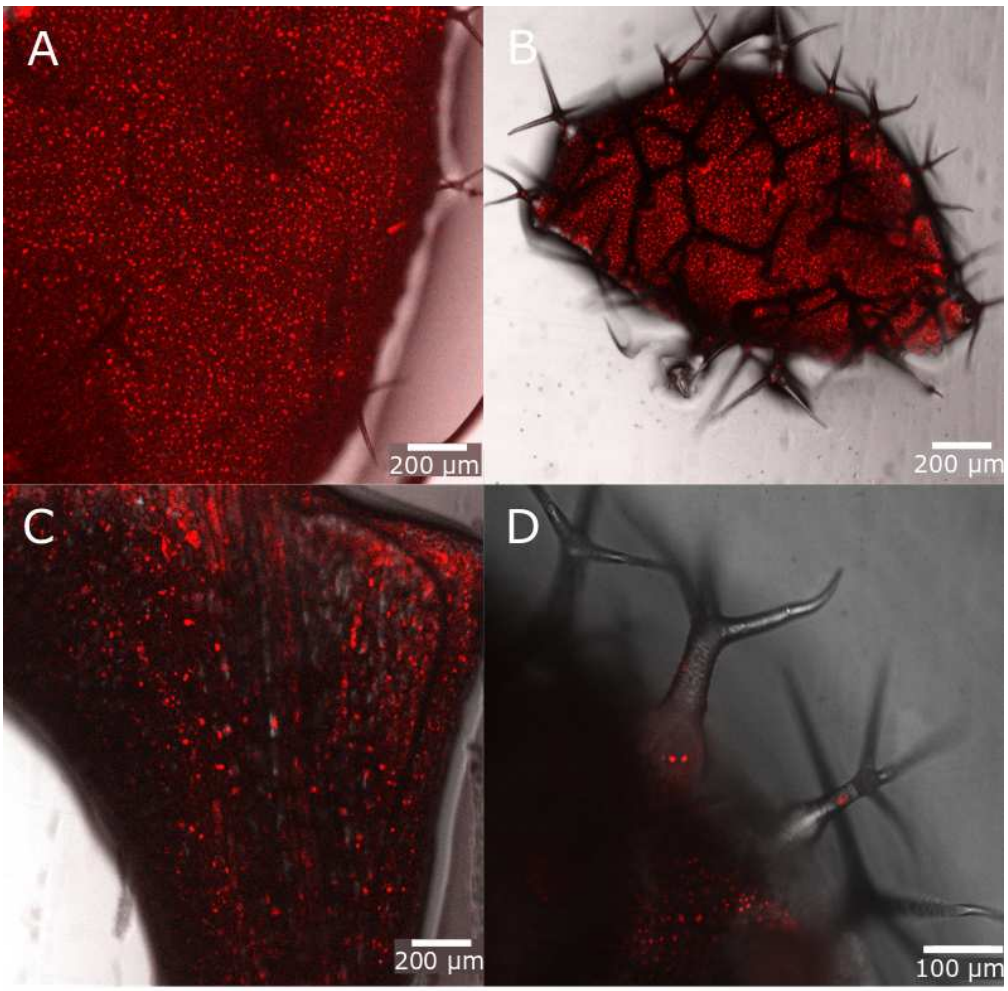

Fig. 23: Promoter activity of pPhLP2 visualized using transcriptional fusion pPhLP2::NLS-mCherry (in red) in T2 plants. **A -** mature leaf, **B -** young leaf, **C -** petiole, **D -** trichomes

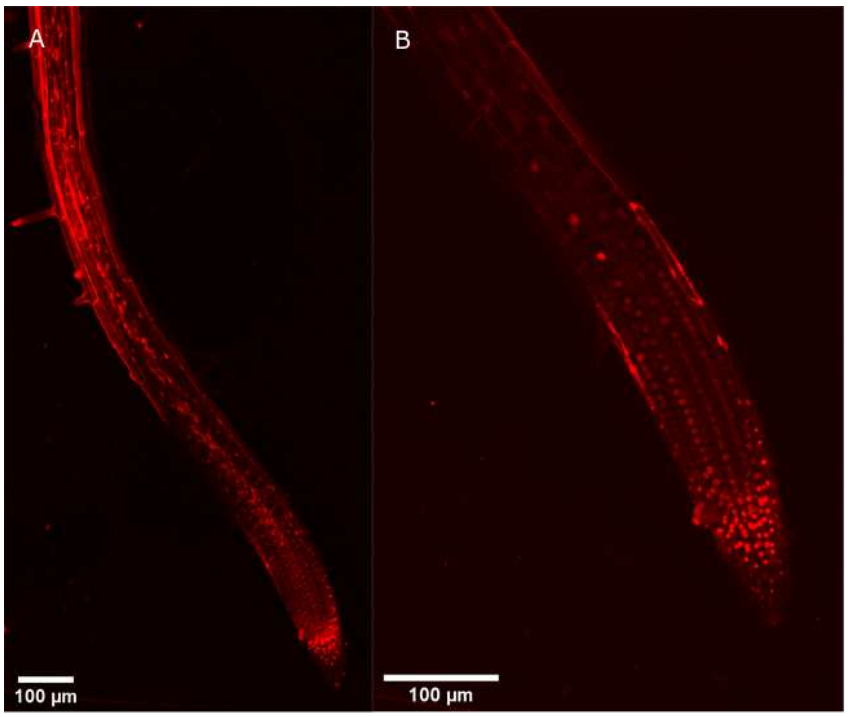

Fig. 24: Promoter activity of PhLP2 in **A -** root tip, **B -** detail of root meristem

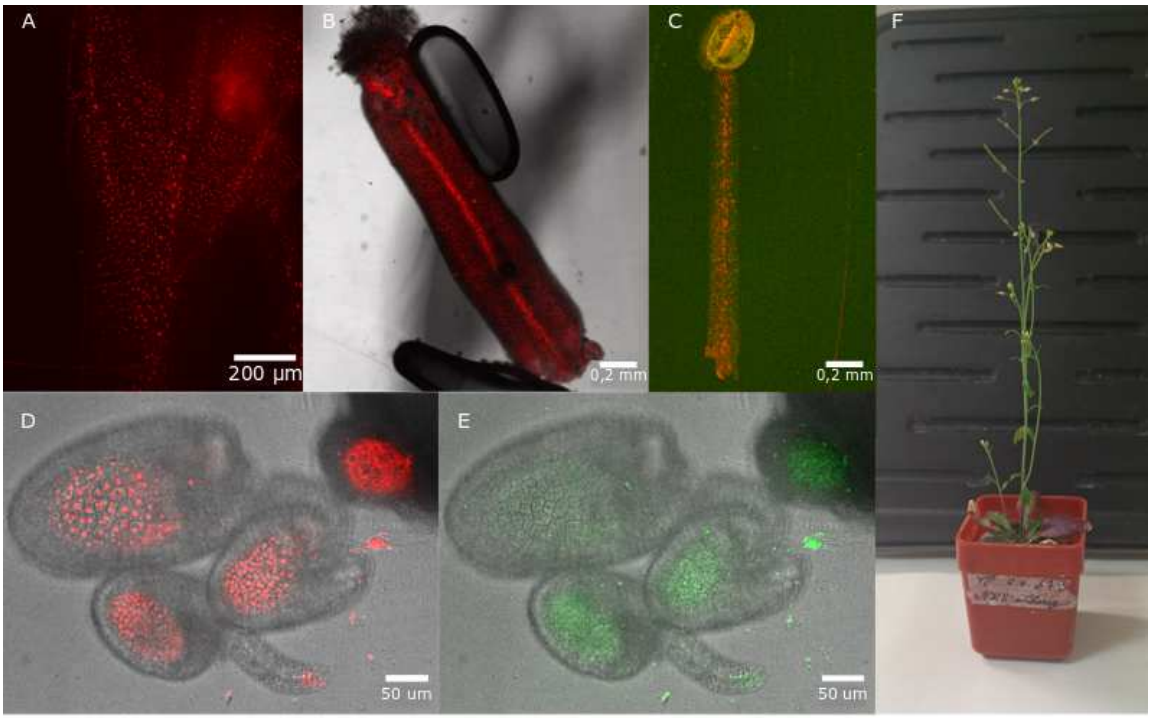

Fig. 25: Promoter activity of pPhLP2 visualized using transcriptional fusion pPhLP2::NLS-mCherry (in red) and autofluorescence (in green) in T2 plants. **A** - petal; **B** - stigma, style; **C** - anther with filament; **D**, **E** - fertilized ovule, **F** - mature pPhLP2::NLS-mCherry T2 plant, flowering stage

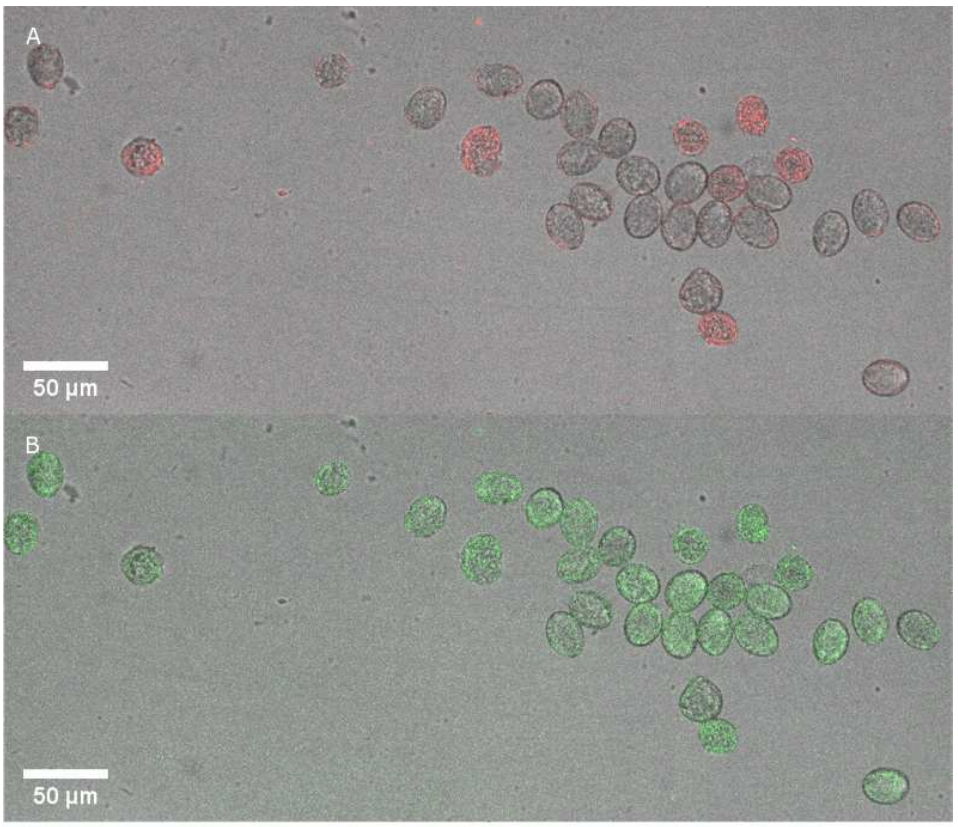

Fig. 26: pPhLP2::NLS-mCherry T2 screening of promoter activity in pollen grains, **A** - mCherry signal in red, **B** - autofluorescence in green

Activity of the promoter corresponds to information about transcript levels obtained from publicly available databases.

3.2.2 Localization of PhLP2 protein in plant tissues

The site of the promoter activity may not always fully correspond to the site of the protein accumulation. To analyze the localization of PhLP2 protein in Arabidopsis tissues, I used a native promoter-driven PhLP2 tagged with mScarlet or mEGFP fluorescent proteins - the pPhLP2::PhLP2-mScarlet and pPhLP2::PhLP2-mEGFP lines created by Denisa Oulehlová.

In roots, localization was observed mainly in the meristem and early elongation zone and vasculature (Fig. 27). At the subcellular level, the signal was localized in the nucleus and cytoplasm. I also observed the PhLP2-mScarlet signal in

petals, mature leaves or trichomes. On the subcellular level, protein is localized mainly in the nucleus and cytoplasm (Fig. 28) as well as in root.

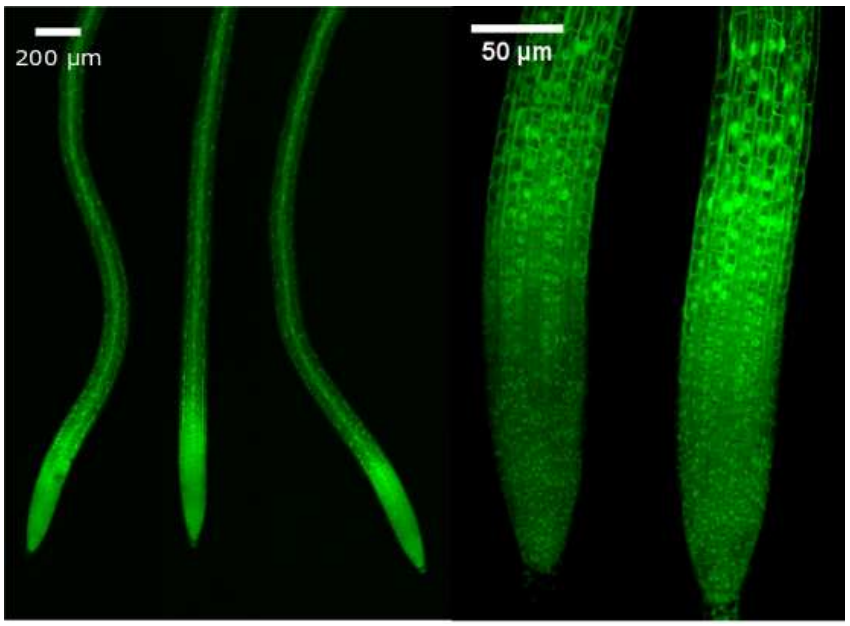

Fig. 27: Localization of PhLP2 visualized in seedlings of pPhLP2::PhLP2-GFP (created and captured by Denisa Oulehlová). mEGFP signal is present in the meristem zone, early elongation zone and vasculature.

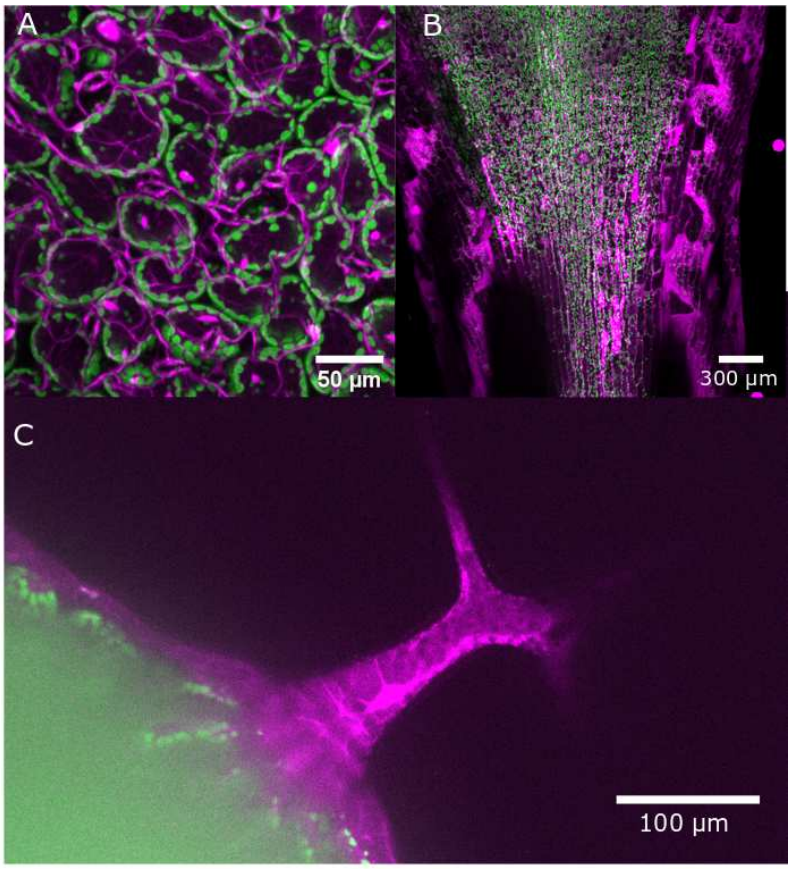

Fig. 28: Localization of PhLP2 visualized by pPhLP2::PhLP2-mScarlet (PhLP2 signal in magenta, autofluorescence of chloroplasts in green) in nucleus and cytoplasm in **A** - leaf epidermal cells, **B** petal base, **C** - trichome

-

According to indications that PhLP2 knock-out lethality might be caused by gametophytic defects, I focused on the expression in pollen grains and tubes. Observation was performed using pPhLP2::PhLP2-mEGFP translational fusion. I observe abundant signal in the cytoplasm in both pollen grains (Fig. 29-A) and pollen tubes (Fig. 29-B).

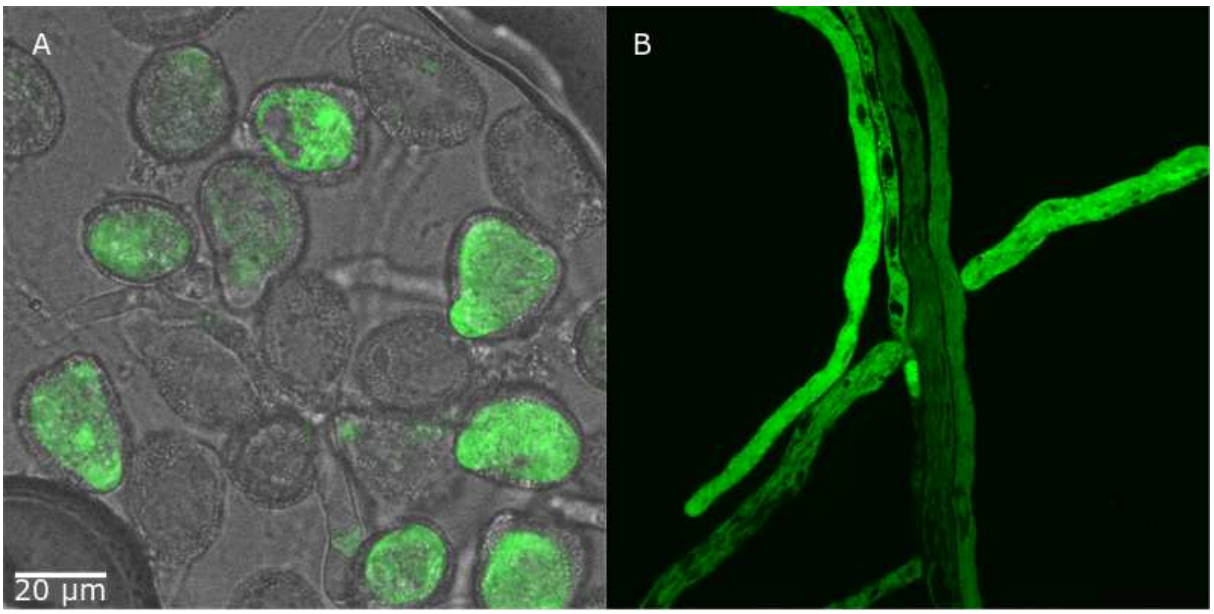

Fig. 29: Localization of PhLP2 in pPhLP2::PhLP2-mEGFP translational fusion in the cytoplasm of **A** - germinating pollen grains, **B** - pollen tubes

According to fluorescent signals observed, protein localization corresponds to the promoter activity. Interestingly, the signal in germination pollen grains and tubes was very strong.

3.3 Phenotype analysis of RNAi *PhLP2*

In comparison to Col-0, mutant in the PhLP2 gene could provide a closer outline of which processes PhLP2 is involved in based on the analysis of the mutant phenotype. However, there were no *phlp2* T-DNA lines containing mutation among the publicly available databases. Subsequently, colleagues in the laboratory used CRISPR-Cas9 technology to create a novel *phlp2-cr* loss-of-function alleles. In the T1 generation, various individuals exhibited consistent phenotype of defects in primary root growth, but *phlp-cr* alleles were not possible to propagate to the next generation, which might indicate gametophytic or embryonic lethality (unpublished data). Since it was not possible to recover homozygous *phlp2* mutant lines from publicly available databases, line with lower expression of PhLP2 was used for phenotype

analysis. RNA interference (RNAi) is a tool for lowering expression of a target gene, in contrast with insertion mutation. Degradation of host mRNA happens via enzymatic machinery, when guided RNA string is led into RNA-induced splicing complex (RISC) by argonaute proteins and double string RNA-binding proteins. Guided strand exiting RISC is subsequently led to complementary mRNA, which is cleaved by argonaute proteins (Taxman et al., 2010).

To observe the function of PhLP2, I wanted to prepare a RNAi *PhLP2* knock-down construct expressed under estimated native promoter, because the phenotype would correspond to natural occurrence of PhLP2. Unfortunately, the cloning process of the knock-down expressed under native promoter failed and it was not possible to continue with transformation to *Arabidopsis thaliana*. For phenotype analysis I used the knock-down line RNAi *PhLP2* already available in the laboratory (created by Denisa Oulehlová) expressed under the 35S promoter that provides strong constitutive expression within the plant.

In T2 generation of RNAi *PhLP2*, *PhLP2* expression level was downregulated to 30,18 % of Col-0 expression (Table 17).

	Col-0	**RNAi *PhLP2***
Gene level (TPM)	92,41	32,66

Table 17: Gene expression level of *PhLP2* in Col-0 and RNAi *PhLP2* in T2 generation, TPM = transcript per million

Observed phenotype of RNAi *PhLP2* line was strongly affected in comparison to Col-0. Among the most prominent phenotype characteristics were distorted siliques, loss of apical dominance in the shoot, retarded growth, strongly waved primary root or decreased number of lateral roots (Fig. 30 and 31).

Fig. 30: Phenotype of adult plant of RNAi *PhLP2* line, flowering stage - disordered siliques, apical dominance loss; T2 generation (left), T1 generation (right), created by Denisa Oulehlová

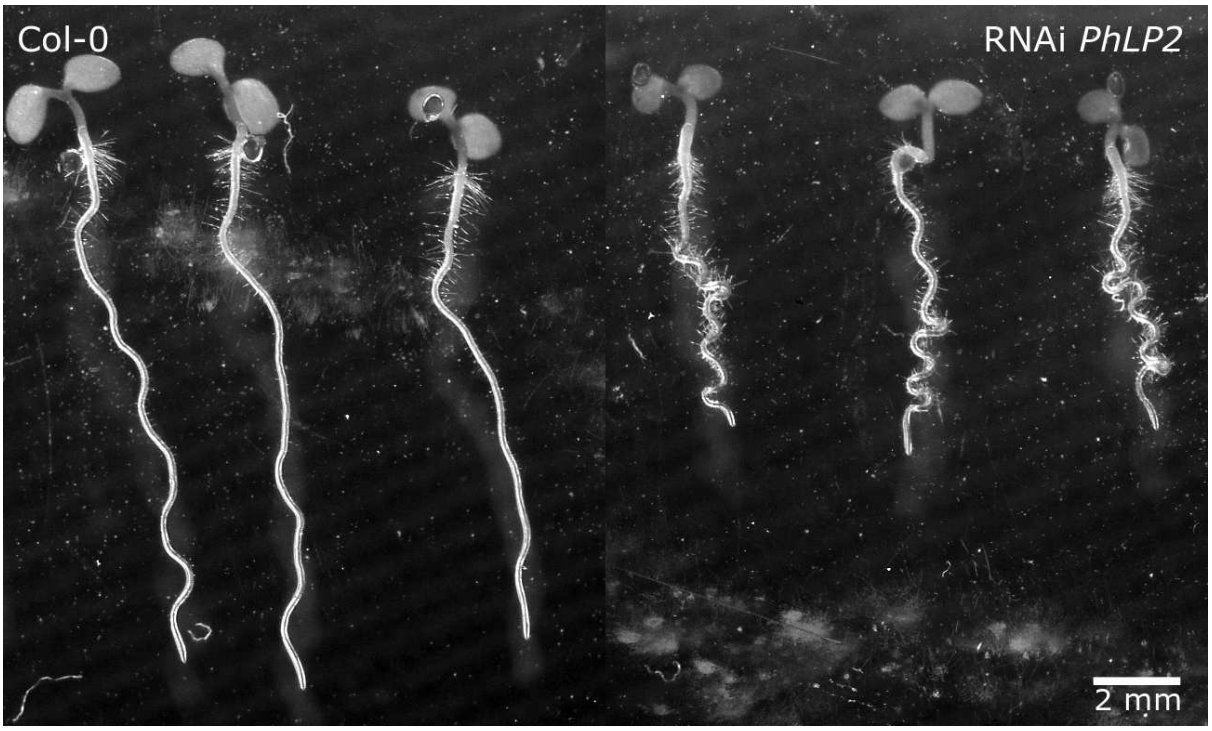

Fig. 31: Phenotype of knock-down line RNAi *PhLP2*, 5-day old seedlings grown of ½ MS medium

3.3.1 Primary root phenotype

One of the most conspicuous characteristics of the RNAi *PhLP2* line is that the primary root was strongly waved in comparison to Col-0 (Fig. 32-A). To quantify the rate of waved phenotype, I measured a VGI as a ratio of whole root length to distance from its base to the tip. VGI of 5-day old seedlings of both lines was compared; the experiment was performed in three replicas. Processed data indicates that the difference of VGIs between lines RNAi *PhLP2* and Col-0 was statistically significant (Fig. 32-B) in all measurements performed. Value of VGI = 1 indicates a perfectly straight root, since the root length and distance from base to tip are equal. Apparently, lower VGI value describes a more curvy root. VGI of Col-0 was significantly higher than in RNAi *PhLP2*, which is a result confirming stronger root waving of RNAi *PhLP2* in comparison to Col-0.

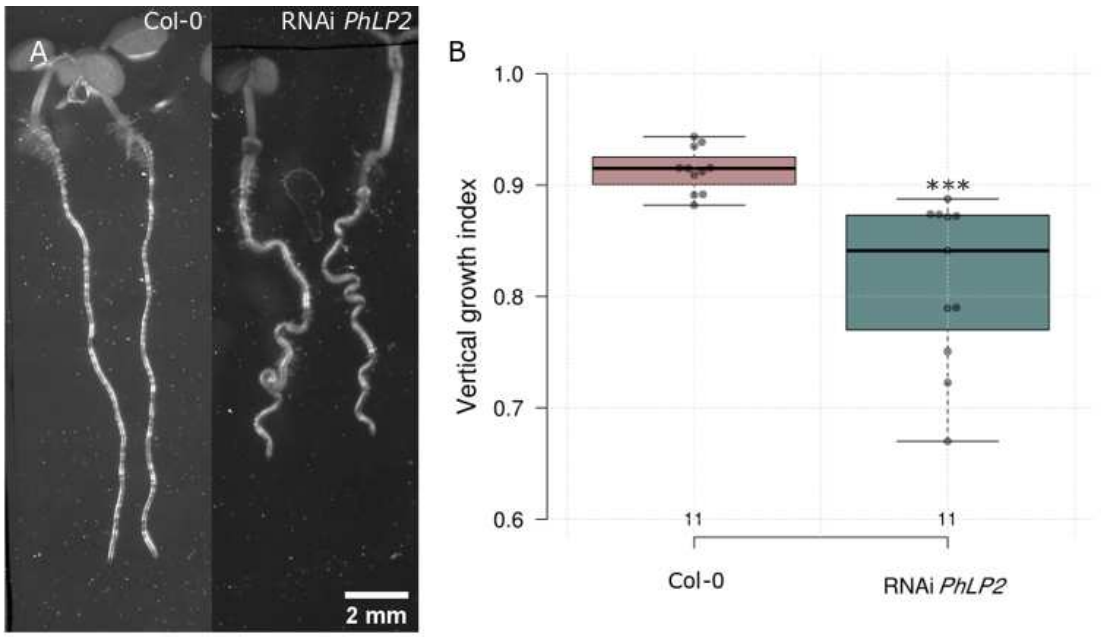

Fig. 32: Representative measurement of VGI, **A** - comparison of Col-0 and RNAi *PhLP2* growing on vertical plates, **B** - difference in VGI of Col-0 compared to RNAi *PhLP2*, Student's t-test ($\alpha = 0{,}05$) was used to determine the significant difference between Col-0 and RNAi *PhLP2*. *$p < 0.05$, **$p < 0.01$, ***$p < 0.001$, ns = not significant

Although the roots of RNAi *PhLP2* knock-down exhibit demonstrably stronger curvature, the wave pattern could not be described by the VGI approach. The number of waves present in the root can describe whether the waving rhythm differs. On plates cultivated vertically it was difficult to distinguish the presence of waves in Col-0 plants so it was hard to compare its pattern to knock down lines. Seedlings of *Arabidopsis thaliana* are known to exhibit a stronger wave pattern of primary root growing on plates tilted on 45 ° (Li et al., 2016). Cultivating the seedlings on 45 ° tilted agar plates can provide visible wave pattern even in Col-0 (Fig. 33-A). Amplitudes of waves of each root were counted and related to root length. Experiment was performed in three replicas. I found that the RNAi *PhLP2* exhibited a higher number of wave amplitudes per mm (Fig. 33-B), and the difference between Col-0 and RNAi *PhLP2* was statistically significant.

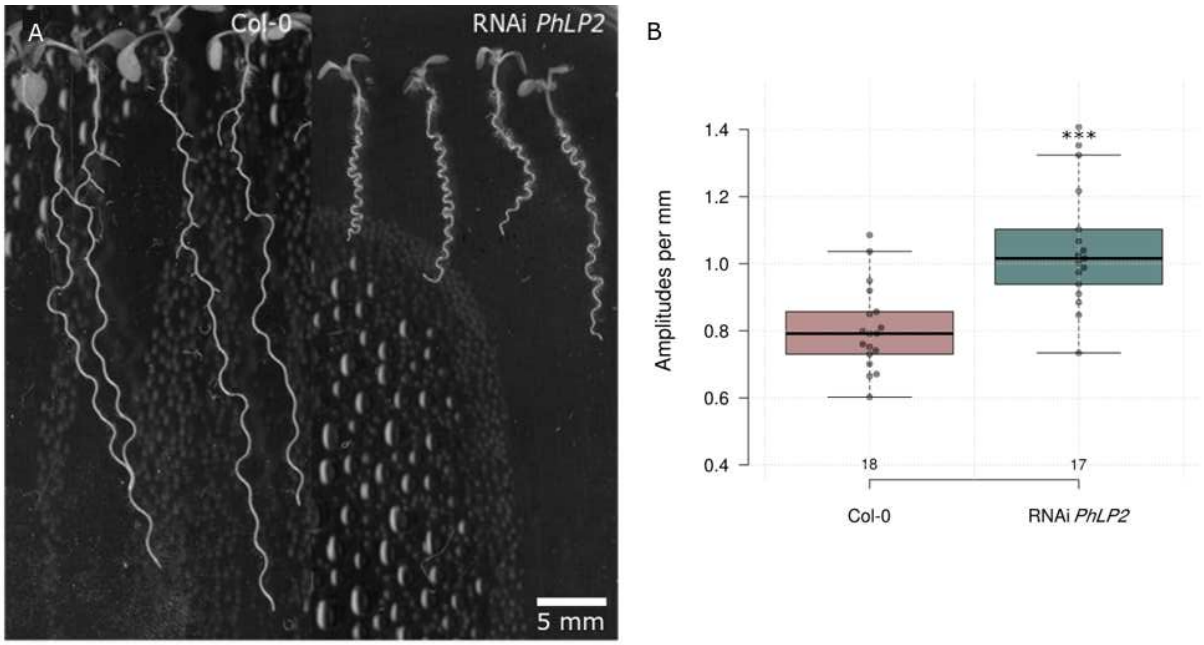

Fig. 33: Waved primary roots in 9-day old seedlings of Col-0 and RNAi *PhLP2* grown on 45 ° tilted plates containing ½ MS medium, **A -** phenotype of Col-0 compared to RNAi PhLP2, **B** - amplitudes of root waving per mm. Student's t-test ($\alpha = 0{,}05$) was used to determine the significant difference between Col-0 and RNAi *PhLP2*. *$p < 0.05$, **$p < 0.01$, ***$p < 0.001$, ns = not significant

Roots of Col-0 growing on the surface of the medium naturally exhibit left-handed growth orientation (from the upper point of view). Waving and skewing are related processes (Oliva and Dunand, 2007) and it might be possible that the phenotype of RNAi *PhLP2* exhibits defects in skewing. Therefore, 5-day old seedlings and 9-day old seedlings were cultivated on 45 ° tilted plates. Angles of the root tip according to the vertical axis were compared in lines Col-0 and RNAi *PhLP2* in three replicas as above. There was no difference in skewness between Col-0 and RNAi *PhLP2* lines in the case of 5-day old seedlings (Fig. 34-A), however, after 9 days of cultivation, I observed a significant difference in skewing between Col-0 and RNAi *PhLP2* (Fig. 34-B) indicating defect in left-handed skewness in the RNAi *PhLP2* line.

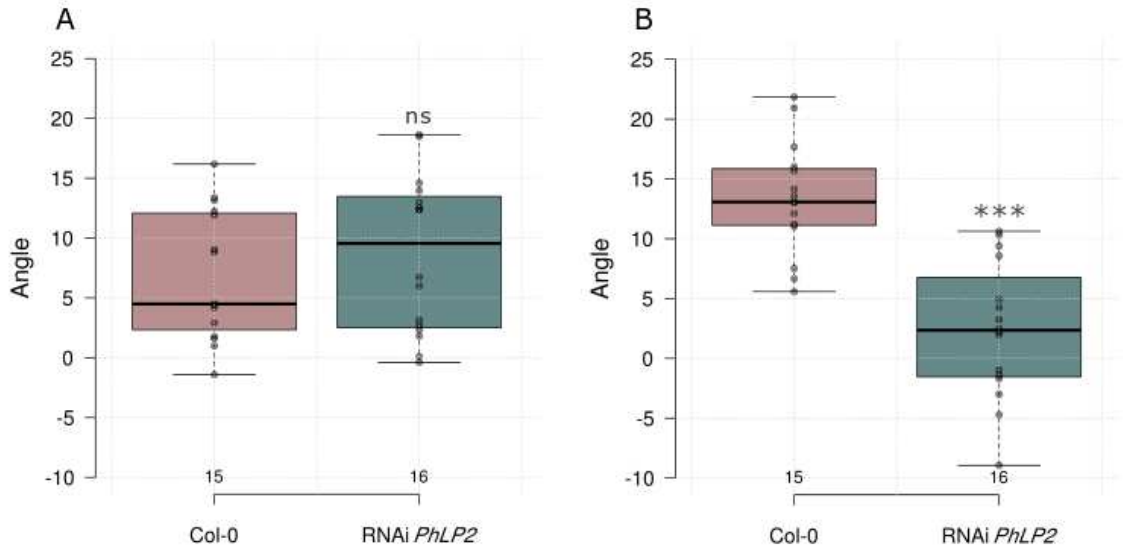

Fig. 34: A - Boxplot showing differences in angle (in degrees) of skewing of **A** - 5-day and **B** - 9-day old Col-0 and RNAi *PhLP2* seedlings. Student's t-test (α = 0,05) was used to determine the significant difference between Col-0 and RNAi *PhLP2*. *p < 0.05, **p < 0.01, ***p < 0.001, ns = not significant

3.3.2 Initiation and outgrowth of lateral roots

The RNAi *PhLP2* line visibly exhibited a reduced number of lateral roots (Fig. 35). Both the initiation and outgrowth of lateral roots depends on the functional

auxin pathway (Torres-Martínez et al., 2020). I analyzed the initiation and outgrowth of primordia to dissect in which step of lateral root formation the RNAi *PhLP2* line is defective. To do so, 8-day old seedlings of Col-0 and RNAi *PhLP2* lines were compared in context of absence / presence and number of lateral roots, their primordia and ratio of these characteristics. Both LRs and primordia were counted on individuals and the number of those structures were compared as absolute values (Fig. 36). The experiment was performed in three replicas. I observed a statistically significant lower number of both LRs and primordias in RNAi *PhLP2* compared to Col-0 in all replicas. Additionally, there was no significant difference in ratio of lateral roots / primordia in all three replicas. Based on results, I concluded that LRs and primordia occur in RNAi *PhLP2*, although their abundance is significantly lower. However, the ratio of LRs and primordia was resembling in Col-0 and knock-down, which indicate that low number of lateral roots is caused rather by lack of primordial initiation than outgrowth disability.

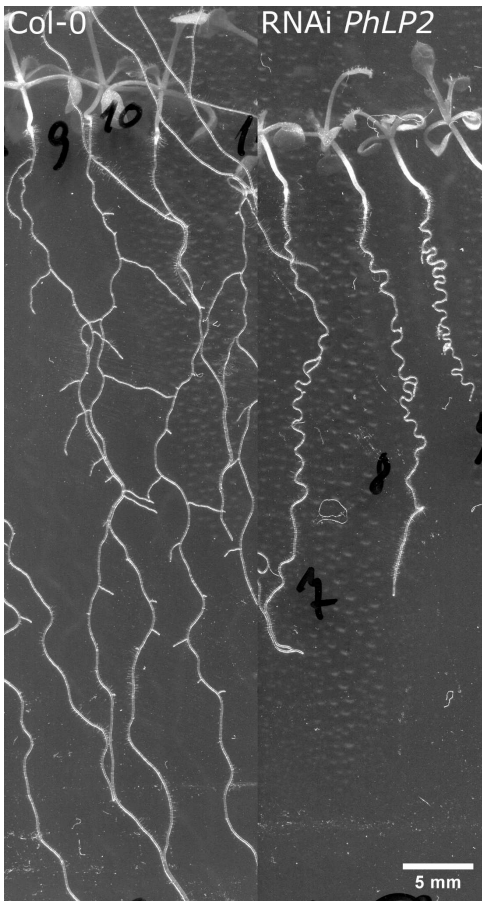

Fig. 35: Comparison of LR in 23-day old seedlings of Col-0 (left) and RNAi *PhLP2* (right). Col-0 seedlings exhibit visible LR emergence, however, RNAi *PhLP2* line possess very little number of LR, moreover poorly developed

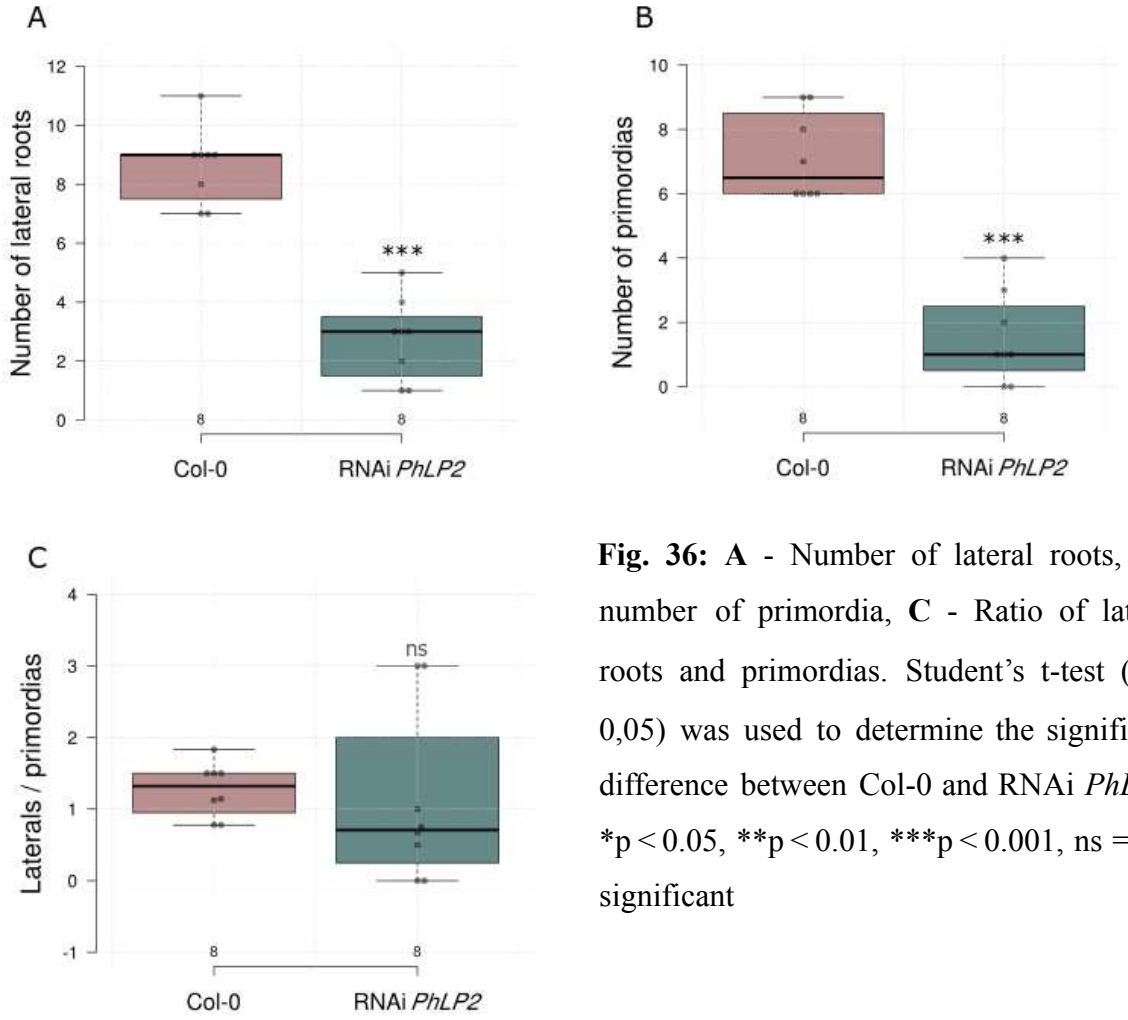

Fig. 36: A - Number of lateral roots, **B** - number of primordia, **C** - Ratio of lateral roots and primordias. Student's t-test (α = 0,05) was used to determine the significant difference between Col-0 and RNAi *PhLP2*. *p < 0.05, **p < 0.01, ***p < 0.001, ns = not significant

3.4 Auxin related processes

Phosphorylation changes in PhLP2 were observed after application of IAA (Table 15). This, together with the altered lateral root phenotype, suggests a possible involvement of PhLP2 in auxin-related processes. Therefore I analyzed whether auxin responses are affected in RNAi *PhLP2*.

3.4.1 IAA-induced root growth inhibition

The application of nanomolar concentrations of IAA inhibits root cell elongation (Dubey et al., 2021). First, I tested whether the RNAi *PhLP2* knock-down is sensitive to exogenous auxin application and if so, whether the rate of inhibition differs in RNAi *PhLP2* compared to Col-0. 6-day old seedlings were transferred to plates containing ½ MS medium with three treatments: 10nM IAA, 50nM IAA and mock. Immediately after transfer, growth of roots was captured using a flatbed scanner for 11,5 hours in 30 minute intervals (Fig. 38).

Analysis was performed in five replicas. According to my measurement there were detectable significant differences in the 50nM IAA treatment (Fig. 39) when inhibition of Col-0 was stronger in comparison to RNAi *PhLP2*. However, one of the replicas showed no significant difference in root inhibition between lines and one of the replicas revealed even stronger inhibition of root growth in RNAi *PhLP2*. In the 10nM IAA treatment, the results were not consistent, only two replicas showed a difference in root growth inhibition between the lines, although one of them showed stronger inhibition in Col-0 compared to RNAi *PhLP2* and the second one showed the opposite, therefore results obtained are not conclusive and do not clearly provide information about how the IAA-induced root inhibition differs in RNAi *PhLP2*. Nevertheless, the results clearly show that the auxin-induced root growth inhibition occurs in the RNAi *PhLP2* line (Fig. 37). To understand the PhLP2 connection to auxin I observed manifestations of auxin-related processes in next experiments.

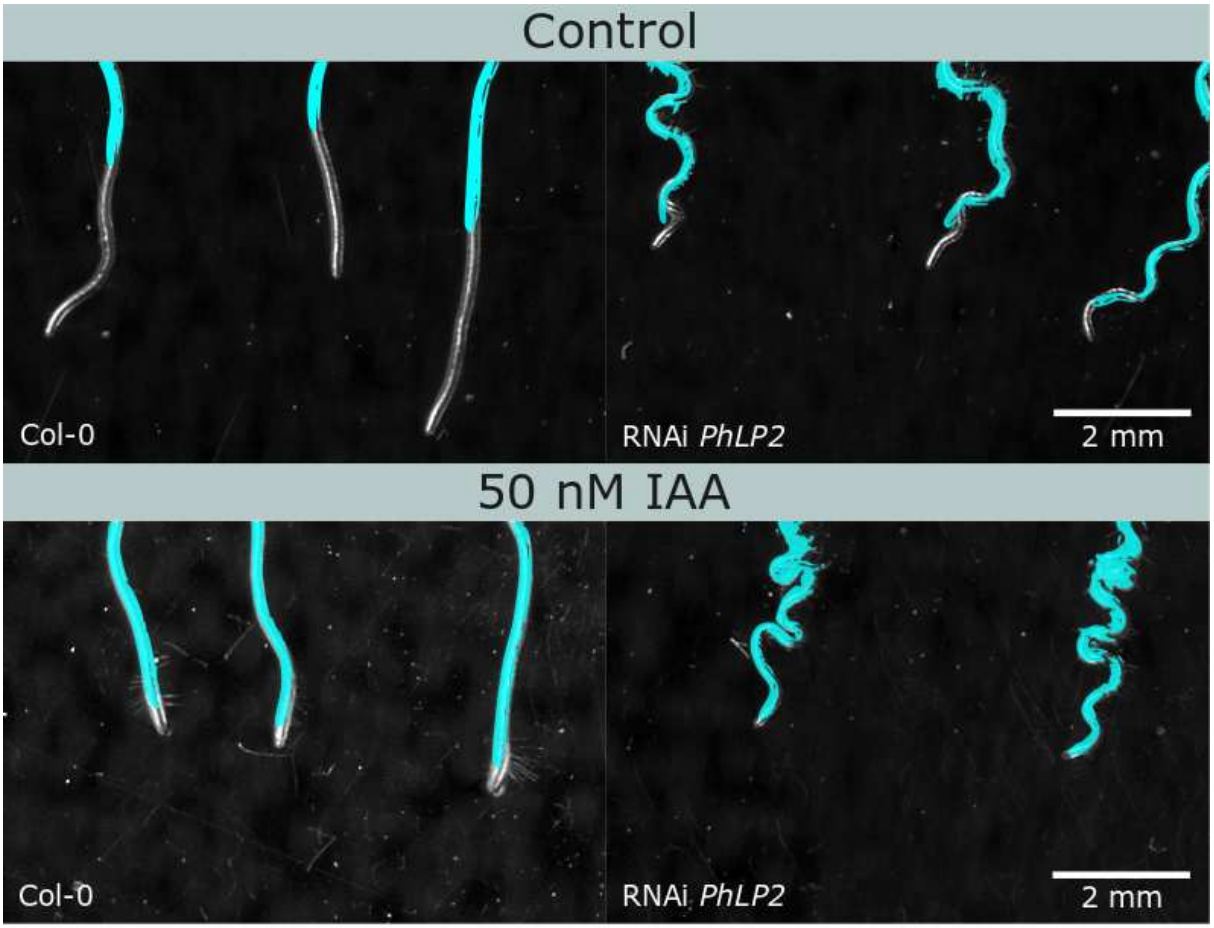

Fig. 37: Example of root inhibition after IAA application: 6-day old seedlings of Col-0 and RNAi *PhLP2* captured at the beginning of the treatment (root position in blue) and after 11,5 h, control (upper) and treated with 50nM IAA (lower)

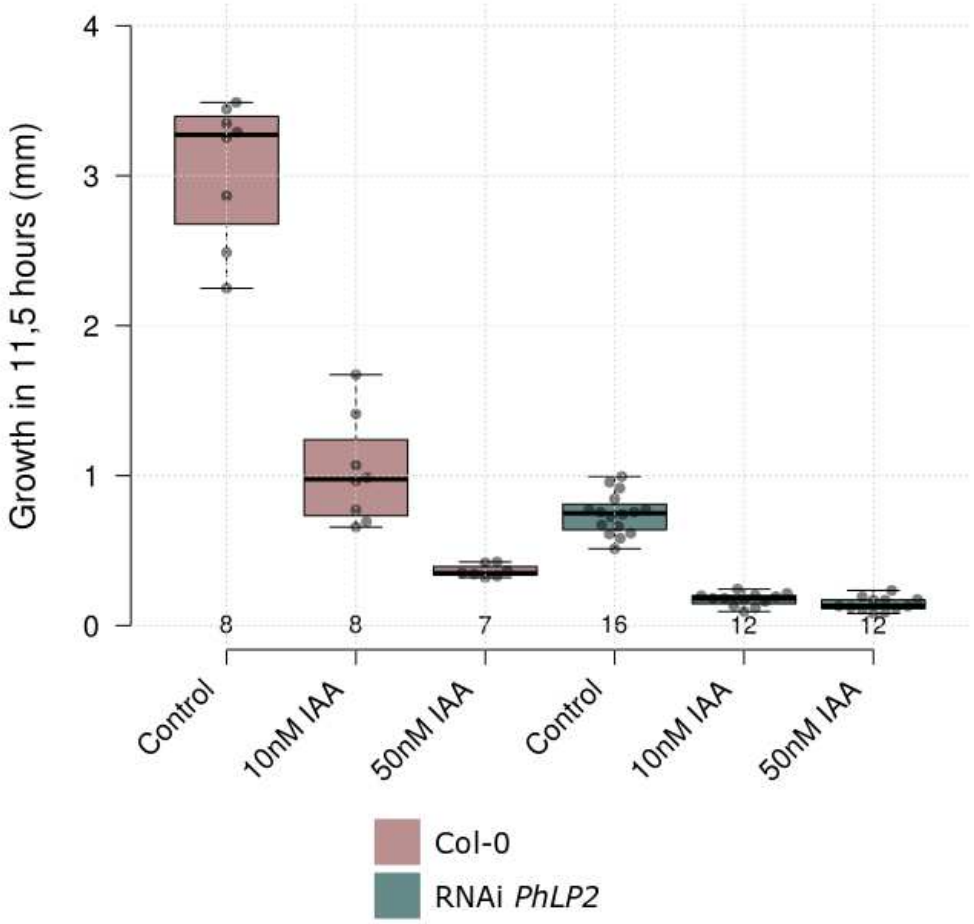

Fig. 38: Increment of roots of 6-day old seedlings of Col-0 and RNAi *PhLP2* 11,5 hours after IAA application

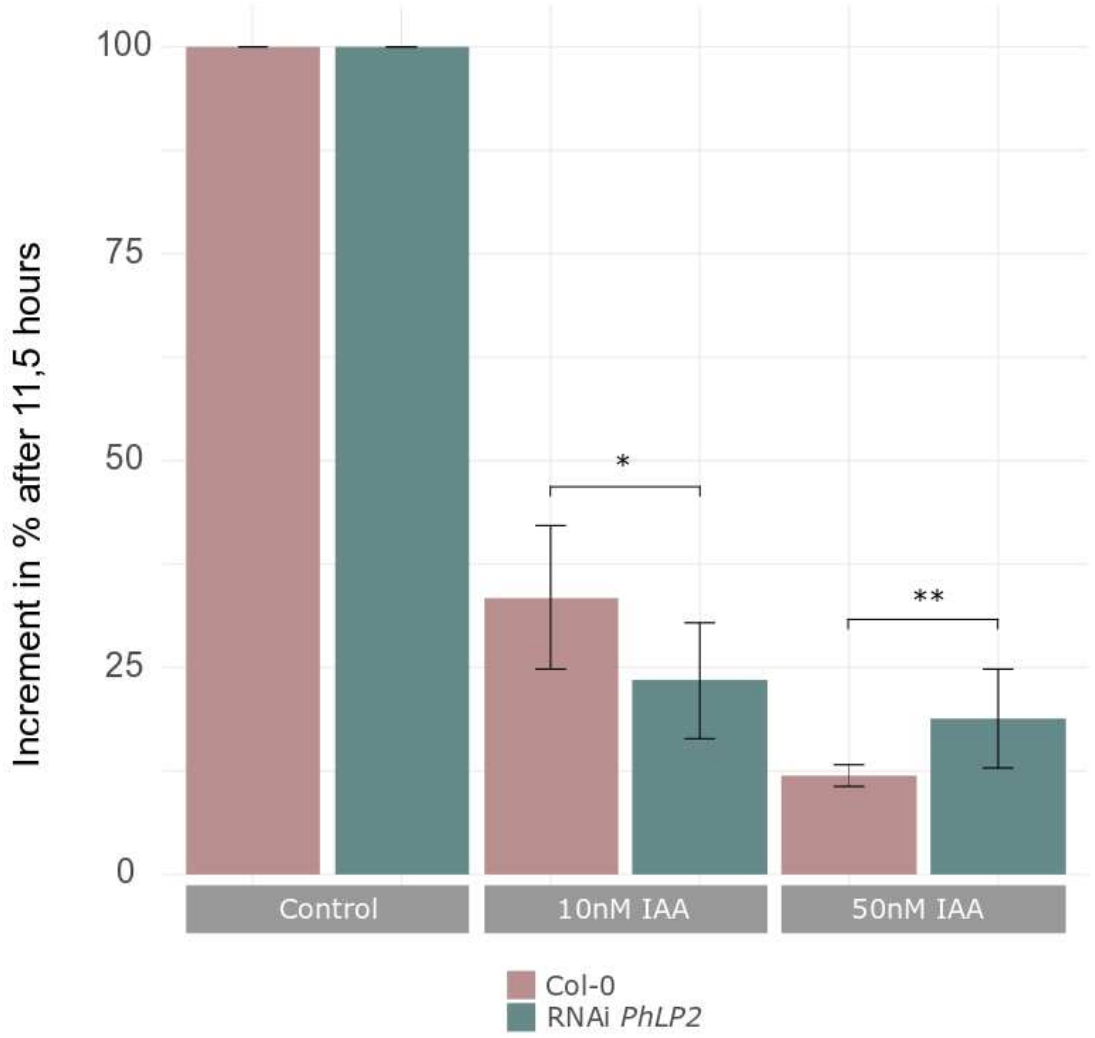

Fig. 39: Representative measurement of root growth inhibition of 6-day old seedlings of Col-0 and RNAi *PhLP2* upon different IAA concentrations described as an increment in 11,5 hours: 100% increment after 11,5 hours is represented by average increment of plants growing on control medium. Seedlings treated with IAA were grown on ½ MS medium containing 10nM or 50nM IAA. Student's t-test ($\alpha = 0{,}05$) was used to determine the significant difference between Col-0 and RNAi *PhLP2*. *$p < 0.05$, **$p < 0.01$, ***$p < 0.001$, ns = not significant

3.4.2 Gravitropic response

Gravitropism of a primary root can be used as a biological readout of the rapid auxin response. As was mentioned above in the Introduction chapter, AFB1 signaling is required for this process and the *afb1* mutant was shown to lack the

initial rapid phase of the gravitropic response. I wanted to observe whether the RNAi *PhLP2* exhibits gravitropic response and if so, I wanted to measure the difference in root bending in comparison to Col-0. Seedlings of both backgrounds were grown inside ½ MS medium. When the seedlings were grown on the surface of the medium, they exhibited a strong waving pattern of their primary roots. After 90 ° rotation of the plates, the primary roots bent in the direction of the gravity vector, but the gravitropic response itself was masked by the waving phenotype. Growing seedlings inside the agar medium creates a pressure on the root, which reduces waving (Fig. 40-B). That was why for this experiment, the seedlings were grown inside of the medium.

Samples were rotated 90° to observe gravitropic response and immediately captured using a scanner for 11,5 hour observation (long term) in a 30-minute interval or using a microscope for ~200 min observation (short term) in 5-minute intervals. Samples of lines Col-0 and RNAi *PhLP2* were compared in four (long term) and five (short term) replicas.

In the case of the long-term gravitropic response, 4 timepoints were selected for comparing a difference in root bending progress (3, 6, 9 and 11,5 hours after gravitropic stimulation). There was no difference in root bending between Col-0 and the RNAi *PhLP2* in 3 hours after gravitropic stimulation in the case of 3 out of 4 replicas. One measurement revealed a significantly lower angle of root bending in the RNAi *PhLP2*. After 6 and 9 hours, a significantly stronger bending was observed in Col-0 compared to the RNAi *PhLP2*, except one replica showing the opposite. In 11,5 hours, no difference in root bending between the genotypes was observed. In general, early stages of the response do not indicate gravitropism disruption in the RNAi *PhLP2*. Differences occurred later during observation, although in the end, root bending of both lines equalized (Fig. 40-A).

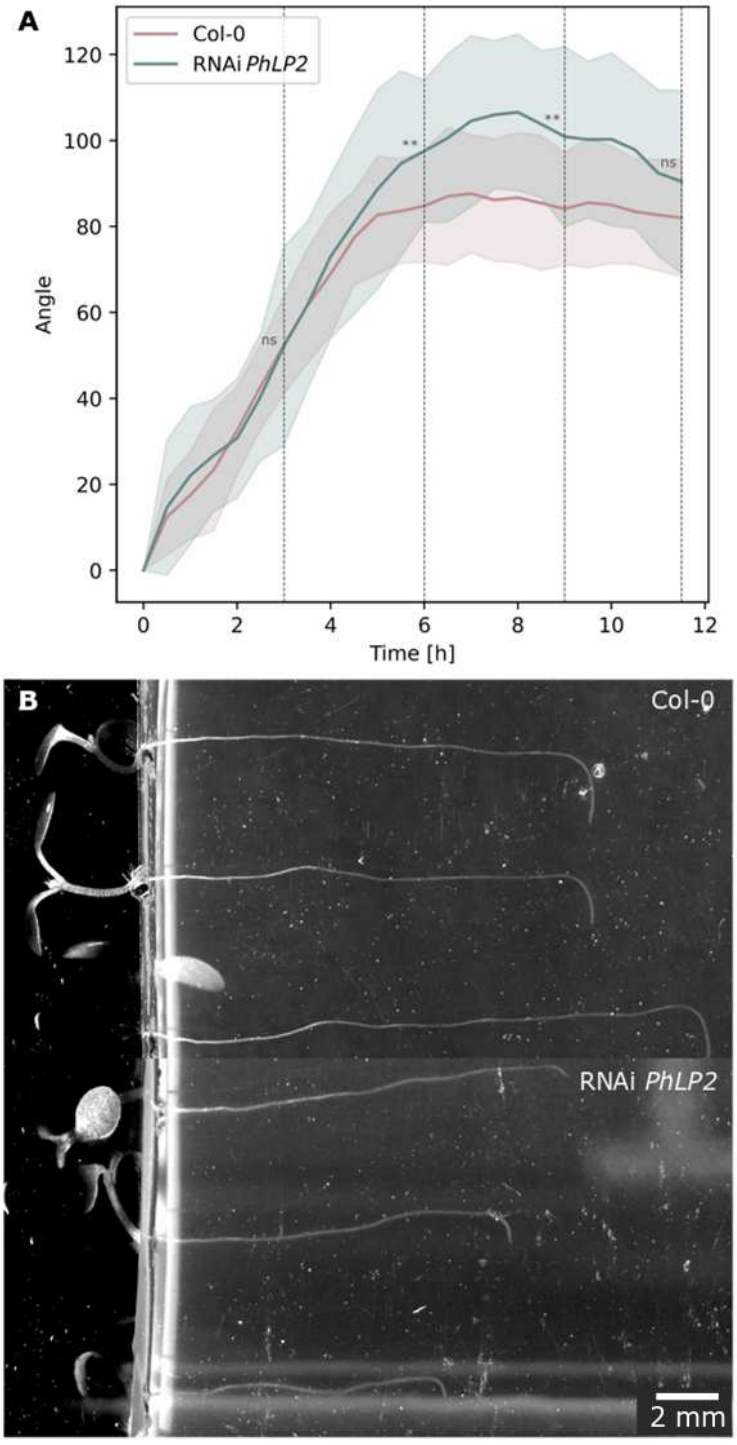

Fig. 40: Long term gravitropic response of 5-day old seedlings of Col-0 and RNAi *PhLP2* in 11,5 hours, **A** - long-term gravitropic response during 11,5 h after rotating samples, angle (degrees) of the bending root in time. Student's t-test ($\alpha = 0{,}05$) was used to determine the significant difference between Col-0 and RNAi *PhLP2*, $^{*}p < 0.05$, $^{**}p < 0.01$, $^{***}p < 0.001$, ns = not significant. **B** - root bending of 5-day old seedlings of Col-0 and RNAi *PhLP2* in ½ MS medium in 11,5 hours after gravitropic stimuli

In case of the short term gravitropism analysis, selected time points for the bending angle comparison were 10, 15, 20 and 25 minutes to evaluate progress of gravitropic response immediately after gravitropic stimulation. I observed no difference in all selected timepoints, which indicates that the gravitropic response in RNAi *PhLP2* remains unaffected (Fig. 41).

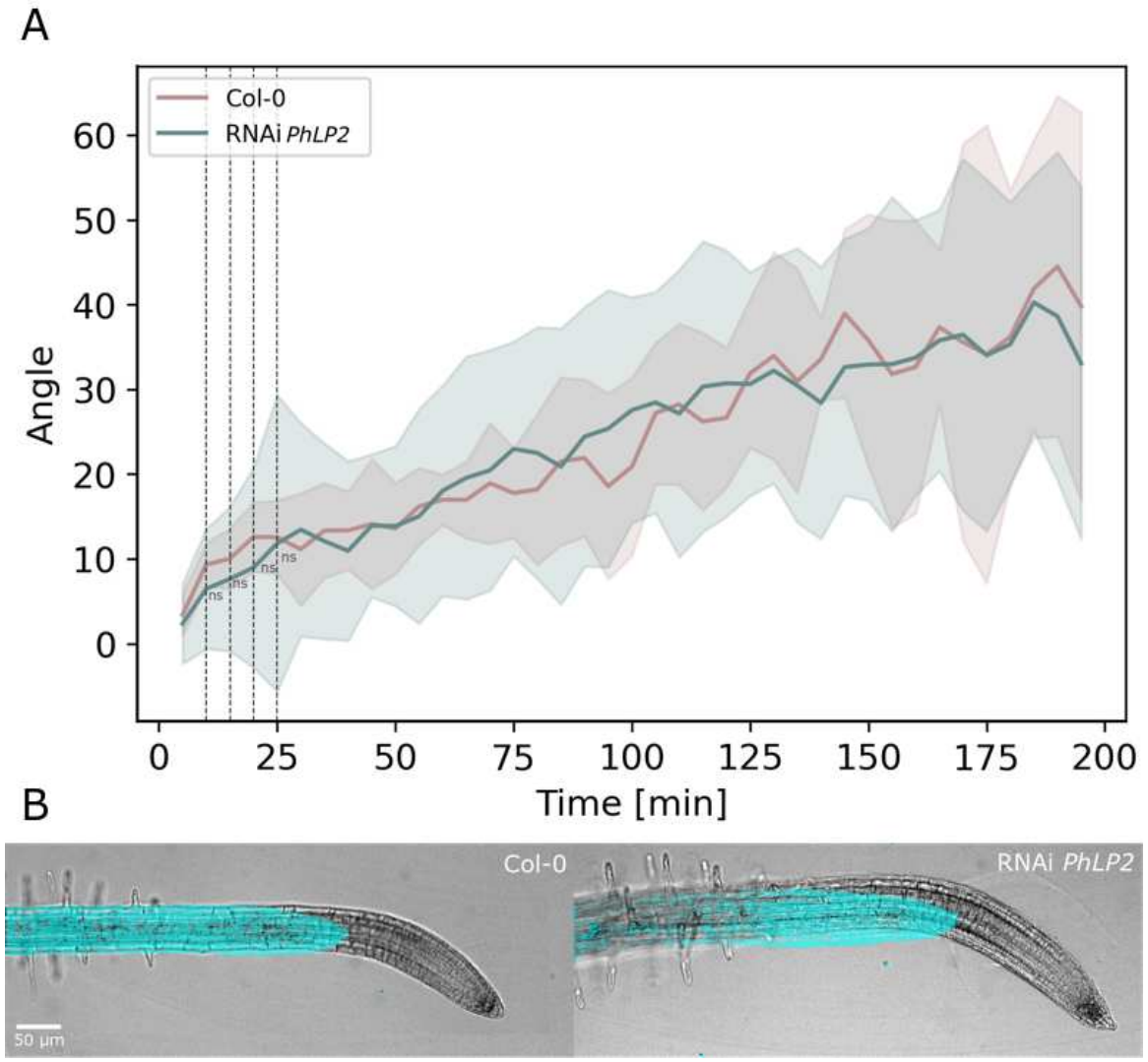

Fig. 41: Short-term gravitropic response of 5-day old seedlings of Col-0 and RNAi *PhLP2* in 195 minutes, **A** - angle (degrees) of the bending root in time, Student's t-test ($\alpha = 0{,}05$) was used to determine the significant difference between Col-0 and RNAi *PhLP2*. *$p < 0.05$, **$p < 0.01$, ***$p < 0.001$, ns = not significant. **B** - the root position 5 minutes after gravitropic stimulus visualized in blue, root position after 195 minutes is visualized in gray

3.4.3 Root zonation

Auxin plays an important role in the root meristem development (Kubalová et al., 2024) and, as it was described above, PhLP2 is distinctly expressed in the root meristem. Therefore, I analyzed the size of the meristem to test whether PhLP2 participated in meristem development. 8-day old seedlings of Col-0 and RNAi *PhLP2* were stained with 1 mM PI and imaged using a spinning disk confocal microscope. The meristem was estimated as an area between quiescent center (pool of stem cells, origin of meristem cells) and a last cell in cell file before elongation occurs. Length of the meristem was measured using ImageJ tools. The measurement was performed in three replicas. I observed that the meristem zone of RNAi *PhLP2* was significantly shorter compared to Col-0 in all three replicas (Fig. 42).

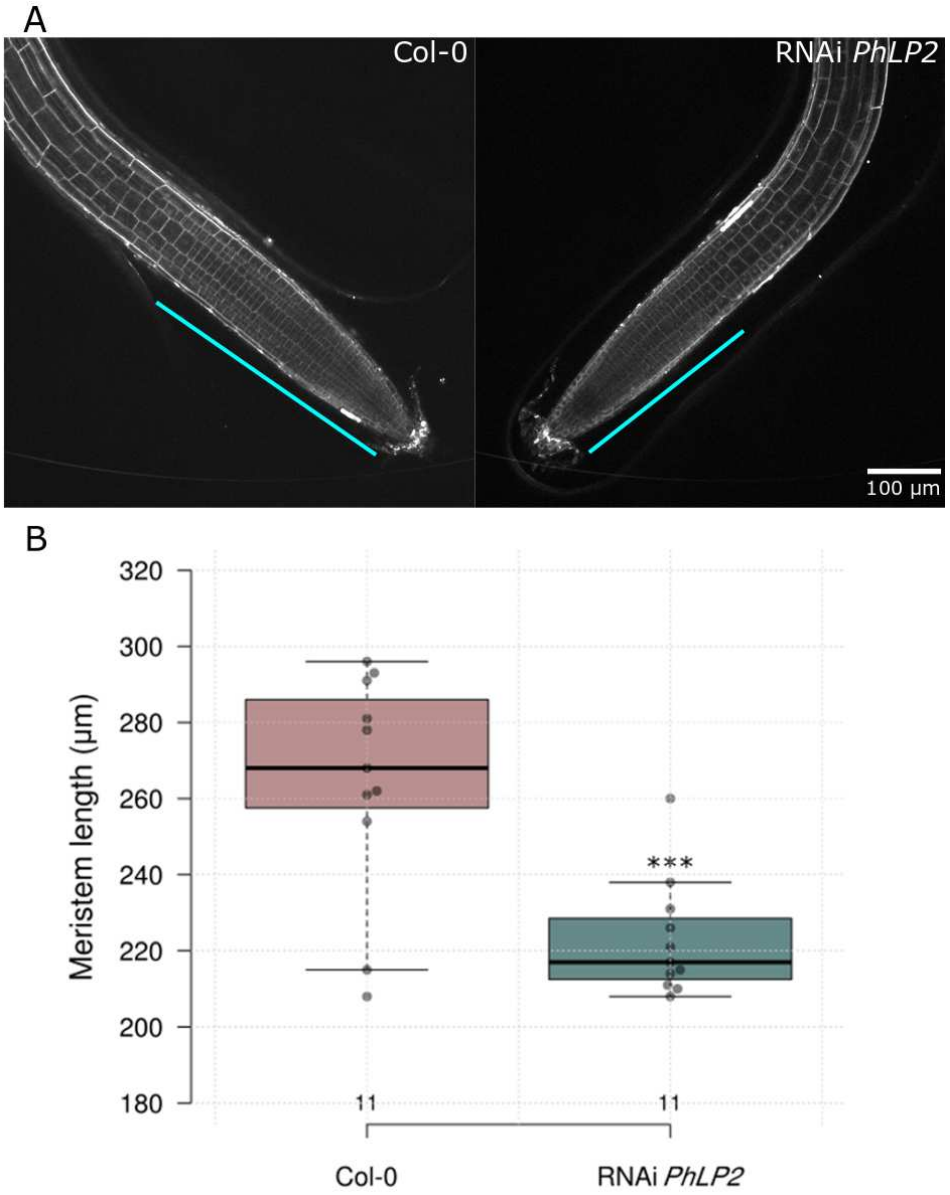

Fig. 42: Meristem length in Col-0 and RNAi *PhLP2* lines, **A** - meristem length of 8-day old seedlings of Col-0 and *PhLP2*, meristem is labeled in blue **B** - root meristem length comparison of Col-0 and RNAi *PhLP2* stained with 1 mM PI, Student's t-test ($\alpha = 0{,}05$) was used to determine the significant difference between Col-0 and RNAi *PhLP2*. *$p < 0.05$, **$p < 0.01$, ***$p < 0.001$, ns = not significant

The length of the meristematic zone can be determined either by the cell division activity or the cell elongation (or both). Difference in cell division activity can be estimated based on cell number. Therefore, the number of cells of RNAi *PhLP2* in a cell file according to the basipetal axes was counted and

compared to Col-0. According to my measurement, in two of three replicas, there was a significantly lower number of cells in RNAi *PhLP2* compared to Col-0 and in one replica, the difference was at the limit of significance (Fig. 43-A). Although, the ratio of cell number compared to the length of meristem equaled in both RNAi *PhLP2* and Col-0 (Fig. 43-B) which indicates that the number of cells is proportional to meristem length in RNAi *PhLP2* in comparison to Col-0.

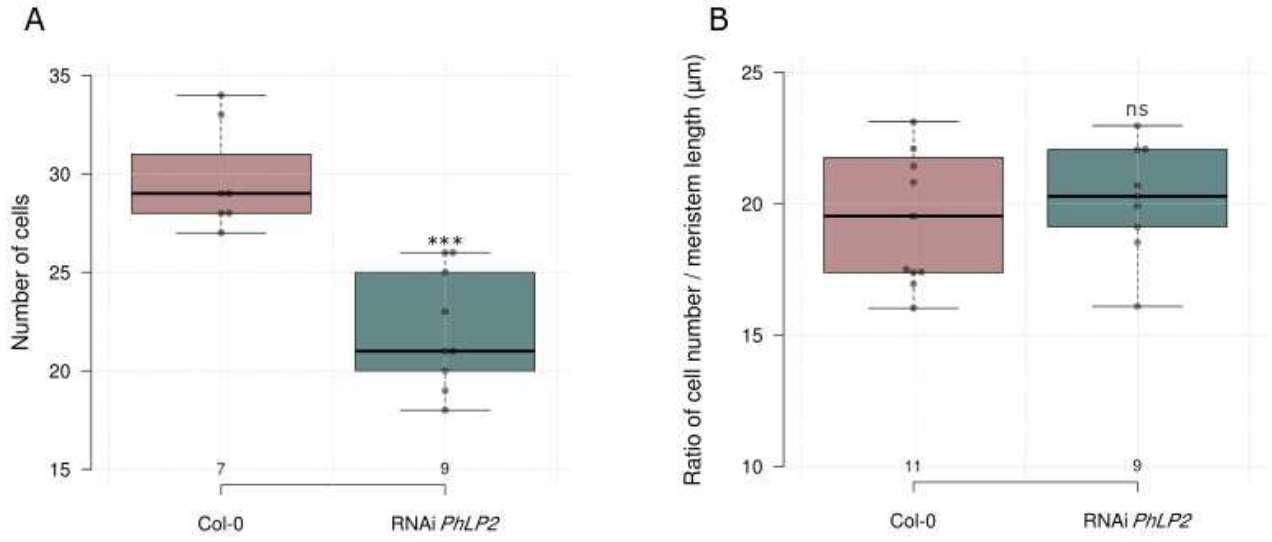

Fig. 43: Cell division activity, **A** - the number of cells in one cell file, **B** - Comparison of cell division activity expressed as the ratio of number of cells / length of meristem. Student's t-test ($\alpha = 0{,}05$) was used to determine the significant difference between Col-0 and RNAi *PhLP2*. *p < 0.05, **p < 0.01, ***p < 0.001, ns = not significant

4. Discussion

PhLP2 phosphorylation is rapidly induced by an exogenous application of IAA. Independently to IAA application, phosphorylation changes of PhLP2 in mutants of *afb1-3*, *tmk1* and *abp1-TD1*, i.e. the main players in the rapid auxin response, indicate that these signaling components are not required for the phosphorylation of PhLP2 (Han et al., 2021b; Kuhn et al., 2024b). Col-0 treated with PEO-IAA (the auxin signaling antagonist) showed a higher rate of phosphorylation of PhLP2 compared to untreated Col-0. This indicates that the PhLP2 phosphorylation is rather variable and is not specific to auxin treatment. Instead, the phosphorylation changes might be connected to the stress, secondarily caused by the treatments application (as could be for example a reaction to excessive cell elongation after the application of PEO-IAA) (Sharma et al., 2012). Phosphorylation of phosducin-family proteins was already reported in the animal system; receptor-like kinase G-PROTEIN COUPLED RECEPTOR KINASE 2 (GRK2) mediates a phosphorylation of their C-terminal domain, which decreases the ability of the protein to bind βγ-subunit of heterotrimeric G-protein (Ruiz-Gómez et al., 2000). In all cases mentioned, the position of phosphorylation of PhLP2 was Ser255, located in the 4th domain, less conserved than the core domain containing the thioredoxin active site. Would a mutation of this site exhibit a phenotype comparable to RNAi *PhLP2*? If not, it would indicate that the vital PhLP2 function is not phosphorylation-dependent.

The promoter activity I observed using pPhLP::NLS-mCherry predominantly corresponded to the expression patterns obtained from publicly available databases. Additionally, I observed its activity also in the trichomes. Protein localization throughout developmental stages corresponded to the PhLP2 promoter activity, which indicates that there are no significant tissue-specific post-translational modifications of the protein. At a cellular level, PhLP2 was present in the cytoplasm and nucleus in all tissues. It corresponds to the

cytosolic localization of the phosducin family proteins in animal systems (Blaauw, 2003). A small fraction of the animal phosducin proteins occurs also in the nucleus (Chen et al., 2005; Margulis et al., 2002). In *Arabidopsis*, plant phosducin PhLP3a and PhLP3b are localized in cytoplasm and nucleus, comparably to PhLP2 (Castellano and Sablowski, 2008).

PhLP2 signal was abundantly observed in the cytoplasm in germinating pollen grains and tubes, which corresponds to the information obtained from databases describing the expression in the mature pollen. Based on this and also based on the impossibility to propagate progeny of the knock-out mutants, PhLP2 might play an important role in the pollen development or fertilization. However, based on current knowledge, no specific function can be predicted. In the future, also the female gametophyte and embryo should be examined in the context of the knock-out lethality.

Biological processes involving PhLP2 could be hinted based on the function of genes, which are co-expressed with PhLP2. Among genes with higher coexpression, several of them participate in vesicular transport. *SNX1* is involved in plenty of processes by sorting cargo in the endosome pathway to vacuoles. For example, the sorting of PIN2 was shown to be mediated by endosomes containing SNX1 (Jaillais et al., 2006). Interestingly, SNX1 is phosphorylated after auxin application and an overexpression of SNX1 leads to the retarded growth of the primary root and lower density of LRs (Kleine-Vehn et al., 2008; Zhang et al., 2013).

SYP23 and SYP51 seem to be also connected to PhLP2. These proteins participate in endomembrane trafficking (De Benedictis et al., 2013; Ibrahim et al., 2020). Since the phenotype exhibits disruptions in auxin-related processes, vesicle trafficking might potentially influence localization of PINs to the plasma membrane and therefore distribution of IAA.

There were shown interactors of PhLP2 participating in heterotrimeric G-protein signalization: RGS1, which regulates G-protein activity by inhibiting

dissociation of its subunits, or PhLP2 predicted interactor *ELK4* encoding its β-subunit (Klopffleisch et al., 2011). These interactors participate in G-protein signaling, which corresponds to the published research about phosducins involvement in the heterotrimeric G-protein signaling in animals (Humrich et al., 2005; Lukov et al., 2005; Stirling et al., 2007).

Another group of PhLP2 interactors belongs the CCT group, which are proteins known to participate in the protein folding, including folding of individual subunits of the heterotrimeric G-proteins (Humrich et al., 2005) or cytoskeleton components (Llamas et al., 2021). However, null-mutations of heterotrimeric G-proteins in plants lead to rather subtle phenotypes, which indicates that sole impairment of this pathway (either by mis-regulation of signaling or aberrant folding of the subunits) cannot explain the strong phenotype of PhLP2 mutants (Lease et al., 2001b; Ullah et al., 2003, 2001; Urano et al., 2016). That indicates engagement of PhLP2 in plant signaling or metabolism beyond this pathway.

IAA-induced (directly or not) phosphorylation of PhLP2 requires the activity of a kinase. There are several kinases identified as co-expressed or interacting with PhLP2 and it might be possible that some of them participate in PhLP2 phosphorylation. One of the co-expressed kinases, *CKA2* was shown to be auxin involved. Transient induction of dominant negative *CKA2* (*CKA2mut*) leads to disruption of auxin transport resulting in a short and wavy primary root. *CK2* kinases are also connected to circadian rhythms regulation (Marquès‐Bueno et al., 2011), which also influence auxin regulation pathways (Covington and Harmer, 2007).

Since phosphorylation of PhLP2 was reported for serine, another relevant hint might be a serine/threonine receptor-like kinase BRL2/VH1. *vh1* mutant is for instance hypersensitive to an exogenous auxin application, which manifested as a retarded root growth (Ceserani et al., 2009).

Cloning of hairpin with native PhLP2 promoter unfortunately failed. As a

backup strategy, I took advantage of the hairpin driven by a 35S promoter available in the laboratory for the phenotype analysis. The idea was to observe the knock-down-mutant phenotype of tissues, where PhLP2 naturally occurs and based on this to suggest which developmental processes might be involved in. However, expression under the 35S promoter might not fully correspond to the native promoter. For example, I observed strong expression of the protein in the pollen where the 35S promoter is not active, therefore some phenotype characteristics could be missed. In general, the phenotype of the available line exhibited strong defects mainly in the primary root development.

The root of RNAi *PhLP2* was significantly waved in comparison to Col-0. This pattern could be explained by multiple reasons including the hypersensitivity to the stimuli connected to waving. The waved phenotype is caused mainly by interplay of the gravity sensing, mechanosensitive reaction and circumnutation. Waved primary root of the mutant *wav2* resembles the RNAi *PhLP* phenotype (Mochizuki et al., 2005). *WAV2* is a gene co-expressed with PhLP2 (although the rate of the co-expression was not high). However, the root of its mutant does not lead to skewing of the primary root. Therefore, connection of *WAV2* to PhLP2 could not fully explain observed root phenotype. The gravitropic reaction is one of the factors influencing the root waving. Distribution of PIN to PM is important for the auxin polar transport maintenance. Its disruption can lead to both waved and agravitropic phenotype, as could be seen in *pin2* mutant (Fig. 2) (Blakeslee et al., 2007; De Smet et al., 2007). However, RNAi *PhLP2* is not agravitropic. Another process participating in root wavy phenotype, circumnutation, describes a spiral movement of the root tip. When the root deviates from the direction of the growth, gravity stimulation leads it back. This coordination enables avoiding obstacles in the soil while growing (Okada and Shimura, 1990). Seedlings growing on tilted plates are constantly in touch with the agar medium surface. As was mentioned in the Results chapter, the wavy root phenotype of RNAi *PhLP2* growing in the stiff medium disappears. The

waving pattern was rescued by uniform external pressure, indicating possible hypersensitivity to the contact with the solid medium.

Col-0 growing on the medium surface naturally exhibits the left-handed skewness of the primary root (Rutherford and Masson, 1996). The angle of the root skewness of 5-day old seedlings did not differ, however, in 9-day old seedlings was significantly lower in RNAi *PhLP2* and Col-0. The longer the root is, the more the angle between root tip, root base and vertical axis increases. In 9 days of the cultivation, due to the retarded growth of RNAi *PhLP2*, roots of Col-0 were significantly longer than RNAi *PhLP2*. It might be possible that the difference is caused by the root length, however, mutant roots seemed to tend to skew in the opposite direction (Fig. 33). The only earlier described *Arabidopsis* phosducin proteins PhLP3a and PhLP3b are responsible for a proper microtubule folding (Castellano and Sablowski, 2008; De Mendoza et al., 2014) which could point to the possible connection of PhLP2 to microtubules. The drug-induced destabilization of microtubules was shown to increase the skewing in *Arabidopsis* roots, however, simultaneously with the coiled primary root (Ishida and Hashimoto, 2007), which I did not observe in RNAi *PhLP2*, so the connection to microtubules is not convincing. As was mentioned in the Literature overview chapter, skewing and waving are related processes and the skewed root phenotype of RNAi *PhLP2* could also be a consequence of defects in the wave pattern.

Lateral roots barely occur in seedlings of RNAi *PhLP2*, and this phenotype is most likely caused by a decrease in the number of established primordia. LR development is connected to auxin transport and signaling and the initiation and the outgrowth are regulated differently (Dubrovsky et al., 2008; Torres-Martínez et al., 2020).

Primordias are grown from the xylem pole of the pericycle, where PhLP2 is expressed according to ePlant. Defects in the primordial initiation were observed in triple *plt3plt5plt7* mutants (Du and Scheres, 2017). *arf7arf9* double

mutant exhibits defects in LRP initiation, which can be rescued by overexpressing *PLT3PLT5PLT7*. In the case of triple mutant *plt3plt5plt7* there were defects in LRP development but not initiation itself (Xie et al., 2021).

Phosphorylation of PhLP2 was increased in the *afb1* mutant in comparison to Col-0. It hints that both could simultaneously contribute to LRP development.

AFB1 is expressed in developing LRP and their overlaying tissues. Interestingly, the *afb1* mutant has a higher number of LRs and the *AFB1* overexpression leads to fewer LRs compared to Col-0. The difference is caused by defects in LR emergence (outgrowth) and not by decreased number of primordia initiated, as it was observed in RNAi *PhLP2* (Dubey et al., 2023). Also, *TMK1* and *TMK4* expression is increased in LR through different developmental stages. *tmk1tmk4* double mutant possess a few LRs, although LRPs are initiated (Huang et al., 2019). PhLP2 is probably not connected to the rapid auxin response players during LR development.

LRPs occur more frequently in mutants of β-subunits of the heterotrimeric G-protein, which are considered as negative regulators of the auxin-induced cell division (Ullah et al., 2003), which lead us again to potential involving of PhLP2 in the heterotrimeric G-protein signaling.

And also, ABERRANT LATERAL ROOT FORMATION 4 (ALF4) regulates the LRP initiation through the cell division ability and lack of LRPs observed in *alf4* mutant was not possible to rescue after the IAA application (DiDonato et al., 2004). The connection of PhLP2 to LRP development might not be connected to auxin as well, since RNAi *PhLP2* seems not to be IAA-insensitive. In future research, this could be revealed based on whether LRP deficiency could be rescued by IAA application.

VH1/BRL2, which is a kinase identified as a PhLP2 interactor in Y2H, is connected to the cell division activity and participating in xylem pole of vascular bounds development in leaves through different developmental stages. It is expressed in root meristem vasculature and its expression is stronger in the

xylem pole and even in LRP (Ceserani et al., 2009; Clay and Nelson, 2002). As was mentioned above, in the context of the vasculature, PhLP2 is expressed rather in the xylem pole, which points to possible connection to BRL2/VH1.

As was mentioned earlier in this work, an exogenous IAA application inhibits root-cell elongation already at nanomolar concentration. Mis-regulation of auxin signaling does not allow such a reaction. Therefore, this process is a conclusive biological readout of the sensitivity to auxin. Based on my measurement, RNAi *PhLP2* root-growth was inhibited after the IAA application, concluding that the auxin signaling itself is not disturbed. However, results in the rate of the IAA-induced inhibition were not fully consistent. Results might be possibly affected due to pipetting error or limits of measuring methods, because root growth in nM IAA concentrations happens on a very small scale and the increment was measured using the scanner, where the resolution of images is limited. Therefore, more accurate results could be obtained using microfluidics in combination with microscopy for better resolution.

As was mentioned in Literature overview, the process of gravitropic response depends on both canonical and non-transcriptional auxin signaling (Dubey et al., 2023; Kubalová et al., 2023). Based on my measurement, rapid auxin response was not impaired and the root of both lines bending equally after 11,5 hours indicates that nor canonical response is disturbed in RNAi *PhLP2*. The differences of root bending between lines in middle points of the response (6 and 9 hours) may be caused by slower growth of RNAi *PhLP2*, since gravitropism is a growth movement. Since the gravitropic response was not disrupted in RNAi *PhLP2*, the conclusion could be that PhLP2 is not required for both rapid and canonical auxin pathways.

The length of RNAi *PhLP2* meristem is significantly shorter compared to Col-0, as well as the cell number in one cell file in the meristem is also lower. Ratio of the cell length per root length did not differ between Col-0 and RNAi *PhLP2* which indicates the number of cells in one cell file is proportional to the length.

In other words, there could be a common denominator for both the less cell division activity and the cell reduced size.

Related proteins PhLP3a and PhLP3b are expressed in similar tissues as PhLP2 including root meristem. Mutation in these proteins led to defects in the cell division, however, cells continued towards DNA replication and abortive cytokinesis, so the phenotype is not comparable with RNAi *PhLP2* (Castellano and Sablowski, 2008).

On the contrary, similarly to RNAi *PhLP2*, the phenotype of mutation in SYNTAXIN OF PLANTS 81 (SYP81) possesses a shorter root meristem and lower cell number, mainly due to the disorder of the stem cell niche activity. SYP81 participates as a regulator of the reactive oxygen species signaling. *PLT1* and *PLT2*, which are participating in the stem cells activity maintenance (Du and Scheres, 2017), were identified as downstream effectors of this machinery (M. Wang et al., 2023) SYP81 belongs to the family of SNARE-proteins participating in Golgi trafficking network as well as PhLP2 interactor SYP23 or co-expressed gene *SYP51* (Saito and Ueda, 2009) which could be considered as a promoter of PhLP2 function.

In the future, further indications about the PhLP2 function could provide observation of its expression upon different treatments. According to the ePlant-expression pattern (Fig. 20) and preliminary results obtained from colleagues (unpublished data), the phenotype is also dependent on the sugar concentrations. Also, there was reported interaction of PhLP2 with RGS1 and RHIP1. RHIP1 mediates an interaction between RGS1 and hexokinase (HXK), the main glucose receptor (Huang et al., 2015). That indicates possible relation of PhLP2 to the sugar signaling. Transcription of *PhLP2* was also upregulated in the darkness period in seedling of Ler-0 growing in the short-day conditions (Todd P Michael et al., 2008). Also in the animal system there was reported decreasing of phosphorylated phosducin-family proteins as a reaction to irradiance (Yoshida et al., 1994; Zhu and Craft, 2000).

No viable mutants indicate lethality in some stage of development. I observed abundant signal of mEGFP-labeled PhLP2 in germinating pollen grains and tubes. In the future, female gametophyte could be observed too.

Another biological readout of root development might be the growth of root hairs. I observed activity of the *PhLP2* promoter also in root hair (Fig. 24). One of co-expressed genes, *WRM*, participates in propper actin cytoskeleton formation and its mutant exhibits short and stubby structure of hair root in comparison to straight root hair in Col-0 (Mathur et al., 2003). Root-hair development is also auxin dependent and its phenotype in RNAi *PhLP2* could be another hint to PhLP2 function.

5. Conclusions and answer to the aims

Does PhLP2 participate in the rapid auxin response? Gravitropic response, as the main biological readout of rapid auxin response, was not affected in early stages, unlike the mutants involved in the rapid auxin response. Also, RNAi *PhLP2* was not insensitive to IAA exogenous application, although the rate of inhibition compared to Col-0 was not conclusive. Therefore, rapid auxin response seems not disrupted. PhLP2 reacts to IAA application by phosphorylation, however, it is not required for rapid auxin response and auxin signaling. What are the other processes PhLP2 might be involved in? A lot remains unclear, although there might be some indications. It seems that in contrast to related PhLP3a and PhLP3b (beside PhLP2 the only identified *Arabidopsis* phosducin-family proteins), PhLP2 is not required for microtubule-dependent processes. Based on interacting partners and co-expressed genes, PhLP2 may play a role even in auxin non-dependent processes, such as vesicle trafficking. According to already known functions of the animal phosducins, PhLP2 might also participate in heterotrimeric G-protein signaling, although the strong phenotype of RNAi *PhLP2* is not possible to explain only by its disruption and there has to be other processes requiring PhLP2. The strong expression of PhLP2 in the germinating pollen indicates its role in gametes development. Current knowledge is not sufficient to make a conclusion about the function of PhLP2 in the *Arabidopsis* development, however, the outcome of my thesis could provide hints for future research.

6. Reference

Aida, M., Beis, D., Heidstra, R., Willemsen, V., Blilou, I., Galinha, C., Nussaume, L., Noh, Y.-S., Amasino, R., Scheres, B., 2004. The PLETHORA Genes Mediate Patterning of the Arabidopsis Root Stem Cell Niche. Cell 119, 109–120. https://doi.org/10.1016/j.cell.2004.09.018

Al-Harrasi, I., Patankar, H.V., Al-Yahyai, R., Sunkar, R., Krishnamurthy, P., Kumar, P.P., Yaish, M.W., 2020. Molecular Characterization of a Date Palm Vascular Highway 1-Interacting Kinase (PdVIK) under Abiotic Stresses. Genes 11, 568. https://doi.org/10.3390/genes11050568

Band, L.R., Wells, D.M., Larrieu, A., Sun, J., Middleton, A.M., French, A.P., Brunoud, G., Sato, E.M., Wilson, M.H., Péret, B., Oliva, M., Swarup, R., Sairanen, I., Parry, G., Ljung, K., Beeckman, T., Garibaldi, J.M., Estelle, M., Owen, M.R., Vissenberg, K., Hodgman, T.C., Pridmore, T.P., King, J.R., Vernoux, T., Bennett, M.J., 2012. Root gravitropism is regulated by a transient lateral auxin gradient controlled by a tipping-point mechanism. Proc. Natl. Acad. Sci. 109, 4668–4673. https://doi.org/10.1073/pnas.1201498109

Barbosa, I.C.R., Zourelidou, M., Willige, B.C., Weller, B., Schwechheimer, C., 2014. D6 PROTEIN KINASE Activates Auxin Transport-Dependent Growth and PIN-FORMED Phosphorylation at the Plasma Membrane. Dev. Cell 29, 674–685. https://doi.org/10.1016/j.devcel.2014.05.006

Barlow, P.W., 1989. Differential growth in plants—A phenomenon that occurs at all levels of organization. Environ. Exp. Bot. 29, 1–5. https://doi.org/10.1016/0098-8472(89)90034-8

Benjamins, R., Quint, A., Weijers, D., Hooykaas, P., Offringa, R., 2001. The PINOID protein kinase regulates organ development in *Arabidopsis* by enhancing polar auxin transport. Development 128, 4057–4067. https://doi.org/10.1242/dev.128.20.4057

Benková, E., Michniewicz, M., Sauer, M., Teichmann, T., Seifertová, D., Jürgens, G., Friml, J., 2003. Local, Efflux-Dependent Auxin Gradients as a Common Module for Plant Organ Formation. Cell 115, 591–602. https://doi.org/10.1016/S0092-8674(03)00924-3

Blaauw, M., 2003. Phosducin-like proteins in Dictyostelium discoideum: implications for the phosducin family of proteins. EMBO J. 22, 5047–5057. https://doi.org/10.1093/emboj/cdg508

Blakeslee, J.J., Bandyopadhyay, A., Lee, O.R., Mravec, J., Titapiwatanakun, B., Sauer, M., Makam, S.N., Cheng, Y., Bouchard, R., Adamec, J., Geisler, M., Nagashima, A., Sakai, T., Martinoia, E., Friml, J., Peer, W.A., Murphy, A.S., 2007. Interactions among PIN-FORMED and P-Glycoprotein Auxin Transporters in *Arabidopsis*. Plant Cell 19, 131–147. https://doi.org/10.1105/tpc.106.040782

Blancaflor, E.B., Fasano, J.M., Gilroy, S., 1998. Mapping the Functional Roles of Cap Cells in the Response of Arabidopsis Primary Roots to Gravity1. Plant Physiol. 116, 213–222. https://doi.org/10.1104/pp.116.1.213

Blancaflor, E.B., Masson, P.H., 2003. Plant Gravitropism. Unraveling the Ups and Downs of a Complex Process. Plant Physiol. 133, 1677–1690. https://doi.org/10.1104/pp.103.032169

Brackley, K.I., Grantham, J., 2009. Activities of the chaperonin containing TCP-1 (CCT): implications for cell cycle progression and cytoskeletal organisation. Cell Stress Chaperones 14, 23–31. https://doi.org/10.1007/s12192-008-0057-x

Califar, B., Sng, N.J., Zupanska, A., Paul, A.-L., Ferl, R.J., 2020. Root Skewing-Associated Genes Impact the Spaceflight Response of Arabidopsis thaliana. Front. Plant Sci. 11, 239. https://doi.org/10.3389/fpls.2020.00239

Cao, M., Chen, R., Li, P., Yu, Y., Zheng, R., Ge, D., Zheng, W., Wang, X., Gu, Y., Gelová, Z., Friml, J., Zhang, H., Liu, R., He, J., Xu, T., 2019. TMK1-mediated auxin signalling regulates differential growth of the apical hook. Nature 568, 240–243. https://doi.org/10.1038/s41586-019-1069-7

Caspar, T., Pickard, B.G., 1989. Gravitropism in a starchless mutant of Arabidopsis: Implications for the starch-statolith theory of gravity sensing. Planta 177, 185–197. https://doi.org/10.1007/BF00392807

Castellano, M.M., Sablowski, R., 2008. Phosducin-Like Protein 3 Is Required for Microtubule-Dependent Steps of Cell Division but Not for Meristem Growth in *Arabidopsis*. Plant Cell 20, 969–981. https://doi.org/10.1105/tpc.107.057737

Ceserani, T., Trofka, A., Gandotra, N., Nelson, T., 2009. VH1/BRL2 receptor‐like kinase interacts with vascular‐specific adaptor proteins VIT and VIK to influence leaf venation. Plant J. 57, 1000–1014. https://doi.org/10.1111/j.1365-313X.2008.03742.x

Chen, J., Yoshida, T., Nakano, K., Bitensky, M.W., 2005. Subcellular localization of phosducin in rod photoreceptors. Vis. Neurosci. 22, 19–25. https://doi.org/10.1017/S0952523805221028

Chen, J.-G., Jones, A.M., 2004. AtRGS1 Function in Arabidopsis thaliana, in: Methods in Enzymology. Elsevier, pp. 338–350. https://doi.org/10.1016/S0076-6879(04)89020-7

Clay, N.K., Nelson, T., 2002. VH1, a Provascular Cell–Specific Receptor Kinase That Influences Leaf Cell Patterns in Arabidopsis. Plant Cell 14, 2707–2722. https://doi.org/10.1105/tpc.005884

Clough, S.J., Bent, A.F., 1998. **Floral dip: a simplified method for *Agrobacterium*‐mediated transformation of *Arabidopsis thaliana*** . Plant J. 16, 735–743. https://doi.org/10.1046/j.1365-313x.1998.00343.x

Collet, J.-F., Messens, J., 2010. Structure, Function, and Mechanism of Thioredoxin Proteins. Antioxid. Redox Signal. 13, 1205–1216. https://doi.org/10.1089/ars.2010.3114

Covington, M.F., Harmer, S.L., 2007. The Circadian Clock Regulates Auxin Signaling and Responses in Arabidopsis. PLoS Biol. 5, e222. https://doi.org/10.1371/journal.pbio.0050222

De Benedictis, M., Bleve, G., Faraco, M., Stigliano, E., Grieco, F., Piro, G., Dalessandro, G., Di Sansebastiano, G.P., 2013. AtSYP51/52 Functions Diverge in the Post-Golgi Traffic and Differently Affect Vacuolar Sorting. Mol. Plant 6, 916–930. https://doi.org/10.1093/mp/sss117

De Mendoza, A., Sebé-Pedrós, A., Ruiz-Trillo, I., 2014. The Evolution of the GPCR Signaling System in Eukaryotes: Modularity, Conservation, and the Transition to Metazoan Multicellularity. Genome Biol. Evol. 6, 606–619. https://doi.org/10.1093/gbe/evu038

De Smet, I., Tetsumura, T., De Rybel, B., Frey, N.F.D., Laplaze, L., Casimiro, I., Swarup, R.,

Naudts, M., Vanneste, S., Audenaert, D., Inzé, D., Bennett, M.J., Beeckman, T., 2007. Auxin-dependent regulation of lateral root positioning in the basal meristem of *Arabidopsis*. Development 134, 681–690. https://doi.org/10.1242/dev.02753

De Smet, S., Cuypers, A., Vangronsveld, J., Remans, T., 2015. Gene Networks Involved in Hormonal Control of Root Development in Arabidopsis thaliana: A Framework for Studying Its Disturbance by Metal Stress. Int. J. Mol. Sci. 16, 19195–19224. https://doi.org/10.3390/ijms160819195

Del Bianco, M., Kepinski, S., 2011. Context, Specificity, and Self-Organization in Auxin Response. Cold Spring Harb. Perspect. Biol. 3, a001578–a001578. https://doi.org/10.1101/cshperspect.a001578

DiDonato, R.J., Arbuckle, E., Buker, S., Sheets, J., Tobar, J., Totong, R., Grisafi, P., Fink, G.R., Celenza, J.L., 2004. *Arabidopsis ALF4* encodes a nuclear‐localized protein required for lateral root formation. Plant J. 37, 340–353. https://doi.org/10.1046/j.1365-313X.2003.01964.x

Dindas, J., Scherzer, S., Roelfsema, M.R.G., Von Meyer, K., Müller, H.M., Al-Rasheid, K.A.S., Palme, K., Dietrich, P., Becker, D., Bennett, M.J., Hedrich, R., 2018. AUX1-mediated root hair auxin influx governs SCFTIR1/AFB-type Ca2+ signaling. Nat. Commun. 9, 1174. https://doi.org/10.1038/s41467-018-03582-5

Du, Y., Scheres, B., 2017. PLETHORA transcription factors orchestrate de novo organ patterning during *Arabidopsis* lateral root outgrowth. Proc. Natl. Acad. Sci. 114, 11709–11714. https://doi.org/10.1073/pnas.1714410114

Dubey, S.M., Han, S., Stutzman, N., Prigge, M.J., Medvecká, E., Platre, M.P., Busch, W., Fendrych, M., Estelle, M., 2023. The AFB1 auxin receptor controls the cytoplasmic auxin response pathway in *Arabidopsis thaliana* (preprint). Plant Biology. https://doi.org/10.1101/2023.01.04.522696

Dubey, S.M., Serre, N.B.C., Oulehlová, D., Vittal, P., Fendrych, M., 2021. No Time for Transcription—Rapid Auxin Responses in Plants. Cold Spring Harb. Perspect. Biol. 13, a039891. https://doi.org/10.1101/cshperspect.a039891

Dubrovsky, J.G., Sauer, M., Napsucialy-Mendivil, S., Ivanchenko, M.G., Friml, J., Shishkova, S., Celenza, J., Benková, E., 2008. Auxin acts as a local morphogenetic trigger to specify lateral root founder cells. Proc. Natl. Acad. Sci. 105, 8790–8794. https://doi.org/10.1073/pnas.0712307105

Fendrych, M., Akhmanova, M., Merrin, J., Glanc, M., Hagihara, S., Takahashi, K., Uchida, N., Torii, K.U., Friml, J., 2018. Rapid and reversible root growth inhibition by TIR1 auxin signalling. Nat. Plants 4, 453–459. https://doi.org/10.1038/s41477-018-0190-1

Friml, J., 2003. Auxin transport — shaping the plant. Curr. Opin. Plant Biol. 6, 7–12. https://doi.org/10.1016/S1369526602000031

Friml, J., Gallei, M., Gelová, Z., Johnson, A., Mazur, E., Monzer, A., Rodriguez, L., Roosjen, M., Verstraeten, I., Živanović, B.D., Zou, M., Fiedler, L., Giannini, C., Grones, P., Hrtyan, M., Kaufmann, W.A., Kuhn, A., Narasimhan, M., Randuch, M., Rýdza, N., Takahashi, K., Tan, S., Teplova, A., Kinoshita, T., Weijers, D., Rakusová, H., 2022. ABP1–TMK auxin perception for global phosphorylation and auxin canalization. Nature 609, 575–581. https://doi.org/10.1038/s41586-022-05187-x

Fukaki, H., Tasaka, M., 2009. Hormone interactions during lateral root formation. Plant Mol.

Biol. 69, 437–449. https://doi.org/10.1007/s11103-008-9417-2
Galinha, C., Hofhuis, H., Luijten, M., Willemsen, V., Blilou, I., Heidstra, R., Scheres, B., 2007. PLETHORA proteins as dose-dependent master regulators of Arabidopsis root development. Nature 449, 1053–1057. https://doi.org/10.1038/nature06206
Geisler-Lee, J., O'Toole, N., Ammar, R., Provart, N.J., Millar, A.H., Geisler, M., 2007. A Predicted Interactome for Arabidopsis. Plant Physiol. 145, 317–329. https://doi.org/10.1104/pp.107.103465
Grabov, A., Ashley, M.K., Rigas, S., Hatzopoulos, P., Dolan, L., Vicente‐Agullo, F., 2005. Morphometric analysis of root shape. New Phytol. 165, 641–652. https://doi.org/10.1111/j.1469-8137.2004.01258.x
Grantham, J., 2020. The Molecular Chaperone CCT/TRiC: An Essential Component of Proteostasis and a Potential Modulator of Protein Aggregation. Front. Genet. 11, 172. https://doi.org/10.3389/fgene.2020.00172
Gray, W.M., Kepinski, S., Rouse, D., Leyser, O., Estelle, M., 2001. Auxin regulates SCFTIR1-dependent degradation of AUX/IAA proteins. Nature 414, 271–276. https://doi.org/10.1038/35104500
Hadfi, K., Speth, V., Neuhaus, G., 1998. Auxin-induced developmental patterns in *Brassica juncea* embryos. Development 125, 879–887. https://doi.org/10.1242/dev.125.5.879
Han, H., Verstraeten, I., Roosjen, M., Mazur, E., Rýdza, N., Hajný, J., Ötvös, K., Weijers, D., Friml, J., 2021a. Rapid auxin-mediated phosphorylation of Myosin regulates trafficking and polarity in Arabidopsis (preprint). Plant Biology. https://doi.org/10.1101/2021.04.13.439603
Han, H., Verstraeten, I., Roosjen, M., Mazur, E., Rýdza, N., Hajný, J., Ötvös, K., Weijers, D., Friml, J., 2021b. Rapid auxin-mediated phosphorylation of Myosin regulates trafficking and polarity in Arabidopsis. https://doi.org/10.1101/2021.04.13.439603
Hilty, J., Muller, B., Pantin, F., Leuzinger, S., 2021. Plant growth: the What, the How, and the Why. New Phytol. 232, 25–41. https://doi.org/10.1111/nph.17610
Hofmann, F., Schon, M.A., Nodine, M.D., 2019. The embryonic transcriptome of Arabidopsis thaliana. Plant Reprod. 32, 77–91. https://doi.org/10.1007/s00497-018-00357-2
Hooper, C.M., Castleden, I.R., Tanz, S.K., Aryamanesh, N., Millar, A.H., 2017. SUBA4: the interactive data analysis centre for Arabidopsis subcellular protein locations. Nucleic Acids Res. 45, D1064–D1074. https://doi.org/10.1093/nar/gkw1041
Huang, C., Wang, Z., Quinn, D., Suresh, S., Hsia, K.J., 2018. Differential growth and shape formation in plant organs. Proc. Natl. Acad. Sci. 115, 12359–12364. https://doi.org/10.1073/pnas.1811296115
Huang, J.-P., Tunc-Ozdemir, M., Chang, Y., Jones, A.M., 2015. Cooperative control between AtRGS1 and AtHXK1 in a WD40-repeat protein pathway in Arabidopsis thaliana. Front. Plant Sci. 6. https://doi.org/10.3389/fpls.2015.00851
Huang, R., Zheng, R., He, J., Zhou, Z., Wang, J., Xiong, Y., Xu, T., 2019. Noncanonical auxin signaling regulates cell division pattern during lateral root development. Proc. Natl. Acad. Sci. 116, 21285–21290. https://doi.org/10.1073/pnas.1910916116
Humrich, J., Bermel, C., Bünemann, M., Härmark, L., Frost, R., Quitterer, U., Lohse, M.J., 2005. Phosducin-like Protein Regulates G-Protein βγ Folding by Interaction with Tailless Complex Polypeptide-1α. J. Biol. Chem. 280, 20042–20050.

https://doi.org/10.1074/jbc.M409233200
Ibrahim, A., Yang, X., Liu, C., Cooper, K.D., Bishop, B.A., Zhu, M., Kwon, S., Schoelz, J.E., Nelson, R.S., 2020. Plant SNAREs SYP22 and SYP23 interact with Tobacco mosaic virus 126 kDa protein and SYP2s are required for normal local virus accumulation and spread. Virology 547, 57–71. https://doi.org/10.1016/j.virol.2020.04.002
Ishida, T., Hashimoto, T., 2007. An Arabidopsis thaliana tubulin mutant with conditional root-skewing phenotype. J. Plant Res. 120, 635–640. https://doi.org/10.1007/s10265-007-0105-0
Jaillais, Y., Fobis-Loisy, I., Miège, C., Rollin, C., Gaude, T., 2006. AtSNX1 defines an endosome for auxin-carrier trafficking in Arabidopsis. Nature 443, 106–109. https://doi.org/10.1038/nature05046
Jin, J., Pawson, T., 2012. Modular evolution of phosphorylation-based signalling systems. Philos. Trans. R. Soc. B Biol. Sci. 367, 2540–2555. https://doi.org/10.1098/rstb.2012.0106
Jumper, J., Evans, R., Pritzel, A., Green, T., Figurnov, M., Ronneberger, O., Tunyasuvunakool, K., Bates, R., Žídek, A., Potapenko, A., Bridgland, A., Meyer, C., Kohl, S.A.A., Ballard, A.J., Cowie, A., Romera-Paredes, B., Nikolov, S., Jain, R., Adler, J., Back, T., Petersen, S., Reiman, D., Clancy, E., Zielinski, M., Steinegger, M., Pacholska, M., Berghammer, T., Bodenstein, S., Silver, D., Vinyals, O., Senior, A.W., Kavukcuoglu, K., Kohli, P., Hassabis, D., 2021. Highly accurate protein structure prediction with AlphaFold. Nature 596, 583–589. https://doi.org/10.1038/s41586-021-03819-2
Kepinski, S., Leyser, O., 2004. Auxin-induced SCF ^{TIR1} –Aux/IAA interaction involves stable modification of the SCF ^{TIR1} complex. Proc. Natl. Acad. Sci. 101, 12381–12386. https://doi.org/10.1073/pnas.0402868101
Kim, H.B., Schaller, H., Goh, C.-H., Kwon, M., Choe, S., An, C.S., Durst, F., Feldmann, K.A., Feyereisen, R., 2005. Arabidopsis *cyp51* Mutant Shows Postembryonic Seedling Lethality Associated with Lack of Membrane Integrity. Plant Physiol. 138, 2033–2047. https://doi.org/10.1104/pp.105.061598
Kleine-Vehn, J., Leitner, J., Zwiewka, M., Sauer, M., Abas, L., Luschnig, C., Friml, J., 2008. Differential degradation of PIN2 auxin efflux carrier by retromer-dependent vacuolar targeting. Proc. Natl. Acad. Sci. 105, 17812–17817. https://doi.org/10.1073/pnas.0808073105
Klepikova, A.V., Kasianov, A.S., Gerasimov, E.S., Logacheva, M.D., Penin, A.A., 2016. A high resolution map of the *Arabidopsis thaliana* developmental transcriptome based on RNA‐seq profiling. Plant J. 88, 1058–1070. https://doi.org/10.1111/tpj.13312
Klopffleisch, K., Phan, N., Augustin, K., Bayne, R.S., Booker, K.S., Botella, J.R., Carpita, N.C., Carr, T., Chen, J., Cooke, T.R., Frick‐Cheng, A., Friedman, E.J., Fulk, B., Hahn, M.G., Jiang, K., Jorda, L., Kruppe, L., Liu, C., Lorek, J., McCann, M.C., Molina, A., Moriyama, E.N., Mukhtar, M.S., Mudgil, Y., Pattathil, S., Schwarz, J., Seta, S., Tan, M., Temp, U., Trusov, Y., Urano, D., Welter, B., Yang, J., Panstruga, R., Uhrig, J.F., Jones, A.M., 2011. Arabidopsis G‐protein interactome reveals connections to cell wall carbohydrates and morphogenesis. Mol. Syst. Biol. 7, 532. https://doi.org/10.1038/msb.2011.66

Konstantinova, N., Korbei, B., Luschnig, C., 2021. Auxin and Root Gravitropism: Addressing Basic Cellular Processes by Exploiting a Defined Growth Response. Int. J. Mol. Sci. 22, 2749. https://doi.org/10.3390/ijms22052749

Kubalová, M., Müller, K., Dobrev, P.I., Rizza, A., Jones, A.M., Fendrych, M., 2024. Auxin co‐receptor IAA17 / AXR3 controls cell elongation in *Arabidopsis thaliana* root solely by modulation of nuclear auxin pathway. New Phytol. 241, 2448–2463. https://doi.org/10.1111/nph.19557

Kubalová, M., Müller, K., Dobrev, P.I., Rizza, A., Jones, A.M., Fendrych, M., 2023. Auxin coreceptor IAA17/AXR3 controls cell elongation in *Arabidopsis thaliana* root by modulation of auxin and gibberellin perception (preprint). Plant Biology. https://doi.org/10.1101/2023.03.15.532805

Kuhn, A., Roosjen, M., Mutte, S., Dubey, S.M., Carrasco, P.C., Monzer, A., Kohchi, T., Nishihama, R., Fendrych, M., Friml, J., Sprakel, J., Weijers, D., 2022. A RAF-like kinase mediates a deeply conserved, ultra-rapid auxin response (preprint). Plant Biology. https://doi.org/10.1101/2022.11.25.517951

Kuhn, A., Roosjen, M., Mutte, S., Dubey, S.M., Carrillo Carrasco, V.P., Boeren, S., Monzer, A., Koehorst, J., Kohchi, T., Nishihama, R., Fendrych, M., Sprakel, J., Friml, J., Weijers, D., 2024a. RAF-like protein kinases mediate a deeply conserved, rapid auxin response. Cell 187, 130-148.e17. https://doi.org/10.1016/j.cell.2023.11.021

Kuhn, A., Roosjen, M., Mutte, S., Dubey, S.M., Carrillo Carrasco, V.P., Boeren, S., Monzer, A., Koehorst, J., Kohchi, T., Nishihama, R., Fendrych, M., Sprakel, J., Friml, J., Weijers, D., 2024b. RAF-like protein kinases mediate a deeply conserved, rapid auxin response. Cell 187, 130-148.e17. https://doi.org/10.1016/j.cell.2023.11.021

Kulich, I., Schmid, J., Teplova, A., Qi, L., Friml, J., 2024. Rapid translocation of NGR proteins driving polarization of PIN-activating D6 protein kinase during root gravitropism. eLife 12, RP91523. https://doi.org/10.7554/eLife.91523.3

Lacoste, C., Barthaux, V., Iborra, C., Seagar, M., Erard-Garcia, M., 2006. MAU-8 is a Phosducin-like Protein required for G protein signaling in C. elegans. Dev. Biol. 294, 181–191. https://doi.org/10.1016/j.ydbio.2006.02.039

Lease, K.A., Wen, J., Li, J., Doke, J.T., Liscum, E., Walker, J.C., 2001a. A Mutant Arabidopsis Heterotrimeric G-Protein β Subunit Affects Leaf, Flower, and Fruit Development. Plant Cell 13, 2631–2641. https://doi.org/10.1105/tpc.010315

Lease, K.A., Wen, J., Li, J., Doke, J.T., Liscum, E., Walker, J.C., 2001b. A Mutant Arabidopsis Heterotrimeric G-Protein β Subunit Affects Leaf, Flower, and Fruit Development. Plant Cell 13, 2631–2641. https://doi.org/10.1105/tpc.010315

Lee, R.H., Fowler, A., McGinnis, J.F., Lolley, R.N., Craft, C.M., 1990. Amino acid and cDNA sequence of bovine phosducin, a soluble phosphoprotein from photoreceptor cells. J. Biol. Chem. 265, 15867–15873. https://doi.org/10.1016/S0021-9258(18)55479-X

Leyser, O., 2010. The Power of Auxin in Plants. Plant Physiol. 154, 501–505. https://doi.org/10.1104/pp.110.161323

Li, C., Wu, H.-M., Cheung, A.Y., 2016. FERONIA and Her Pals: Functions and Mechanisms. Plant Physiol. 171, 2379–2392. https://doi.org/10.1104/pp.16.00667

Li, M., Chen, Y., Ou, J., Huang, J., Zhang, X., 2022. PDCL2 is essential for spermiogenesis

and male fertility in mice. Cell Death Discov. 8, 419. https://doi.org/10.1038/s41420-022-01210-2

Li, X., Zhao, R., Liu, J., Li, Z., Chen, A., Xu, S., Sheng, X., 2024. Dynamic changes in calcium signals during root gravitropism. Plant Physiol. Biochem. 208, 108481. https://doi.org/10.1016/j.plaphy.2024.108481

Lin, W., Zhou, X., Tang, W., Takahashi, K., Pan, X., Dai, J., Ren, H., Zhu, X., Pan, S., Zheng, H., Gray, W.M., Xu, T., Kinoshita, T., Yang, Z., 2021. TMK-based cell-surface auxin signalling activates cell-wall acidification. Nature 599, 278–282. https://doi.org/10.1038/s41586-021-03976-4

Llamas, E., Torres-Montilla, S., Lee, H.J., Barja, M.V., Schlimgen, E., Dunken, N., Wagle, P., Werr, W., Zuccaro, A., Rodríguez-Concepción, M., Vilchez, D., 2021. The intrinsic chaperone network of Arabidopsis stem cells confers protection against proteotoxic stress. https://doi.org/10.1101/2021.01.19.427268

Lukov, G.L., Hu, T., McLaughlin, J.N., Hamm, H.E., Willardson, B.M., 2005. Phosducin-like protein acts as a molecular chaperone for G protein βγ dimer assembly. EMBO J. 24, 1965–1975. https://doi.org/10.1038/sj.emboj.7600673

Mähönen, A.P., Tusscher, K.T., Siligato, R., Smetana, O., Díaz-Triviño, S., Salojärvi, J., Wachsman, G., Prasad, K., Heidstra, R., Scheres, B., 2014. PLETHORA gradient formation mechanism separates auxin responses. Nature 515, 125–129. https://doi.org/10.1038/nature13663

Marconi, M., Wabnik, K., 2021. Shaping the Organ: A Biologist Guide to Quantitative Models of Plant Morphogenesis. Front. Plant Sci. 12, 746183. https://doi.org/10.3389/fpls.2021.746183

Margulis, A., Dang, L., Pulukuri, S., Lee, R., Sitaramayya, A., 2002. Presence of phosducin in the nuclei of bovine retinal cells. Mol. Vis. 8, 477–482.

Marquès‐Bueno, M.M., Moreno‐Romero, J., Abas, L., De Michele, R., Martínez, M.C., 2011. A dominant negative mutant of protein kinase CK2 exhibits altered auxin responses in Arabidopsis. Plant J. 67, 169–180. https://doi.org/10.1111/j.1365-313X.2011.04585.x

Mathur, J., Mathur, N., Kernebeck, B., Hülskamp, M., 2003. Mutations in Actin-Related Proteins 2 and 3 Affect Cell Shape Development in Arabidopsis. Plant Cell 15, 1632–1645. https://doi.org/10.1105/tpc.011676

Michael, Todd P., Mockler, T.C., Breton, G., McEntee, C., Byer, A., Trout, J.D., Hazen, S.P., Shen, R., Priest, H.D., Sullivan, C.M., Givan, S.A., Yanovsky, M., Hong, F., Kay, S.A., Chory, J., 2008. Network discovery pipeline elucidates conserved time-of-day-specific cis-regulatory modules. PLoS Genet. 4, e14. https://doi.org/10.1371/journal.pgen.0040014

Michael, Todd P, Mockler, T.C., Breton, G., McEntee, C., Byer, A., Trout, J.D., Hazen, S.P., Shen, R., Priest, H.D., Sullivan, C.M., Givan, S.A., Yanovsky, M., Hong, F., Kay, S.A., Chory, J., 2008. Network Discovery Pipeline Elucidates Conserved Time-of-Day–Specific cis-Regulatory Modules. PLoS Genet. 4, e14. https://doi.org/10.1371/journal.pgen.0040014

Milo, R., Jorgensen, P., Moran, U., Weber, G., Springer, M., 2010. BioNumbers—the database of key numbers in molecular and cell biology. Nucleic Acids Res. 38,

D750–D753. https://doi.org/10.1093/nar/gkp889
Mizzotti, C., Rotasperti, L., Moretto, M., Tadini, L., Resentini, F., Galliani, B.M., Galbiati, M., Engelen, K., Pesaresi, P., Masiero, S., 2018. Time-Course Transcriptome Analysis of Arabidopsis Siliques Discloses Genes Essential for Fruit Development and Maturation. Plant Physiol. 178, 1249–1268. https://doi.org/10.1104/pp.18.00727
Mochizuki, S., Harada, A., Inada, S., Sugimoto-Shirasu, K., Stacey, N., Wada, T., Ishiguro, S., Okada, K., Sakai, T., 2005. The Arabidopsis WAVY GROWTH 2 Protein Modulates Root Bending in Response to Environmental Stimuli. Plant Cell 17, 537–547. https://doi.org/10.1105/tpc.104.028530
Monshausen, G.B., Miller, N.D., Murphy, A.S., Gilroy, S., 2011. Dynamics of auxin‐dependent Ca $^{2+}$ and pH signaling in root growth revealed by integrating high‐resolution imaging with automated computer vision‐based analysis. Plant J. 65, 309–318. https://doi.org/10.1111/j.1365-313X.2010.04423.x
Mudgett, M., Shen, Z., Dai, X., Briggs, S.P., Zhao, Y., 2023. Suppression of *pinoid* mutant phenotypes by mutations in *PIN-FORMED 1* and PIN1-GFP fusion. Proc. Natl. Acad. Sci. 120, e2312918120. https://doi.org/10.1073/pnas.2312918120
Narsai, R., Law, S.R., Carrie, C., Xu, L., Whelan, J., 2011. In-Depth Temporal Transcriptome Profiling Reveals a Crucial Developmental Switch with Roles for RNA Processing and Organelle Metabolism That Are Essential for Germination in Arabidopsis. Plant Physiol. 157, 1342–1362. https://doi.org/10.1104/pp.111.183129
Ng, J., Perrine-Walker, F., Wasson, A., Mathesius, U., 2015. The Control of Auxin Transport in Parasitic and Symbiotic Root–Microbe Interactions. Plants 4, 606–643. https://doi.org/10.3390/plants4030606
Obayashi, T., Hibara, H., Kagaya, Y., Aoki, Y., Kinoshita, K., 2022. ATTED-II v11: A Plant Gene Coexpression Database Using a Sample Balancing Technique by Subagging of Principal Components. Plant Cell Physiol. 63, 869–881. https://doi.org/10.1093/pcp/pcac041
Okada, K., Shimura, Y., 1990. Reversible Root Tip Rotation in *Arabidopsis* Seedlings Induced by Obstacle-Touching Stimulus. Science 250, 274–276. https://doi.org/10.1126/science.250.4978.274
Okada, K., Ueda, J., Komaki, M.K., Bell, C.J., Shimura, Y., 1991. Requirement of the Auxin Polar Transport System in Early Stages of Arabidopsis Floral Bud Formation. Plant Cell 677–684. https://doi.org/10.1105/tpc.3.7.677
Okumura, K., Goh, T., Toyokura, K., Kasahara, H., Takebayashi, Y., Mimura, T., Kamiya, Y., Fukaki, H., 2013. GNOM/FEWER ROOTS is Required for the Establishment of an Auxin Response Maximum for Arabidopsis Lateral Root Initiation. Plant Cell Physiol. 54, 406–417. https://doi.org/10.1093/pcp/pct018
Oliva, M., Dunand, C., 2007. Waving and skewing: how gravity and the surface of growth media affect root development in Arabidopsis. New Phytol. 176, 37–43. https://doi.org/10.1111/j.1469-8137.2007.02184.x
Oliveira, C.C., Jones, A.M., Fontes, E.P.B., Reis, P.A.B.D., 2022. G-Protein Phosphorylation: Aspects of Binding Specificity and Function in the Plant Kingdom. Int. J. Mol. Sci. 23, 6544. https://doi.org/10.3390/ijms23126544
Péret, B., Swarup, K., Ferguson, A., Seth, M., Yang, Y., Dhondt, S., James, N., Casimiro, I.,

Perry, P., Syed, A., Yang, H., Reemmer, J., Venison, E., Howells, C., Perez-Amador, M.A., Yun, J., Alonso, J., Beemster, G.T.S., Laplaze, L., Murphy, A., Bennett, M.J., Nielsen, E., Swarup, R., 2012. *AUX/LAX* Genes Encode a Family of Auxin Influx Transporters That Perform Distinct Functions during *Arabidopsis* Development. Plant Cell 24, 2874–2885. https://doi.org/10.1105/tpc.112.097766

Petricka, J.J., Winter, C.M., Benfey, P.N., 2012. Control of *Arabidopsis* Root Development. Annu. Rev. Plant Biol. 63, 563–590. https://doi.org/10.1146/annurev-arplant-042811-105501

Prigge, M.J., Platre, M., Kadakia, N., Zhang, Y., Greenham, K., Szutu, W., Pandey, B.K., Bhosale, R.A., Bennett, M.J., Busch, W., Estelle, M., 2020. Genetic analysis of the Arabidopsis TIR1/AFB auxin receptors reveals both overlapping and specialized functions. eLife 9, e54740. https://doi.org/10.7554/eLife.54740

Reig, J.A., Yu, L., Klein, D.C., 1990. Pineal transduction. Adrenergic----cyclic AMP-dependent phosphorylation of cytoplasmic 33-kDa protein (MEKA) which binds beta gamma-complex of transducin. J. Biol. Chem. 265, 5816–5824. https://doi.org/10.1016/S0021-9258(19)39436-0

Remy, E., Cabrito, T.R., Baster, P., Batista, R.A., Teixeira, M.C., Friml, J., Sá-Correia, I., Duque, P., 2013. A Major Facilitator Superfamily Transporter Plays a Dual Role in Polar Auxin Transport and Drought Stress Tolerance in *Arabidopsis*. Plant Cell 25, 901–926. https://doi.org/10.1105/tpc.113.110353

Roosjen, M., Kuhn, A., Mutte, S.K., Boeren, S., Krupar, P., Koehorst, J., Fendrych, M., Friml, J., Weijers, D., 2022. An ultra-fast, proteome-wide response to the plant hormone auxin (preprint). Plant Biology. https://doi.org/10.1101/2022.11.25.517949

Routier-Kierzkowska, A.-L., Smith, R.S., 2013. Measuring the mechanics of morphogenesis. Curr. Opin. Plant Biol. 16, 25–32. https://doi.org/10.1016/j.pbi.2012.11.002

Roy, R., Bassham, D.C., 2014. Root growth movements: Waving and skewing. Plant Sci. 221–222, 42–47. https://doi.org/10.1016/j.plantsci.2014.01.007

Roychoudhry, S., Kepinski, S., 2021. Auxin in Root Development. Cold Spring Harb. Perspect. Biol. a039933. https://doi.org/10.1101/cshperspect.a039933

Ruiz-Gómez, A., Humrich, J., Murga, C., Quitterer, U., Lohse, M.J., Mayor, F., 2000. Phosphorylation of Phosducin and Phosducin-like Protein by G Protein-coupled Receptor Kinase 2. J. Biol. Chem. 275, 29724–29730. https://doi.org/10.1074/jbc.M001864200

Rutherford, R., Masson, P.H., 1996. Arabidopsis thaliana sku Mutant Seedlings Show Exaggerated Surface-Dependent Alteration in Root Growth Vector. Plant Physiol. 111, 987–998. https://doi.org/10.1104/pp.111.4.987

Saito, C., Ueda, T., 2009. Chapter 4 Functions of RAB and SNARE Proteins in Plant Life, in: International Review of Cell and Molecular Biology. Elsevier, pp. 183–233. https://doi.org/10.1016/S1937-6448(08)02004-2

Salem, M.A., Li, Y., Bajdzienko, K., Fisahn, J., Watanabe, M., Hoefgen, R., Schöttler, M.A., Giavalisco, P., 2018. RAPTOR Controls Developmental Growth Transitions by Altering the Hormonal and Metabolic Balance. Plant Physiol. 177, 565–593. https://doi.org/10.1104/pp.17.01711

Santner, A.A., Watson, J.C., 2006. The WAG1 and WAG2 protein kinases negatively regulate

root waving in Arabidopsis. Plant J. 45, 752–764. https://doi.org/10.1111/j.1365-313X.2005.02641.x

Sarrion-Perdigones, A., Vazquez-Vilar, M., Palaci, J., Castelijns, B., Forment, J., Ziarsolo, P., Blanca, J., Granell, A., Orzaez, D., 2013. GoldenBraid 2.0: A Comprehensive DNA Assembly Framework for Plant Synthetic Biology. PLANT Physiol. 162, 1618–1631. https://doi.org/10.1104/pp.113.217661

Sato, E.M., Hijazi, H., Bennett, M.J., Vissenberg, K., Swarup, R., 2015. New insights into root gravitropic signalling. J. Exp. Bot. 66, 2155–2165. https://doi.org/10.1093/jxb/eru515

Schmid, M., Davison, T.S., Henz, S.R., Pape, U.J., Demar, M., Vingron, M., Schölkopf, B., Weigel, D., Lohmann, J.U., 2005. A gene expression map of Arabidopsis thaliana development. Nat. Genet. 37, 501–506. https://doi.org/10.1038/ng1543

Schultz, E.R., Zupanska, A.K., Sng, N.J., Paul, A.-L., Ferl, R.J., 2017. Skewing in Arabidopsis roots involves disparate environmental signaling pathways. BMC Plant Biol. 17, 31. https://doi.org/10.1186/s12870-017-0975-9

Serre, N.B., Wernerová, D., Vittal, P., Dubey, S.M., Medvecká, E., Jelínková, A., Petrášek, J., Grossmann, G., Fendrych, M., 2023. The AUX1-AFB1-CNGC14 module establishes a longitudinal root surface pH profile. eLife 12, e85193. https://doi.org/10.7554/eLife.85193

Serre, N.B.C., Kralík, D., Yun, P., Slouka, Z., Shabala, S., Fendrych, M., 2021. AFB1 controls rapid auxin signalling through membrane depolarization in Arabidopsis thaliana root. Nat. Plants 7, 1229–1238. https://doi.org/10.1038/s41477-021-00969-z

Sharma, P., Jha, A.B., Dubey, R.S., Pessarakli, M., 2012. Reactive Oxygen Species, Oxidative Damage, and Antioxidative Defense Mechanism in Plants under Stressful Conditions. J. Bot. 2012, 1–26. https://doi.org/10.1155/2012/217037

Shih, H.-W., DePew, C.L., Miller, N.D., Monshausen, G.B., 2015. The Cyclic Nucleotide-Gated Channel CNGC14 Regulates Root Gravitropism in Arabidopsis thaliana. Curr. Biol. 25, 3119–3125. https://doi.org/10.1016/j.cub.2015.10.025

Stateczny, D., Oppenheimer, J., Bommert, P., 2016. G protein signaling in plants: minus times minus equals plus. Curr. Opin. Plant Biol. 34, 127–135. https://doi.org/10.1016/j.pbi.2016.11.001

Stirling, P.C., Srayko, M., Takhar, K.S., Pozniakovsky, A., Hyman, A.A., Leroux, M.R., 2007. Functional Interaction between Phosducin-like Protein 2 and Cytosolic Chaperonin Is Essential for Cytoskeletal Protein Function and Cell Cycle Progression. Mol. Biol. Cell 18, 2336–2345. https://doi.org/10.1091/mbc.e07-01-0069

Su, S.-H., Gibbs, N.M., Jancewicz, A.L., Masson, P.H., 2017. Molecular Mechanisms of Root Gravitropism. Curr. Biol. 27, R964–R972. https://doi.org/10.1016/j.cub.2017.07.015

Tanaka, H., Dhonukshe, P., Brewer, P.B., Friml, J., 2006. Spatiotemporal asymmetric auxin distribution: a means to coordinate plant development. Cell. Mol. Life Sci. 63, 2738–2754. https://doi.org/10.1007/s00018-006-6116-5

Taxman, D.J., Moore, C.B., Guthrie, E.H., Huang, M.T.-H., 2010. Short Hairpin RNA (shRNA): Design, Delivery, and Assessment of Gene Knockdown, in: Sioud, M. (Ed.), RNA Therapeutics, Methods in Molecular Biology. Humana Press, Totowa, NJ, pp. 139–156. https://doi.org/10.1007/978-1-60761-657-3_10

Torres-Martínez, H.H., Hernández-Herrera, P., Corkidi, G., Dubrovsky, J.G., 2020. From one cell to many: Morphogenetic field of lateral root founder cells in *Arabidopsis thaliana* is built by gradual recruitment. Proc. Natl. Acad. Sci. 117, 20943–20949. https://doi.org/10.1073/pnas.2006387117

Torres-Martínez, H.H., Rodríguez-Alonso, G., Shishkova, S., Dubrovsky, J.G., 2019. Lateral Root Primordium Morphogenesis in Angiosperms. Front. Plant Sci. 10, 206. https://doi.org/10.3389/fpls.2019.00206

Ullah, H., Chen, J.-G., Temple, B., Boyes, D.C., Alonso, J.M., Davis, K.R., Ecker, J.R., Jones, A.M., 2003. The β-Subunit of the Arabidopsis G Protein Negatively Regulates Auxin-Induced Cell Division and Affects Multiple Developmental Processes[W]. Plant Cell 15, 393–409. https://doi.org/10.1105/tpc.006148

Ullah, H., Chen, J.-G., Young, J.C., Im, K.-H., Sussman, M.R., Jones, A.M., 2001. Modulation of Cell Proliferation by Heterotrimeric G Protein in *Arabidopsis*. Science 292, 2066–2069. https://doi.org/10.1126/science.1059040

Ung, K.L., Winkler, M., Schulz, L., Kolb, M., Janacek, D.P., Dedic, E., Stokes, D.L., Hammes, U.Z., Pedersen, B.P., 2022. Structures and mechanism of the plant PIN-FORMED auxin transporter. Nature 609, 605–610. https://doi.org/10.1038/s41586-022-04883-y

Urano, D., Miura, K., Wu, Q., Iwasaki, Y., Jackson, D., Jones, A.M., 2016. Plant Morphology of Heterotrimeric G Protein Mutants. Plant Cell Physiol. 57, 437–445. https://doi.org/10.1093/pcp/pcw002

Van Leene, J., Han, C., Gadeyne, A., Eeckhout, D., Matthijs, C., Cannoot, B., De Winne, N., Persiau, G., Van De Slijke, E., Van De Cotte, B., Stes, E., Van Bel, M., Storme, V., Impens, F., Gevaert, K., Vandepoele, K., De Smet, I., De Jaeger, G., 2019. Capturing the phosphorylation and protein interaction landscape of the plant TOR kinase. Nat. Plants 5, 316–327. https://doi.org/10.1038/s41477-019-0378-z

Vermeer, J.E.M., Von Wangenheim, D., Barberon, M., Lee, Y., Stelzer, E.H.K., Maizel, A., Geldner, N., 2014. A Spatial Accommodation by Neighboring Cells Is Required for Organ Initiation in *Arabidopsis*. Science 343, 178–183. https://doi.org/10.1126/science.1245871

Villaecija-Aguilar, J.A., Hamon-Josse, M., Carbonnel, S., Kretschmar, A., Ljung, K., Bennett, T., Gutjahr, C., 2019. KAI2 regulates root and root hair development by modulating auxin distribution. https://doi.org/10.1101/539734

Von Wangenheim, D., Fangerau, J., Schmitz, A., Smith, R.S., Leitte, H., Stelzer, E.H.K., Maizel, A., 2016. Rules and Self-Organizing Properties of Post-embryonic Plant Organ Cell Division Patterns. Curr. Biol. 26, 439–449. https://doi.org/10.1016/j.cub.2015.12.047

Wang H, Chevalier D, Larue C, Ki Cho S, Walker JC. The Protein Phosphatases and Protein Kinases of Arabidopsis thaliana. Arabidopsis Book. 2007;5:e0106. doi: 10.1199/tab.0106. Epub 2007 Feb 20. PMID: 22303230; PMCID: PMC3243368.https://doi.org/10.1105/tpc.106.048777

Wang, M., Zhang, H., Zhao, X., Zhou, J., Qin, G., Liu, Y., Kou, X., Zhao, Z., Wu, T., Zhu,

J.-K., Feng, X., Li, L., 2023. SYNTAXIN OF PLANTS81 regulates root meristem activity and stem cell niche maintenance via ROS signaling. Plant Physiol. 191, 1365–1382. https://doi.org/10.1093/plphys/kiac530

Wang, S., Sass, M.I., Kwon, Y., Ludlam, W.G., Smith, T.M., Carter, E.J., Gladden, N.E., Riggi, M., Iwasa, J.H., Willardson, B.M., Shen, P.S., 2023. Visualizing the chaperone-mediated folding trajectory of the G protein β5 β-propeller. Mol. Cell 83, 3852-3868.e6. https://doi.org/10.1016/j.molcel.2023.09.032

Wu, G., Lewis, D.R., Spalding, E.P., 2007. Mutations in *Arabidopsis Multidrug Resistance-Like* ABC Transporters Separate the Roles of Acropetal and Basipetal Auxin Transport in Lateral Root Development. Plant Cell 19, 1826–1837. https://doi.org/10.1105/tpc.106.048777

Xie, X., Wang, Y., Datla, R., Ren, M., 2021. Auxin and Target of Rapamycin Spatiotemporally Regulate Root Organogenesis. Int. J. Mol. Sci. 22, 11357. https://doi.org/10.3390/ijms222111357

Xu, T., Dai, N., Chen, J., Nagawa, S., Cao, M., Li, H., Zhou, Z., Chen, X., De Rycke, R., Rakusová, H., Wang, W., Jones, A.M., Friml, J., Patterson, S.E., Bleecker, A.B., Yang, Z., 2014. Cell Surface ABP1-TMK Auxin-Sensing Complex Activates ROP GTPase Signaling. Science 343, 1025–1028. https://doi.org/10.1126/science.1245125

Yoshida, T., Willardson, B.M., Wilkins, J.F., Jensen, G.J., Thornton, B.D., Bitensky, M.W., 1994. The phosphorylation state of phosducin determines its ability to block transducin subunit interactions and inhibit transducin binding to activated rhodopsin. J. Biol. Chem. 269, 24050–24057.

Yu, H., Zhang, Y., Moss, B.L., Bargmann, B.O.R., Wang, R., Prigge, M., Nemhauser, J.L., Estelle, M., 2015. Untethering the TIR1 auxin receptor from the SCF complex increases its stability and inhibits auxin response. Nat. Plants 1, 14030. https://doi.org/10.1038/nplants.2014.30

Zhang, H., Zhou, H., Berke, L., Heck, A.J.R., Mohammed, S., Scheres, B., Menke, F.L.H., 2013. Quantitative Phosphoproteomics after Auxin-stimulated Lateral Root Induction Identifies an SNX1 Protein Phosphorylation Site Required for Growth. Mol. Cell. Proteomics 12, 1158–1169. https://doi.org/10.1074/mcp.M112.021220

Zhao, Y., 2012. Auxin Biosynthesis: A Simple Two-Step Pathway Converts Tryptophan to Indole-3-Acetic Acid in Plants. Mol. Plant 5, 334–338. https://doi.org/10.1093/mp/ssr104

Zhu, X., Craft, C.M., 2000. Modulation of CRX Transactivation Activity by Phosducin Isoforms. Mol. Cell. Biol. 20, 5216–5226. https://doi.org/10.1128/MCB.20.14.5216-5226.2000

Online sources:

https://gbcloning.upv.es/ (GoldenBraid)

https://www.geneious.com/ (Geneious)

https://www.graphpad.com/quickcalcs/ttest1/?format=C (online t-test calculator)

https://alphafold.ebi.ac.uk/ (AlphaFold)

https://bar.utoronto.ca/eplant/ (bar.utoronto)

https://bar.utoronto.ca/interactions2/#%7B%7D (bar.utoronto, *Arabidopsis* interactions)

https://atted.jp/ (ATTED-II)

https://thebiogrid.org/ (BioGRID)